Changes made to the revised manuscript are described in red.

General response

We thank all three references for their constructive comments and suggestions. Overall, there seem to be two main categories of issues/suggestions:

1) Writing: (a) the aims and conclusions of the research are not communicated clearly enough and (b) the comparison against observations/proxies is too detailed for an EMIC. We agree and have addressed as detailed below. We also agree that the strengths of the study have not been sufficiently emphasised, and address this as well.

2) Analyses: It is suggested that doing additional analyses would be helpful if feasible (specifically incorporating ^{13}C and performing sensitivity analyses). These analyses would be interesting, but are unfortunately infeasible as the research was performed during a PhD and there are no resources for additional simulations. Note that applying all our ensemble members to the simulation of one stage represents at least 0.5 CPU years of computing. We will instead deal with these helpful suggestions through an existing sensitivity not previously discussed, and re-emphasise caveats as appropriate, and as detailed below.

We note that this paper was intended as part one of two related papers. This paper describing the relationships between ensemble outputs, and the second, currently being finalised for submission, describing dependencies on ensemble parameters to isolate mechanisms. We are happy to provide a draft of the second manuscript as part of the review process if deemed necessary, as it may help to put this current paper in perspective. Even accounting for the increased focus of the revisions, however, we still believe there to be far too much material overall to cram into a single paper.

Response to referee #1

We thank referee #1 for useful and constructive comments. Our response is provided below in black, with original referee comments in blue.

General comments

I like it very much that the authors provided an comprehensive review of the mechanisms that governing the LGM atm. CO2 drop. And I really appreciate that an extensive body of related work are mentioned during the discussion of model results. However, I do have several major concerns.

1) Research aim:

P1 l15-16 and P3 l19 suggest that the aim of this study is "to investigate the causes of the LGM atmospheric CO2 drop". To me, this research aim is not appropriate. Previous studies have already proposed some hypotheses regarding the mechanisms that governing the decrease of atmospheric CO2 concentration relative to preindustrial (as have been summarised in the Introduction). What is not yet clear is the interplay of these mechanisms and the relative quantitative contribution of each mechanism to the LGM atmospheric CO2 drop. In this study, the authors did not explicitly propose any new hypothesis. Yet, the quantification of the contribution of different mechanisms using GENIE is not possible due to the simplification of the model and due to that many processes are not accounted for.

We agree that the research aim should be reframed. We are using a large ensemble of LGM forced simulations to explore changes in physical and biogeochemical variables thought to influence the drawdown of CO_2. We now make it clearer that the objective is not to explain definitively the causes of CO_2 drop as we strongly believe the inevitable uncertainty surrounding simulations makes it impossible to accurately resolve the relative contributions of individual processes in models of any complexity as a result of irreducible uncertainty regarding processes. Instead our aim is to account for as many sources of model uncertainty as we can and from there describe the model output space we see. Intermediate complexity is demanded for such an uncertainty-based study, which carried out 471x40,000-year simulations, intractable in high complexity models.

We rephrased our research aim in the abstract and introduction, in the manner proposed above.

I think a more specific research aim/question is needed for this study. When setting up the aim/question, the authors might consider: What are the novel aspects of the model or the EFPC2 ensemble? In this manuscript, is it the first time that an interactive carbon cycle model is applied to LGM? Is it for the first time the sensitivity to process parameters is investigated for LGM climate (Holden et al 2013 pointed out that EMICs are important tools for exploring sensitivities and quantifying uncertainty)? Which mechanism(s) the authors would like to focus on? terrestrial carbon preservation? carbonate weathering?

Agreed, the revision addresses this and the introduction lays out the research objective and novelties of our approach, being:

- Investigating the range of physical and biogeochemical changes (and hence implicitly also specific mechanisms) which may have accompanied the LGM atmospheric CO_2 drop, when taking into account model uncertainty in a large ensemble approach.

- Attempting to simulate the LGM atmospheric CO_2 drop with the simulated CO_2 feeding back to the simulated climate, which is still infrequently done in LGM CO_2 experiments, and the first time it is done with GENIE-1.
- Simulating the burial of land carbon by glacial ice sheets: there have been only a limited number of studies doing this and none that have attempted it in an LGM equilibrium experiment set-up.

The novelties of our approach have been laid out in the introduction, in the manner proposed above.

2) Key findings/conclusions:
The current version of the Conclusion reads more like a summary of the model results. It's not clear what are the key findings of this study. I think the key message would become clear once the research aim/question is given.

Agreed, the revision will address this and summarise the key conclusions, being:

- Despite our extensive exploration of model uncertainty, we struggle to achieve -90 ppmv. We attribute this to the potential LGM CO_2 drivers not included in the model as well as error in the model's process representations (and which was not captured by the ensemble). The total effect on is estimated at up to ~60 ppmv, yielding an acceptable, or "plausible", range of ~-30 to ~90 ppmv.
- Within this plausible ΔCO_2 range, there are multiple potential ΔCO_2 "solutions", simply in terms of the sign and magnitude of physical and biogeochemical changes. However, plausible CO_2 is more frequently associated with some changes than others, namely: decreasing SSTs, increasing sea ice area, a weakening of the AMOC, a strengthening of the AABW cell in the Atlantic Ocean, a decreasing ocean biological productivity, an increasing $CaCO_3$ weathering flux, an increasing terrestrial biosphere carbon inventory and an increasing deep-sea $CaCO_3$ burial flux.
- The paper focuses on these dominant changes: (1) showing that the change in terrestrial carbon is positive both because of ice sheet carbon burial and reduced soil respiration, and (2) suggesting ways in which the other physical and biogeochemical changes may have occurred, based on their spatial patterns and relationship to other changes.
- The dominant changes are also found to be broadly consistent with observations, and based on a qualitative attempt to reconcile the sign of the terrestrial carbon change with carbon isotopes, we show that a positive terrestrial carbon change is not immediately in contradiction. However, a quantitative assessment would be needed to obtain a more definitive answer. Since a detailed and comprehensive assessment of modelled results against observations was not an objective of the current paper, this is a direction for future research.

The key conclusions have been incorporated in the revised conclusions section.

3) Comparison of model results to field/proxy data or to results of other models:
A large body of text is devoted to the comparison between model results and data and to the explanation of differences between the two. To me this is a bit overdone. Holden et al. (2010), who used the same model and had the same principle for the design of the ensemble, clearly stated that the ensemble is developed to reproduce the main features, but not the precise observation.

We agree and will compare modelled results in less detail in the revision, focusing on spatial patterns at a coarser resolution, and making it more explicit that globally aggregated estimates are to be treated in a similar way.

We have reduced the comparison of model results to observations/paleo-proxies and other models, in the manner described above.

Specific comments (the following comments mainly concern the suggestions for improving the structure and presentation of model results.)

Abstract

P1 l15-16: It would be helpful to specifically state the research aim here.
We agree that our research aim needs to be clearly laid out at the beginning of the abstract. We propose to briefly introduce the research problem, followed by our aim, and then our key results.

We have rearranged the abstract in the manner described above.

Introduction

P3 l27: "unknown error" – does it mean the discrepancy between e.g. the modelled circulation and that obtained from proxy data? To me it sounds like a mistake one accidentally made in the model.

Our meaning here is that there is no direct two-way, persistent, interaction between ocean and ice sheets (as is the case in some higher complexity models), and the error caused by the absence of this process is unknown.

P3 l28: "unknown error" – Maybe "missing processes" is more suitable here? Agreed, this would be clearer and will be changed.

We removed the following sentence: "It is recognised, however, that what constitutes an implausible or plausible climate state is somewhat subjective, and that not all sources of model uncertainty, such as the unknown error due to interacting ice sheets and ocean circulation, or the unknown error due to potential ΔCO_2 mechanisms not included in the model (although see below for some estimates), are accounted for."

The concern about not all sources of uncertainty being accounted for is largely addressed through: "Despite our ensemble varying many of the parameters thought to contribute to variability in glacial-interglacial atmospheric CO2, not all sources of uncertainty can be captured, and this is reflected in our simulated DCO2 distribution. We estimate that up to ~60 ppmv of DCO2 could be due to processes not included in our model and error in our process representations (see section 2.4 for details)."

Please add at the end of the Introduction an overview of the upcoming sections, viz., what will be presented in each section.

Yes, thank you for the useful suggestion. We will include a paragraph detailing our main sections: (i) description of the model, ensemble and simulation set-up used; (ii) brief analysis of preindustrial simulations to verify that plausible given that the way we spin-up the model is not exactly the same as in Holden et al., 2013a, and we also wanted to include evaluation of a few metrics not used to constrain the original ensemble; (iii) analysis of LGM simulation results to determine range of physical and biogeochemical changes that may have accompanied LGM drop. This section includes direct drivers of CO_2 change (e.g. terrestrial carbon inventory change) as well as indirect drivers (e.g. precipitation change).

The new sections are broadly as outlined above.

We have added an overview section at the end of the introduction

Method

P5, Table 1: what is OLR? Outgoing longwave radiation

We have replaced OLR with Outgoing longwave radiation

P6: I think a table or a flow chart summarising the conditions for the four stages would be helpful for readers to understand the set-up of experiments.

We made some minor changes to the text and feel like this clarifies the description significantly.

How long is the stage 2? 10,000 years

Is the total carbon inventory (that is, sum of atmospheric, terrestrial, ocean and lithospheric carbon inventory) unchanged over the four simulation stage? We checked that carbon is being approximately conserved over stage 3 in PGCAF-16, by calculating the sum of ATMC, TERRC, OCEANC and LITHC for each of the 16 ensemble members. We found that each sum, in absolute terms, was less than 10 PgC.

LGM ensemble simulations

P9: Please explain here why the subset PGACF-16 is needed. This can be done by moving p37 l30-32 to section 4.1. We agree that the need for PGACF-16 should be explained more clearly when introducing it. The main reason is to determine whether the patterns identified for PGACF as a whole also appear to hold for the lower end of the ΔCO_2 range more strictly. Assessing variation across the plausible ΔCO_2 spectrum is not a dominant objective of the study, however, and we will update the writing to reflect this.

We explain the need for subset PGACF-16 towards the end of the Introduction section.

It would be very helpful if a brief overview of the following text of this section 4 is presented: which variables of which set will be presented. Agreed. In the current manuscript, for all model outputs of interest, we discuss PGACF, PGACF-16 and EFPC2, albeit focusing on the first ensemble. The other two ensembles are discussed to show extent to which similar to PGACF, despite their different ΔCO_2 ranges and number of ensemble members included. In the revised manuscript, we will reduce discussion of PGACF-16 and EFPC2 and have this reflected in the overview section.

Instead an overview section in Section 4, we include the above information towards the end of the Introduction section.

P25 l6-7: this is not true because in Table 6 none previous observation/model data study shows negative delta_OceanC. We agree that this statement is misleading as two of the studies make use of soil carbon measurements, and the third is a modelling study which does not explicitly report the change in ocean carbon. The statement was based on the assumption that if ~90% of the atmospheric perturbation caused by the reported increase in terrestrial biosphere carbon was removed by oceans and sediments, the change in ocean carbon inventory would still be negative (between ~-9 and ~350 PgC), after adding remaining carbon to be lost from the atmosphere to the ocean. We will rephrase our statement in the revision.

The statement has been replaced with "we can see that the mean ΔTerrC is only aligned with a handful of estimates and no studies so far report a negative ΔOceanC. Instead, ΔOceanC is estimated to be positive, primarily based on carbon isotope data".

P36 bottom: Fig. 18 should be Fig. 17. We will update the figure number.
The figure number has been updated.

P36 l3: "North Atlantic" and "North Pacific" should be switched. We agree that the text is confusing here and we will clarify this by replacing “large increases” with “ maxima”

We implemented the aforementioned edit.

Comparison of global-integrated numbers and spatial distribution between model results and data: I suggest to first compare the spatial distribution and then the globalintegrated numbers because the latter is just the sum of the former. Agreed, we will switch the order in the revision.

While it is a useful suggestion, we came to the conclusion, in revising the text, that the latter would be easier to follow with the globally integrated numbers presented first.

Colour slots showing spatial distributions of variables, e.g. Fig 3, 6, 7, ...: please add contour line for land-ocean border. These will be included in the revision.

Plots showing standard deviation in e.g. Fig 3, 6, ...: These plots are shown but never mentioned/used/discussed. So please consider move them to a supplementary information file – there are already many figures in the manuscript. Agreed, we included the standard deviation plots for information but they are not central to our arguments. We will move them to a SI file in the revised manuscript.

Conclusions

P39 l15: The positive delta_TerrC has been discussed and justified many times through out the manuscript. Thus, I have the impression that this is one key finding the authors would like to stress. I think this is a bit dangerous because this point is not well supported by data. The authors also seem de-stressing this point several times by stating there are other 4 ways of "achieving a plausible delta_CO2 interns of the sign of individual carbon reservoir changes (although Table 5 suggests those 4 ways are much likely to occur). I have to say I am confused by the above statements.

We agree that the statements are confusing and we will clarify these in the revision as follows: we find that plausible ΔCO_2 can be achieved in 5 different ways in terms of the sign of individual carbon reservoir changes. However, positive ΔTerrC combined with positive ΔLithC and negative ΔOceanC is by far the most common way, encompassing 89% of simulations, and we focus our discussion on these simulations. This includes proposing explanations for the positive ΔTerrC and discussing the change in the light of observational constraints.

The aforementioned revisions have been implemented.

P39 l39 - P41 l15: I understand that it is a pity that carbon isotopes were not simulated. However, I don't think it is appropriate to extensively present inferred results in the Conclusion section.

Agreed. In the revision, we will move the discussion of carbon isotopes, focused on the positive ΔTerrC, to the section on carbon reservoir changes.

Instead of moving the discussion of carbon isotopes to the section on carbon reservoirs, we created a separate sub-section for it, at the end of the results and discussion section.

Response to Pearse Buchanan (referee #2)

We thank Pearse Buchanan for his very detailed and constructive comments. As above, our replies are in black, and original comments in blue.

1 General comments

This study provides some unique perspectives on the glacial drawdown of atmospheric pCO_2. This problem has been at the forefront of climate research for many decades. So far, many mechanisms have been proposed, but a recipe of changes that is physical and biogeochemically consistent with proxy records and known mechanisms is still elusive. The authors of this study set out to try and achieve this difficult task.

The authors employ a unique set of methods to attack their exploration of what might plausibly reduce atmospheric pCO_2 under glacial conditions. The method involves simulating 315 individual parameter sets using the same Earth System Model (ESM) of intermediate complexity in four stages. From what I can tell, each stage involves the full 315-member ensemble, unless numerical instability problems were encountered. Each ensemble member was therefore independent from another at all stages through the study. Each stage was initialised from the final year solution of its previous stage, except stage 1 which I am unsure about what fields have been used for intialisation. The only boundary conditions that were prescribed to the Earth System Model that I can tell were orbital parameters, aeolian iron deposition rates, detrital flux rate to ocean sediments, and ice-sheet fraction and their orography. The 4 stages are as follows:

1. Stage 1 (PI 10,000 years): relaxed pCO_2 to 278 ppmv; no interaction between carbon reservoirs; conserved alkalinity in the ocean.
2. Stage 2 (PI 10,000 years): freely evolving pCO_2; interacting reservoirs; freely evolving ocean alkalinity.
3. Stage 3 (LGM 10,000 years) freely evolving pCO_2; interacting reservoirs; freely evolving ocean alkalinity; ice-sheet growth and corresponding sea level loss

years 0-1000.
4. Stage 4 (LGM 10,000 years) freely evolving pCO2; interacting reservoirs; freely evolving ocean alkalinity.

We will revise the text to clarify our method, which is the following:
In total, 471 runs were applied to preindustrial and then LGM simulations. At the LGM (stage 3), however, 75 runs either “snowballed” or crashed, leaving 396 ensemble members (EM). By “snowballed” we mean that the runs predicted highly implausible global annual SATs, between ca. -67.8 and -56.8°C, likely as a result of global or near-global sea and land ice cover developing in the simulations. Out of the remaining 396 EM, we then removed those simulations with preindustrial CO2 outside of 280 ± 10 ppmv (18 EM), and subsequently any EM that predicted large abrupt changes in atmospheric CO2 over the LGM simulation that likely caused by instabilities rather than by some physical mechanism (63 EM).

Regarding inititialisation, the model spins up from its default state. Only the CaCO3 weathering fluxes are taken from Holden et al., 2013a, diagnosed from their 25 kyr preindustrial spin-up. However, the prescribed fluxes are automatically and continuously rescaled in the model to balance the modelled CaCO3 burial rate. Thus, their value is not important (Ridgwell, 2017).

The boundary conditions in our simulations are indeed orbital parameters, aeolian iron deposition rates, detrital flux rate to ocean sediments, and ice sheet fraction and their orography. For the latter, we will make it more explicit in the revision that since our ice sheets are as described in Holden et al., 2010b, only the Laurentide and Eurasian Ice Sheets are allowed to change from their preindustrial form and rather than being extracted uniformly, freshwater to build the LGM ice sheets is routed from the Atlantic, Pacific and Arctic, assuming modern topography.

l. 24-26 on p. 4 should also say that a freshwater flux scaling parameter (FFX) value of 1.5 is applied in GENIE to correct for un-modelled isostatic depression at the ice-bedrock interface due to ice sheet growth, and for assuming a fixed land-sea mask. We vary the parameter in the ensemble to capture the uncertainty in the magnitude of the glacial sea level drop and its effects on the carbon cycle.

The revised manuscript now reads: “(FFX) scales ice sheet meltwater fluxes to correct for un-modelled isostatic depression at the ice-bedrock interface due to ice sheet growth, and for assuming a fixed land-sea mask. We vary the parameter in the ensemble to capture the uncertainty in the magnitude of the glacial sea level drop and its effects on the carbon cycle.”

The first paragraph of section 2.3 was modified to clarify what happens in stages 1 and 2.

We have described our ice sheet setup in more detail.

For clarity, we moved the section regarding which ensemble runs were removed to section 2.3 and made some minor changes to our wording.

Following on from this methodology, the authors lead the reader through the results in a methodical manner, taking on changes in some key environmental variables. In each address of a variable, the authors undergo a detailed assessment of PI versus LGM changes in their model and in proxy records. This is done both in a global sense and a regional sense, sometimes being highly specific. The ground-truthing and comparison to observations and other studies is commendable. It one of the largest comparisons that I have come across in a modelling paper. However, the sheer size of comparison makes the paper unwieldy, and loses the major findings amongst the details. It is also unexpected that the authors concentrate on highly specific regional comparisons because they use an ESM of intermediate complexity that will simply not perform well in many ways. Rather, the authors should focus on the sheer size of their parameter spread and in diagnosing the effect that certain changes have on carbon and climate. I therefore suggest that the authors make an effort to reduce the emphasis on comparison, and focus on how their interesting results might explain the LGM carbon cycle in only a broad sense.

Agreed, in the revision we will modify the text to better take into account the complexity of our model, and to better emphasize the links between the changes we see and CO2.

In the revised manuscript, we reduce the level of comparison and attempt the link between non-CO2 variables and CO2 more apparent.

It occurs to me that the authors seem to forget some obvious strengths of their study. Their parameter space is enormous, includes an interactive carbon cycle with carbon-climate feedbacks, as well as many other processes (sea level) that have not been included in other model studies of the LGM. This is of interest to the LGM pCO2 drop problem. I suggest that the authors try and convey these strengths more clearly in their abstract and the final paragraph of the introduction.

Agreed, the abstract will be reduced to one paragraph and the aim and strengths of our study will introduced at the beginning at the paragraph. We will also clarify these in the current final paragraph of the introduction section, and which now focuses on a description of the ensemble.

The abstract has been reduced to one paragraph, with the aim stated at the beginning. In the introduction, we state more clearly our advantage of big parameter space, interactive carbon cycle and uniqueness of carbon burial.

A particularly interesting result of this study is the increase in terrestrial carbon under LGM conditions. The authors more often than not find that LGM conditions are associated with greater carbon held in soils because (1) ice-sheet growth covers previously fertile regions and traps the carbon in the soil, (2) soil respiration rates decrease more than primary production, and (3) terrestrial carbon in exposed continental shelves due to sea level drop increases. The authors do not simulate point 3, and there is a possible methodological problem with point 1, in that the authors grow the LGM ice sheets from pre-industrial to LGM state in only 1,000 years. It is unclear in the manuscript presented here whether this rapid growth of ice sheets that is prescribed overtakes highly productive regions that have not yet evolved to become arid tundra land, which have lower carbon content in the soils. A rapid trapping of soil carbon by the unrealistic growth of the ice sheets (almost 100x faster than in reality) would likely overestimate the terrestrial carbon reservoir at the LGM. The authors state in the methods that "Sensitivity simulations were performed to verify the simulated equilibrium state is insensitive to the choice of timescale of ice-sheet growth", and yet the authors do not present any evidence of this sensitivity. I am therefore sceptical of the validity of this result, which I would say is their most important and interesting contribution to the field.

We agree that our statement on sensitivity simulations is confusing, and realise here that the following statement may also need updating in the revision to avoid confusion: “The increases in terrestrial biosphere carbon are predominantly due to our choice to preserve rather than destroy carbon in ice sheet areas. However, the ensemble soil respiration also tends to decrease significantly more than net photosynthesis, resulting in relatively large increases in non-burial carbon”. We briefly address the latter point first.

The statement is based on an analysis of terrestrial carbon partitioning between ice-sheet and non-ice sheet carbon pools in PGACF-16 and from there inference about what happens in PGACF. If the LGM burial carbon inventories in PGACF-16 were to be removed, DTERRC would be negative in 13 out of 16 simulations, despite the fact that terrestrial carbon also increases outside of the ice sheet areas in 15 out of 16 simulations. However, it is not strictly correct to attribute the carbon inventories that are buried to the burial itself. It is the combination of our ice sheet carbon stocks increasing rather than decreasing when exposed to LGM climate, and our choice to preserve rather than destroy this carbon. If most of the carbon that was present in ice sheet areas at the end of the preindustrial runs had been lost to climate forcings, it would not matter much whether the remaining stocks had been destroyed or preserved. From the literature, it is not clear how much of the carbon in ice sheet areas is thought to have been lost strictly in response to ice sheet "bulldozing" versus climate impacts. We will update the revised manuscript to reflect this logic.

With regard to the statement "Sensitivity simulations were performed to verify the simulated equilibrium state is insensitive to the choice of timescale of ice-sheet growth",
This refers to the sensitivity of the LGM burial carbon amount to the timescale of ice sheet growth. To test this, we took one ensemble member from PGACF-16 and applied it to two 11,000-year LGM simulations with 1000-year ice sheet growth and 10,000-year ice sheet growth respectively. Both simulations were started from the end of the same equilibrium preindustrial simulation. We then compared the LGM burial carbon inventories in each run and found that these differed by just 34.2 PgC, which, assuming ~90% of removal of atmospheric CO_2 perturbation by ocean and sediments, amounts to a mere 1.6 ppmv CO_2 difference. Our assumption is that applying the same ensemble member to a transient simulation of the full glacial cycle (and therefore a more realistic ice sheet build-up history) would not have yielded a dramatically different burial carbon inventory. Given that we did a sensitivity experiment with just one ensemble member, we are also assuming that the diagnosed sensitivity is roughly representative of the ensemble as a whole. In the revision, we will highlight these as potential caveats.

With regard to the sign of the ice sheet carbon response at the LGM, we argue that it was not necessarily negative and analysis of PGACF-16 indeed suggests that the sign is consistently positive. Most of this increase is due to a reduction in soil respiration as vegetation carbon change is only positive in one simulation. We also find that extending the timescale of ice sheet growth increases rather than decreases the burial carbon inventory. A likely explanation is that the soil carbon inventory was not yet in equilibrium by 1000 years.

We have clarified our description of LGM terrestrial carbon changes, and our statement on the sensitivity simulations.

Finally, the conclusion needs complete re-writing. It reads as a re-stating of the methods and then the results, which is simply not useful for the reader. The authors do discuss carbon isotope changes, which are appropriate records to discuss given the main result of an increase terrestrial carbon reservoir. I strongly suggest that the authors re-assess their strengths and major findings, present them concisely, and provide some comments regarding how a higher terrestrial carbon reservoir and low ocean reservoir could have occurred despite most studies indicating the opposite. If this is possible, then this would be a useful contribution to the field.

Agreed, our revised conclusions section will summarise our research objective and the novelties of our approach and then the key conclusions, detailed in the author reply on p. 3. Most of the discussion on carbon isotopes will be shifted to the section on carbon reservoir changes.

The aforementioned changes have been included in the revised manuscript.

Major revisions are needed. If the authors can provide some evidence that changes in the timescale over which the ice-sheets are grown do not play a large role in determining how much carbon is present in the terrestrial reservoir, and the manuscript is rewritten addressing the points above and below, then I advocate publication.

Some other general points:

• Regarding the figures, I strongly suggest that the authors overlay the red (PGACF-16) over the yellow (PGACF) bars in the histograms. This would reduce a lot of unnecessary replication in the figures. The authors could use a transparency setting to ensure that the red and yellow are easily seen if they have the same number of experiments (frequency). Agreed, we will include these changes in the revision.

• The writing is generally okay, but this manuscript definitely requires re-writing in some places. There are too many adjectives and unnecessarily difficult acronyms. OK, we will revise this aspect of our writing.

We have sought to make the writing more concise and change acronyms where relevant (e.g. below).

• The presentation of results suffers from the use of opaque acronyms that are easily forgotten after reading the methods section. I strongly suggest that the references to EFPC2, PGACF and PGACF-16 are changed to be more interpretable. PI315, LGM104, LGM16... or equivalent, would be much more helpful. Agreed, the proposed names will be used in the revision.

We changed EPFC2, PGACF and PGACF-16 to ENS315, ENS104 and ENS16 respectively with "EN" denoting ensemble and the number, the associated number of members.

2 Specific comments

Abstract

The abstract is quite long. The message that this study delivers could be made considerably more poignant if it were condensed for the reader. The authors make some very interesting findings, such as the increase in non-burial carbon in the terrestrail reservoir due to the slow-down in respiration" and "there are 5 different ways to achieve an atmospheric pCO2 drop". These findings (mostly in para 2) should be the focus of the abstract, and I advocate for the more technical aspects (para 1) and comparisons with observations (para 3) be removed. In fact, the entire paragraph 3 of the abstract could be reduced to one important sentence without affecting the findings of this study.

Agreed, we will shorten the abstract, highlighting our key conclusions, with brief sentences on comparison against observations, and before this our research problem and aim.
The abstract has been rewritten in the manner described above, and reduced to just one paragraph.

Introduction

• Page 3, Line 13 - "dissolve organic carbon inventory" of what? the ocean? soils? Ocean
We have made the connection to the ocean explicit in the revision: "decreasing dissolved organic carbon inventory due to a more stratified deep ocean"

• Page 3, Paragraph 2 - This entire paragraph simply lists the changes that may be assocaited with a glacial ocean. If these mechanisms are to be called upon by the authors, they should be accompanied by at least a brief discussion of why they influence atmospheric pCO2. For any non-specialist of palaeoceanographic literature specifically relating to the LGM, this paragraph is totally opaque. I would either expand on these mechanisms or remove entirely when accounting for them in the discussion of the results. Agreed, we will briefly describe the referenced mechanisms in the revision.

We have provided brief descriptions of the referenced mechanisms.

• Page 3, Line 19 - "utilises an ensemble of sets of parameters" a bit clunky. What about "uses a large ensemble (471 parameter sets)"? OK, we will include this change in the revision.

This sentence got removed as we re-wrote the introduction.

• Page 3, Line 23 - probably no need to mention Holden (2010a) or cite other literature. Just state philosophy. OK.

We simply state the philosophy in the revised manuscript.

• Page 3, Line 26 - move this to methodology. Not necessary here. Agreed, this would make the message clearer.

We have deleted this section from the revised manuscript.

Methods

• Table 2 - define acronym SAT in caption. What is EFPC2 and EFPC? Must define these here or introduce the Table later on. It is true that the acronyms are difficult to remember and we will change EFPC2 and EFPC to PI315 and PI471, and also add surface air temperature to the caption.

We have replaced "SAT" with "surface air temperature" in the table. We do not refer to EFPC by any acronym in the revised manuscript and as such no renaming was required. EFPC2 on the other hand is referred to as ENS315 (and as explained above).

• Page 5, Line 5 - please clarify what a closed biogeochemistry system is. Does it mean no interaction between land-ocean-atmosphere-lithorsphere reservoirs? It means $CaCO_3$ weathering and deep sea sediment burial forced into balance, no sediment-ocean interactions. We will clarify this in the revision.

We have clarified this in the revision.

how are these reservoirs initiated in Stage 1? Using the fields from Holden 2013a?

As described above (general comments), the model spins up from its default state and takes the weathering fluxes diagnosed from 25 kyr preindustrial spin-up of Holden et al., 2013a.

• Page 7, Lines 1-3 - I don't think it's useful to mention this. Yes, we agree and will delete the sentences from the revision.

These sentences are excluded from the revised manuscript.

Preindustrial simulations

• Page 7, Line 5 - First of all, it would be helpful to change the title of section 3 to "Results: Preindustrial simulations". OK, we will make the change.

In the revised manuscript, we keep the title of Preindustrial Simulations but the section now is also numbered 3.1 and falls under Section 3. Results and discussion.

• Page 7, Lines 7-12 - Why present results and talk about EFPC ensemble when the authors only use the EFPC2 315-member ensemble? It seems to be an unnecessary inclusion that confuses the reader, rather than helps understanding. I think given the length of this study that it would be helpful to simply cut any inclusion of EFPC 471-member ensemble and simply present the results of the 315-member ensemble.

We use EFPC to refer to both our 471-member ensemble and that of Holden et al., 2013a. Our EFPC ensemble is mentioned in the context of explaining where the EFPC2 ensemble came from, and we subsequently compare the response of the latter ensemble with that of Holden et al., 2013a (Table 2), to verify that the values taken by the eight modern plausibility metrics are similar to their values in Holden et al., 2013a. To avoid confusion in the revision, we will move the details of the "ensemble filtering" to a SI file, alongside Table 2 as suggested below.

For enhanced clarity, we decided to move the details of the ensemble filtering to section 2.3 and move Table 2 to a SI file.

• Table 2 - change "31/12" to 31st Dec. OK, will include in the revision.

We have incorporated the change in the revised manuscript.
In revising Table 2 – we spotted a mistake. Namely, that the values we reported for the Atlantic Overturning stream function maximum and minimum were erroneous. These have been rectified in the revised manuscript.

• Table 2 - change "wt% CaCO3" to "wt% ocean CaCO3" wt% refers to surface sediment wt% . We will clarify in the revision.

The revised manuscript incorporates the above clarification.

• page 7, Lines 15-23 - Tables 2 and 3 could be moved to supplementary material. Table 2 discussion could be reduced to a single sentence saying that the preindustrial simulations of the 315-member ensemble reproduced all aspects of the Holden 2013a simulations. Table 3 discussion could be reduced to note that there was good agreement with observations of ocean carbon inventory, SSTs and sea ice extent relative to known values.
• Based on what I've said above, I suppose that this section could actually be reduced to one paragraph, or completely removed if the authors wished to use address PI conditions via comparisons with LGM conditions in the next section.

Agreed, we will reduce discussion of the results, and move Tables 2 and 3 to a SI file.

The section has been reduced to a couple of sentences and Tables 2 and 3 have been moved to a SI file.

LGM ensemble simulations

• Page 9, Line 7 - "104 ensemble members". Are these presented in yellow in Figure 1? If so, mention it here in the text. Yes, “as shown in yellow in Fig. 1” will be added in the revision.

This section has now been moved to a new section, Section 2.4, titled Ensemble subsets.

• Page 9, Lines 7-16 - These sentences are confusing for the reader. I understood once reading further on in the paragraph that you do not include these processes in the model, and you are saying that their inclusion would push LGM pCO2 decrease even further, which justifies your choice of a -30 ppmv threshold to define a successful solution of LGM conditions. However, this is not clear. Please re-write.

• Page 9, Lines 16-26 - This needs to be moved to the methods section. From how I understand your thinking: lines 5-16 justify your choice of -30 ppmv threshold; lines 16-26 justify your methodology in treating the LGM simulations.

• Page 9, Lines 22-25 - The lower threshold of -60 ppmv should belong with your choice of the -30 ppmv upper limit. discuss these together, not separated by other sentences and concepts.

With regard to the above 3 comments, we will address these jointly through revision of p9 l6-26: firstly describing our ΔCO_2 results, and secondly justifying our choice of ΔCO_2 ranges to focus on. Our general approach to analyzing the results will be laid out in the introduction.

In the revised manuscript, the different ensemble subsets are now described in a new, separate section (Section 2.4).

• Page 9, Lines 28-33 - This is a very interesting results. Why can’t you define the mechanisms that lead or do not lead to the snowball Earth scenario? Surely if you can define a plausible set of mechanisms need to achieve glacial conditions, you can do the same by comparing the 471 PIs, 16 LGMs, and 47 snowballs??? This would mark a significant contribution to the field.

In this paragraph what we were trying to convey, and we will rephrase in the revision, is that in our EFPC2 ensemble we struggle to achieve LGM atmospheric $CO_2 \leq 200$ ppmv (only ~1.6% of simulations). Not included in this ensemble are 47 LGM simulations which completed but which also predicted global annual average SATs between ca. -67.8 and -56.8°C (and which we assumed are the result of global or near-global sea and land ice cover developing in the simulations, i.e. “snowball earth” type conditions). In 96% of these simulations, atmospheric CO_2 drops to ≤ 200 ppmv at least temporarily. We thus hypothesised that the CO_2 and the “snowballing” may be linked. Establishing causal mechanisms would be interesting but analysis of stage 3 CO_2 time series suggests that the CO_2 is far from equilibrium in many of the “snowball earth” simulations by 10 kyr. We expect different dynamics to operate in the snowball and non-snowball earth states. We hope to investigate this further in the future, in a separate manuscript.

There are significant complexities here and interpretation is not straightforward, thus we have removed this tangential discussion from the revised manuscript.

• Figure 1 - Overlay red bars on the yellow bars to make 1 panel. We will implement these changes in the revision for this figure, as well as figures 2 and 4 as suggested below.

• Page 11, Line 11 - define SAT . We will specify that SAT means surface air temperature.

In the revised manuscript, SAT is replaced with surface air temperature (SAT).

• Figure 2 - Again, overlay red on yellow to reduce unnecessary replication. Use transparency perhaps to show where yellow and red are both present at the same frequency.

• Page 12, Lines 4-16 - Comparisons with obs not necessary at this detail given the focus of the work and the fact that you use an ESM of intermediate complexity. I would expect a discussion of global temperature changes, with perhaps a little bit of basin-wide, regional discussion if those are important points for later on. Please reduce this paragraph and combine with the next.

We evaluate the spatial distributions of SAT and SST changes as these are likely to influence our CO2 solution through impacts on the solubility pump, land carbon storage etc. We will articulate this more clearly in the revision and make the comparison with observations less detailed to reflect the focus of our work and the complexity of our model. We will also combine SAT and SST evaluations into one paragraph as the two variables are closely linked.

In the revised manuscript, the description is less detailed and SAT and SST changes are dealt with jointly.

• Page 15, Line 5 - I'd say there is no relationship. Our statement of a weak relationship is based on r greater or equal than 0.12, in line with our chosen 0.05 significance level. We will clarify this in the revision.
We clarify our significance level earlier in the manuscript in the revision.

• Page 15, Line 10 - too many adjectives. We will change "The PGACF ensemble LGM global annual sea ice area anomaly (SIA) has a mean of" to "the mean LGM global annual sea ice area anomaly in the PGACF ensemble is"
The revised manuscript now reads "The ENS_{104} mean LGM global annual sea ice area anomaly (ΔSIA) is"

• Figure 4 - overlay red on yellow.

• Page 18, Lines 11-13 - confusing sentence please re-write. What we wanted to convey here is that the observed precipitation decreases are as negative as -1.1 mm in Southern Europe (SE) and Middle East (ME) whereas the ensemble mean decreases are no greater than ~- 0.5 mm in SE and increases of up to +0.1 mm are simulated in ME. We will make the sentences in the precipitation section more concise and also adapt them to better reflect the complexity of model and the focus of our study.

We have reduced the level of detail in the section on precipitation changes.

• Page 19, Lines 11-15 - when talking about AABW formation rates, it is better to present this in positive units. Oceanographers are familiar that the units are negative in the calculation of the streamfunction. It is less confusing for the reader to present your changes as negatives if the AABW formation rate declines. THis also removes the need to explain that a positive anomaly is actually a decrease. Agreed, we will convert our values into negative units in the revision.

• Page 20, Line 2-3 - Don't understand. I thought you said that weaker AMOC and stronger AABW was coincident with the glacial runs, these being PGACF-16? Please make this clearer. WHat are you comparing?

There is a typo in the text which we will fix in the revision. The sentence currently reads: "Although not show here, the PGACF-16 ensemble members tend to exhibit a shoaling of the AMOC and enhanced penetration of AABW. With regard to Δ and Δ, these tend to be more negative (i.e. weaker AMOC and stronger AABW) than in the PGACF-16. The Δ and Δ in the EFPC2 ensemble tend to conversely be more positive".

The second mention of "PGACF-16" should be "PGACF".

We have rectified this in the revised manuscript.

• Page 20, Lines 3-8 - These relationships are made more confusing for the reader because you define AABW formation rates as being stronger when they are negative. It owuld be more helpful if strong = more positive. In the revision, we will make sure that changes and relationships are reported in a way that avoids confusion about direction.

• Page 20, Line 15 - Please see study of Yu et al (2014) Deep ocean carbonate chemistry and glacial-interglacial atmospheric CO2 changes. We will add an appropriate citation.

We reference Yu et al., 2014 at the end of the sentence.

• Page 20, final sentence - This has already been covered above? The relationship between sea ice and ocean circulation changes has already been discussed so we agree that the sentence is somewhat redundant. The aim was simply to point out that CO_2 may have had an impact on the ocean circulation changes as well as vice versa. We will make this clearer in the revision, and also include discussion of the proposed link between Antarctic sea ice expansion and ocean circulation in Ferrari et al., 2014 cited below.

We removed the final sentence from the revised manuscript.

Also, see Ferrari et al (2014) Antarctic sea ice control on ocean circulation in present and glacial climates. PNAS.

• Figure 9 - please ensure that your colour bars are the same scale! I initially thought that your LGM simulation had strong AMOCs, despite the discussion of weaker AMOCs in the text. The scales of the colour bars will be updated as part of the revision.

• Page 23 - Very interesting result. I think that this is a unique and interesting contribution to the field and should be a focus of this study. We will highlight these and other key results by reorganizing the abstract in manner suggested above, and by rewriting conclusions section.

• Table 5 - why does the order change? Please clarify in caption of correct. There is no particular reason for this. For clarity, we will update the table so that column 1 shows $\Delta\mathrm{TerrC}$, column 2 $\Delta\mathrm{OceanC}$ and column 3 $\Delta\mathrm{LithC}$.

We have updated the table in manner described above.

Also,
add the subheadings "Total counts" and "% of total" or their equivalent to the other columns. OK, we will apply the subheadings to all relevant columns in the revision.

The table has been changed in manner described above.

• Table 5 - Please quantify the increases and decreases in this table that accompany the scenarios (i.e. mean). Ok, we will include these in the revised table.

• Page 25, Line 6 - Is table 6 mentioned previously? This introduction of table 6 is jarring. It is indeed mentioned for the first time on line 6. Rather than referring to it at the beginning of a new sentence, we will introduce table 6 more explicitly.

Table 6 now introduced as follows: "The ENS_{104} mean $\Delta\mathrm{TerrC}$, $\Delta\mathrm{OceanC}$ and ΔLithC, the signs of which are consistent with scenario 1, are reported in Table 6, alongside previous estimates from observational data- and model-based studies"

• Table 6 - Great Table. Could the acronyms for studies you cite be organised into alphabetical order? Yes, we will change their order.

The acronyms have been organized in alphabetical order in the revised manuscript.

• Page 25, Lines 9-10 - I'm (and probably many readers) not sure what "Carbonate compensation of the increased terrestrial carbon storage" means. It's not clear whether you refer to carbon compensation mechanism in the land or the ocean. Do you mean a loss in oceanic DIC due to terrestrial carbon storage, causing an increase in alkalinity that increases CaCO3 burial? If changing terrestrial carbon reservoir does have a direct effect on ocean alkalinity and CaCO3 burial, maybe by weathering changes you account for, then please explain more fully.

We mean here carbonate compensation in response to/of the terrestrial carbon uptake: the loss of $\mathrm{CO_2}$ from the ocean leads to an increase in surface $[\mathrm{CO_3^{2-}}]$ and subsequently deep ocean $[\mathrm{CO_3^{2-}}]$, which reduces $\mathrm{CaCO_3}$ dissolution. The latter in turn decreases $[\mathrm{CO_3^{2-}}]$ and increases $[\mathrm{CO_2}]$, which is communicated back to the surface, with a resultant increase in atmospheric CO_2. The modelled change in $CaCO_3$ deep sea burial flux causes ALK to change (Kohfeld and Ridgwell, 2009). We will clarify the above in the revised manuscript.

The term carbonate compensation is not utilized in the revised manuscript but a description of the underlying process is still included.

• Page 25, Line 17 - I find this hard to believe. "The PGACF ensemble mean ΔTerrC is of the same sign and order of magnitude as the ΔTerrC predicted by Zimov et al. (2006, 2009), Zech et al. (2011) and Zeng (2003, 2007). ΔOceanC is not directly calculated in these studies". The issue here is likely with the second rather than first sentence. We will remove the sentence from the revised manuscript as our meaning here was that was not reported in the modelling-based studies, and was not calculated in the observations-based studies.

The sentence "ΔOceanC is not directly calculated in these studies" has been removed from the revised manuscript.

• Page 25, Line 22 - and yet present day continental shelves that are inundated are also regions of effective carbon burial through marine export production. Yes, agreed.

• Tables 7 and 8 - Please make "% Total Land" and its relation to Ice-Sheet carbon more clear in the caption. THis takes time to figure out from the reader. In the revised manuscript, we will change the captions to something like "Ice sheet carbon: amount stored (PgC) and % of total land carbon stock"

As suggested below, Tables 7 and 8 have been combined into one table and this table has been renamed Ice sheet and non-ice sheet terrestrial carbon stocks, and includes a description of each column heading.

• Tables 7 and 8 - I think that these tables could be combined to solely show the LGM changes.

We include Table 7 for 2 reasons: (1) to make it possible to compare our preindustrial ice sheet carbon values with those of previous studies (e.g. Zeng, 2003 or O'ishi and Abe-Ouchi, 2013); (2) to allow estimation of what the impact on ΔCO_2 would have been if this carbon was assumed to be released to the atmosphere as has been done previously (e.g. O'ishi and Abe-Ouchi, 2013). For the revision, we propose combining table 7 and table 8 into one table, but keeping the preindustrial ice sheet carbon inventory column. Columns 3-5 of table 7 can be removed as we do not discuss these in-text.

We combine Tables 7 and 8 in the manner described above, in the revised manuscript.

We also note here that the following sentence will be changed for improved understanding (p27 l1-3): "Analysis of the PGACF-16 ensemble members' terrestrial carbon reservoirs suggests that if the preindustrial ice sheet carbon inventory (the terrestrial biosphere carbon in grid cells to be buried by the LGM ice sheets) were to be destroyed instead of preserved at the LGM, the $\Delta\mathrm{TerrC}$ would be negative in all but 3 simulations (Tables 7 and 8)". What we mean here is that if we did not bury carbon, $\Delta\mathrm{TerrC}$ would be negative in all but 3 simulations. This includes the amount of carbon initially present in ice sheet areas (preindustrial ice sheet carbon inventory) and the subsequent increase in terrestrial carbon over the ice sheet growth period. If only the preindustrial ice sheet carbon inventory was substracted from $\Delta\mathrm{TerrC}$, the latter would be negative in all but 7 simulations. As a reminder, one of the 16 simulations predicts negative $\Delta\mathrm{TerrC}$ to begin with.

The revised manuscript now reads: "However, if this "extra" carbon (accumulated in response to climate forcings), and the carbon already present in the ice sheet areas at the end of the preindustrial spin-up, were to have been destroyed rather than preserved, ΔTerrC would be negative in all but 3 simulations, as opposed to positive in all but one simulation (Tables 7 and 8)."

• Page 27, Lines 1-16 - The relationship between ice-sheet carbon, non-ice sheet carbon and soil burial carbon needs to be made clearer. We will clarify this through the use of subscripts: , , , etc.

We have re-arranged the text on ice sheet vs non-ice sheet carbon changes and this will hopefully make the text easier to read.

• Page 31, Line 7 - re-write sentence please. We re-write the sentence as "The mean LGM total POC export flux anomaly () in the PGACF ensemble is"

The manuscript now reads "The ENS_{104} mean LGM total POC export flux anomaly ($\Delta\mathrm{POC}_{\mathrm{exp}}$) is -0.19 $\pm$ 1 PgC yr^{-1}".

• Page 31, Lines 14-15 - Also the relationship with AABW production and decreased AMOC, which you have just discussed. Agreed, we will update this sentence to include sea ice effects on ocean circulation.

The revised manuscript reads "One possible mechanism is enhanced deep ocean stratification due to increasing AABW formation leading to not only more efficient trapping of DIC at depth (see above), but also nutrients and therefore reduced availability in the euphotic zone. All else held constant, a weaker and shallower AMOC cell would also inhibit the transfer of nutrients from the deep ocean to the surface."

• Page 33, Section 4.5 - This tight description of the main effects is what the other sections should emulate, and would tighten up the manuscript considerably. Agreed. The discussion of spatial changes will be considerably reduced in the revised manuscript.

We reduced the text in other sections but to make section 4.5 more consistent with the other sections, we removed the sentence that says: "The total effect of varying GWS over its full range is ~ 40 ppmv (Fig. 15)", as well as fig. 15.

• Page 35, Line 3 - Again, this sentence is awful to read. Too many adjectives. Agreed. We will replace it with "the mean global deep-sea $\mathrm{CaCO_3}$ burial flux anomaly ($\Delta\mathrm{CaCO3_{bur}}$) in the PGACF ensemble is"

The revised manuscript reads "The $\mathrm{ENS_{104}}$ mean global deep-sea $\mathrm{CaCO_3}$ burial flux anomaly ($\Delta\mathrm{CaCO3_{bur}}$) is".

• Page 36, Line 7 - I don't see a decline in the figure, just no change. The current colour legend indeed makes it difficult to distinguish between no change, small positive and small negative changes. We will center the legend on white and update the text to reflect the plotted changes.

We reduced the level of detail in the comparison against observations, in line with other sections.

Conclusion

• Page 38, Line 26 - A decrease in ocean POC export is not necessarily associated with an increase in atmospheric pCO2. Please see Sigman et al (2010) The polar ocean and glacial cycles in atmospheric CO2 concentration. Nature. for an explanation. Briefly: it is not total POC export, but the efficiency of carbon fixation relative to outgassing that matters. Agreed, we will clarify in the revision that the assumption here is that the impact of our decrease in POC export is not offset by a decrease in the rate at which remineralised carbon is returned to the surface. We will, however, re-discuss potential caveat of no increase in remineralisation depth with decreasing ocean temperature.

In revising the conclusions section, and making it more concise, we removed this section.

• Page 39, Line 13 - Why are you now talking about terrestrial carbon here?
Terrestrial carbon gets mentioned here as we are summarizing our results. However, the text will become easier to follow as we re-write the conclusions section to summarise our research objective, novelties of our approach and then the key conclusions.

• Page 40, Lines 1-11 - Please see Menviel et al (2017) Poorly ventilated deep ocean at the Last Glacial Maximum inferred from carbon isotopes: A data-model comparison study. Paleoceanography.

Here we attempt to broadly reconcile our positive $\Delta\mathrm{TerrC}$ with the mean ocean $\delta^{13}C$ change and do not indeed discuss the spatial distribution of $\delta^{13}C$, which is another useful constraint, as highlighted by the study of Menviel et al., 2017 (and which interestingly suggests weaker, not stronger AABW transport). We will acknowledge this as an added source of uncertainty in the revision.

We have added the following line "A further test would be to compare the simulated spatial distribution of $\delta^{13}C$ with observations (e.g. Menviel et al., 2017)."

• Page 40, Lines 13-14 - But atmospheric _13C at the LGM and preindustrial climates were similar at -6.46 ‰ and -6.36 ‰, respectively.

Agreed. We discuss the role that a glacial increase in terrestrial carbon inventory may have played in the glacial-interglacial $\delta^{13}C$ record but do not attempt to definitely close the $\delta^{13}C$ cycle as a detailed evaluation against observations was not the focus of the paper. In the revision, we will make the similarity between preindustrial and LGM atmospheric $\delta^{13}C$ levels more explicit when discussing the deglacial record.

We have changed the sentence "As discussed in Zeng (2003) the glacial increase in terrestrial carbon inventory may also potentially explain the increase in atmospheric $\delta^{13}C$ over the glaciation, as well as the decrease of about 0.3 ‰ at the beginning of the deglaciation (Smith et al., 1999)." to "As discussed in Zeng (2003) the glacial increase in terrestrial carbon inventory may also potentially explain transient trends in the glacial-interglacal atmospheric $\delta^{13}C$ record, such as the increase in atmospheric $\delta^{13}C$ over the glaciation, and the decrease of about 0.3 ‰ at the beginning of the deglaciation (Smith et al., 1999)"

• Page 40, Line 28 - And what do these new records show?

As above, our aim was not to go into the $\Delta^{14}C$ records in detail but simply acknowledge that there have so far not been attempts to reconcile glacial increases in terrestrial carbon with higher resolution atmospheric CO_2 and $\Delta^{14}C$ deglacial records. These include a significant decline in atmospheric $\Delta^{14}C$ around 14.6 kyr BP, which Köhler et al., 2014 attribute to permafrost thawing in high northern latitudes, as well as possibly flooding of the Siberian continental shelf. Marcott et al., 2014 in turn show that a significant fraction of the deglacial CO_2 rise direct radiative forcing occurred in steps of 10-15 ppm, over less than two centuries, and was followed by no notable change in atmospheric CO_2 for ~1000-1500 years.

• Page 40, Line 30 - The deglacial decrease in atmospheric _14C could also be caused by the exchange of highly negative ocean _14C with the atmosphere. The argument here is not clear.

Our argument here, which we will clarify in the revision is that if ^{14}C-depleted carbon was released from the land to the atmosphere during deglaciation, and subsequently absorbed by the ocean, one might expect to see this signal in ocean Δ^{14}C records. Instead, for the deep ocean at least, we see an increase in Δ^{14}C and the size of the perturbation has been argued to support an overall positive ΔOceanC. Hence, there are potential caveats with the enhanced LGM terrestrial carbon hypothesis. However, we also discuss limitations of Δ^{14}C data: p.41, l5-12.

We have added “a terrestrial biosphere-induced” in front of “early deglacial decrease in atmospheric Δ^{14}C would have also led to a decrease in ocean Δ^{14}C and this is yet to be reconciled with ocean Δ^{14}C data”.

3 Technical corrections

We will revise the manuscript to include the technical corrections below.

1. Page 7, Line 9 - "did not evidence numerical instability" –> "did not show evidence of numerical instability"

2. Page 7, Line 15 - "has" –> "had". Please use past tense in results sections.

3. Page 9, Line 7 - "impact of error" –> "error"

4. Page 9, Line 7 - "impact of certain" –> "certain"

5. Page 9, Line 7 - ", such as changing" –> ", such as changing" (two spaces)

6. Page 15, Line 4 - "thereis" –> "there is"

7. Page 15, Line 15 - "may have for instance" –> "may have"

8. Page 20, Line 21 - "for instance is that" –> "is that"

9. Page 23, Line 3 - "Most of the ensemble members" –> "Most members"

10. Page 26, first line of table - there is a tab separating -1160 from 530.

11. Page 36, Line 11 - double space –> single space

12. Page 38, Line 19 - "Terr" –> "TerrC"

13. Page 38, Line 27 - remove /

The above corrections have been incorporated in the revised manuscript.

Response to referee #3

We thank referee #3 for the constructive comments and suggestions. As above, our replies are in black, and original comments in blue.

This article presents an ensemble of Last Glacial Maximum (LGM) simulations using the GENIE intermediate complexity model with varying parameter values. The model simulates the carbon cycle allowing the authors to compare the CO2 values obtained from the model with the 90 ppm decrease from ice core data and analyses carbon stocks, in addition to the study of climate variables. They select two subsets of simulations with increasing constraints and analyses the changes obtained in these simulations in terms of temperature, precipitation, sea ice, ocean circulation and carbon stocks with respect to the pre-industrial. The CO2 drawdown in most simulations is due to an increase of carbon storage on land and in the lithosphere while the ocean gets depleted in carbon.

Using an ensemble of simulations to study the change of climate and of the carbon cycle during the LGM is a great idea and GENIE is an adequate model as it is fast enough for the long simulations required. However, concerning the carbon cycle part, the lack of carbon isotopes in the simulations prevents any real conclusion to be drawn on the plausibility of the results obtained and the likelihood of the associated mechanisms and carbon stocks changes. As the carbon isotopes are already incorporated within GENIE, providing that this is feasible, I suggest to rerun the simulations and redo the analyses with the isotopes (at least carbon 13) in comparison to data, which is crucial to properly evaluate the results.

As suggested in replies to previous comments, we will clarify our research aim, which was not to explain definitively the causes of CO_2 but rather take an uncertainty-based approach to exploring the physical and biogeochemical changes which may have accompanied the LGM CO_2 decrease. Given our focus, we seek to compare our simulation results with observations only more broadly.

<u>General comments</u>

1. As I said before, the main point is the absence of carbon isotopes which precludes any strong conclusion to be drawn, it would be best to redo the simulations with the carbon isotopes (at least C13, if possible C14) and compare with ocean and atmosphere data to evaluate which simulations are really plausible. How long would this take?

We address this comment in the general response but also note here that spinning up the δ^{13}C of the ocean would take > 100,000 years, and that the model ensemble does not simulate Δ^{14}C and δ^{13}C in the terrestrial biosphere.

2. From the simulations done so far, we can’t know which processes are responsible for the carbon changes, it would be great to have a few additional sensitivity tests (for example taking one set of parameters from the PGACF ensemble) to evaluate the impact of each process on CO2.

We agree that these experiments would be interesting but are not essential to our study, which focuses on the ensemble as a whole rather than the response of individual ensemble members. We also note again here that while this paper describes the relationships between ensemble outputs, the second (related) paper to be submitted describes dependencies on ensemble parameters to isolate mechanisms.

3. In the figures with maps, it would be good to draw the coastlines of continents to make it easier to see where the changes take place. Agreed, we will add these in the revised manuscript.

4. Â´n conversely Â˙z appears 28 times in the manuscript, it could probably be removed or replaced a few times. There seems to be a typo here which precludes understanding?

5. On the bar charts, all ensembles (grey, yellow and orange) could be drawn on the same plot to avoid having two subplots, which would help the comparison between the ensembles and reduce the space taken by figures. Agreed, we will combine all 3 ensembles in the revision.

6. The hypothesis that carbon stays below the ice sheets is a strong one, it could be interesting to evaluate its impact by doing one (or a few) simulations from the PGACF ensemble without carbon kept under ice sheets.

We agree that it would be interesting to test this directly if there were resources for additional simulations. However, we do show how much carbon is stored below the ice sheets in PGACF-16 and from there one can at least try to estimate what the impact of releasing it would have been on CO_2.

Indeed, the LGM burial carbon inventory varies between ~300 and 1300 PgC and if we assume that 90% of the initial atmospheric CO_2 perturbation removed by the oceans and sediments, atmospheric CO_2 would increase by between ~14 and 61 ppmv.

However, it is important to note here (as also emphasized in an earlier reply) that the importance of assumptions regarding what happens to carbon in ice sheet areas depends on how much carbon is there. Our LGM burial carbon estimates include the initial preindustrial carbon inventories, plus carbon accumulated in response to glacial forcings.

Specific comments

p.1-2: The abstract is quite long, and could be better organized, with the problematic explained at the beginning before stating what is the main scientific question raised in this article, how it is raised, and then the main results.

Agreed, the abstract will be reorganized in manner suggested above and reduced to just one paragraph.

The changes to the abstract described above have been implemented.

p. 2-3: Permafrost is not mentioned in the introduction; it would be good to include it.

Yes, thank you, permafrost growth should here be mentioned as a separate mechanism. The text will be revised accordingly.

We have revised the second paragraph of the introduction to include permafrost growth.

It would also be interesting to introduce here which data will be later used to constrain the results.

Agreed. We will include an overview of upcoming sections at the very end of the introduction section, and in this overview describe which model variables will be compared against observations.

We include which variables will be compared against observations/paleo-proxies towards the end of the introduction.

p. 6: During the second stage of the simulations, how does CO2 evolve, does it stay stable? We plotted the evolution of atmospheric CO_2 from stage 1 through 4 in PGACF-16: CO_2 stays stable, except for maybe 3 runs where CO_2 changes by ~< 10 ppmv but then reaches an equilibrium again.

p. 7 l. 12: In the EFPC ensemble, are the simulations at equilibrium at the end of stage 3? What is meant here is probably the EFPC2 ensemble. We again have plots of atmospheric CO_2 and surface sediment %wt $CaCO_3$ for a subset of this ensemble (PGACF-16). Both metrics either in or nearing equilibrium by 10 kyr.

p.7 l.21: The SST value is too high compared to data, how does that compare to other models? Is it in the range?

We deem the mean value (18.9 °C) to be comparable to other previous model-based estimates, in that e.g. Kim et al., 2003 predict modern SST of ~18 °C, Zhang et al., 2012 predict preindustrial SST of 17.1 °C. The range is 16.4 to 21.9 °C, which is potentially larger than the range of previous model-based estimates.

p.7 l.22 The sea ice value is given for the Northern and Southern Hemispheres, how is the comparison with data when split between the North and the South?

Our model is set up to output time series of annual average global sea ice area, 31/12 NH and 31/12 SH sea ice areas. The latter is one of the modern plausibility metrics used in Holden et al., 2013a and as shown in Table 2, our estimates are comparable to those of Holden et al., 2013a.
For 31/12 NH sea ice area, the mean of the EFPC2 ensemble is 15.1 $\pm$ 1.4 million km^2, and the range is 12.6 to 19.2 million km^2. The mean is within the range of typical late winter Arctic sea ice cover today (14-16 million km^2) (NSIDC). Note that the preindustrial NH sea ice extent during the month of maximum (winter) extent simulated by the 13 PMIP2 and PMIP3 models shown in Fig. 4 of Goosse et al., 2013 ranges between ~ 13 and 27 million km^2.

p. 7: The vegetation and soil carbon values are given in table 2 but are not discussed. How does it compare to data ? Is the vegetation distribution ok? Given that it plays an important role in the change of CO2 for the LGM it would be good to know if the preindustrial terrestrial biosphere is well represented or if it has important biases. There is also no discussion of the overturning values given, how does it compare to other models?

We kept discussion of the preindustrial results to a minimum to cut down on the amount of text. It is true that we do not compare any of the values in table 2 (including overturning values) against observations - this is not intentional and we will add a note that there are no major differences between our results (EFPC2) and those of Holden et al., 2013a (EFPC), which meet previously chosen modern plausibility criteria (i.e. modelled values within acceptable distance of observations). We did plot the spatial distribution of vegetation and soil carbon in EFPC2 but did not feel that the discrepancies were large enough to significantly bias our LGM results and therefore did not include the plots in the manuscript. There is however, one potential exception and we mention this on p. 28: "However, it is also noteworthy that, although not shown here, the regions with the largest decreases in terrestrial carbon density, namely northwest North America, Beringia and the Tibetan plateau area, are also the regions with the largest terrestrial carbon densities in the preindustrial simulations". This refers to the terrestrial carbon densities in the EFPC2 ensemble mean and we will clarify in the revision that in the preindustrial EFPC2 ensemble mean: (i) the Tibetan soil carbon peak is overestimated and (ii) the North American soil carbon peak misplaced (compared to observations). We attribute (i) to the lack of soil weathering in the model and the inclusion of land use effects in the observational data-based estimate (Holden et al., 2013b; Williamson et al., 2006). We attribute (ii) to the lack of explicit representation of permafrost (instead the model only attempts to capture the soil respiration rates characteristic of permafrost by utilising a distinct soil respiration temperature sensitivity for land temperatures below freezing) (Williamson et al., 2006) and the absence of moisture control on soil respiration.

We add the above clarification to our description of terrestrial carbon changes, and also include the following: "Comparison of the preindustrial response of ENS_{315} (i.e. the original, non-ΔCO_2 filtered ensemble) against the preindustrial ensemble response of Holden et al., 2013a confirms that the two are very similar."

p. 9 l. 28-29 I'm not sure I understand or agree with this sentence as the simulations are for the LGM and not the other glacial maxima in terms of orbital parameters.
Agreed, conclusions we draw for the LGM may not be generalizable to other glacial maxima. We will rephrase this in the revision.

p. 10 figure 1: maybe replace PRE by PI and explain it somewhere: Pre-industrial (PI).
We consistently use PRE to denote preindustrial but can change this to PI for improved understanding.

We kept the PRE denotation for consistency in the revised manuscript.

p. 11 l.10 and following: Could you use temperature and salinity data to select ensemble members that are supported by data?
Although a useful suggestion, it goes against our approach of looking at the ensemble more widely and not putting too much emphasis on individual ensemble members/strongly constraining these. This will be clarified in the revised introduction, which will help understand the current presentation of results.

The introduction has been rewritten to reflect the above.

p. 15 line 10: how does sea ice distribution compare with data?

As mentioned above, our model is set up to output time series of 31/12 NH and 31/12 SH sea ice areas, and we also have maps of the annual average spatial distribution of sea ice. There are no obvious observation-based estimates to compare the latter against, or 31/12 NH sea ice area. For 31/12 SH sea ice area, our estimates can be compared against the estimates of Gersonde et al., 2005 and Roche et al., 2012. In the first study, LGM summer sea ice extent is estimated to have increased by between 1-2 million km^2, which is much smaller than our PGACF ensemble mean of 11.4 $\pm$ 6 million km^2, and falls outside of our 3 to 32.6 million km^2 PGACF ensemble range. However, as noted in Gersonde et al., 2005, major uncertainties concern the reconstruction of summer sea ice extent. Roche et al., 2012 predict increases in LGM summer sea ice extent between ~2 and 12 million km^2. We also note here that based on Fig. 4 in Goosse et al., 2013, the LGM change in SH sea ice extent during the month of minimum (summer) extent predicted by the 13 PMIP2 and PMIP3 models ranges between ~ -3 and 25 million km^2.

To estimate how our simulated 31/12 NH sea ice compares with data, we will, in the revision, compare our LGM change in the annual average spatial distribution of sea ice with reconstructed changes in winter and summer sea ice extents in the NH. We note here, however, that the mean LGM change in NH 31/12 sea ice area in the PGCAF ensemble is 7.3 $\pm$ 2.1 million km^2, and the range is 3.6 million to 13.2 million km^2. For comparison again, based on Fig. 4 in Goosse et al., 2013, the range of estimates predicted by the 13 PMIP2 and PMIP3 models included therein goes from -7 to 4 million km^2.

We also note here an error in the current manuscript: l13-16 p.12. Contrary to our statement, it is unlikely (or at least not more likely than not) that the LGM increase in annual average SH sea ice is underestimated given that the LGM increase in 31/12 SH sea ice lies at the upper end of observed estimates. Winter SH sea ice also here means 31/12 SH sea ice not austral winter sea ice. We will revise the paragraph.

In revising the paragraph to reduce the level of detail in the description of LGM SAT changes (and comparison against observations), we deemed this section to no longer be necessary and removed it.

p. 20 l. 3 Is it really “than in the PGACF-16”? Is this not the ensemble that you are talking about? Thank you, there is a typo, it should indeed say “PGACF”.

We have corrected this in the revision.

p. 20 line 10: NADW instead of AABW? We use the brackets here to mean that expanding AABW cell may restrict the AMOC cell (i.e. the upper cell of the AMOC) to lower depths and expanding AMOC cell may restrict AABW to higher latitudes. We will clarify this in the revised manuscript.

In the revision, we only consider changes in AABW cell strength leading to changes in the AMOC.

Figure 9: It looks like the NADW is stronger for the LGM than the Pre-industrial , while from the text and figure 8 I understood the opposite: : :
We will put the colour bars on the same scale to avoid confusion in the revised manuscript.

Figure 10: could you add the PGACF-16 ensemble? Yes, good suggestion.

p. 23 and following: could you show a map of where the carbon is stored on land ?
We show the spatial distribution of vegetation, soil and total land carbon changes on p.30. As per suggestion of referee #1, we will show the spatial distributions first, then the globally-integrated numbers, in the revised manuscript.

p. 37: the conclusion is long and more descriptive than conclusive, it might be good to re-organize it.

Agreed. We will shorten the current conclusions section, succinctly summarizing the objective of our research and research strengths, and then describe the key conclusions.

The revised conclusion incorporates the above changes.

References

Gersonde, R., Crosta, X., Abelmann, A. and Armand, L.: Sea-surface temperature and sea ice distribution of the Southern Ocean at the EPILOG Last Glacial Maximum - A circum-Antarctic view based on siliceous microfossil records, Quat. Sci. Rev. 24, 869–896, 2005.

Goosse, H., Roche, D.M., Mairesse, A., Berger, M.: Modelling past sea ice changes, Quat. Sci. Rev., 79, pp. 191–206, 2013.

Holden, P. B., Edwards, N. R., Wolff, E. W., Lang, N. J., Singarayer, J. S., Valdes, P. J. and Stocker, T. F.: Interhemispheric coupling, the West Antarctic Ice Sheet and warm Antarctic interglacials, Clim. Past, 6(4), 431–443, doi:10.5194/cp-6-431-2010, 2010b.

Holden, P. B., Edwards, N. R., Müller, S. A., Oliver, K. I. C., Death, R. M. and Ridgwell, A.: Controls on the spatial distribution of oceanic δ13CDIC, Biogeosciences, 10(3), 1815–1833, doi:10.5194/bg-10-1815-2013, 2013a.

Holden, P. B., Edwards, N. R., Gerten, D. and Schaphoff, S.: A model-based constraint on CO2 fertilisation, Biogeosciences, 10(1), 339–355, doi:10.5194/bg-10-339-2013, 2013b.

Kim, S.-J., Flato, G. and Boer, G.: A coupled climate model simulation of the Last Glacial Maximum, Part 2: approach to equilibrium, Clim. Dyn., 20(6), 635–661, doi:10.1007/s00382-002-0292-2, 2003.

Kohfeld, K. E. and Ridgwell, A.: Glacial-Interglacial Variability in Atmospheric CO2, Surf. Ocean. Atmos. Process., 251–286, doi:10.1029/2008GM000845, 2009.

Köhler, P., Knorr, G. and Bard, E.: Permafrost thawing as a possible source of abrupt carbon release at the onset of the Bølling/Allerød, Nat. Commun., 5, doi:10.1038/ncomms6520, 2014.

Marcott, S. A., Bauska, T. K., Buizert, C., Steig, E. J., Rosen, J. L., Cuffey, K. M., Fudge, T. J., Severinghaus, J. P., Ahn, J., Kalk, M. L., McConnell, J. R., Sowers, T., Taylor, K. C., White, J. W. C. and Brook, E. J.: Centennial-scale changes in the global carbon cycle during the last deglaciation, Nature, 514(7524), 616–619, doi:10.1038/nature13799, 2014.

O'Ishi, R. and Abe-Ouchi, A.: Influence of dynamic vegetation on climate change and terrestrial carbon storage in the Last Glacial Maximum, Clim. Past, 9(4), 1571–1587, doi:10.5194/cp-9-1571-2013, 2013.

Ridgwell, A.: Examples for cGENIE: 'muffin' pre-release version. January 5, 2017. http://www.seao2.info/cgenie/docs/cGENIE.muffin.Examples.pdf

Roche, D. M., Crosta, X. and Renssen, H.: Evaluating Southern Ocean sea-ice for the Last Glacial Maximum and pre-industrial climates: PMIP-2 models and data evidence, *Quat. Sci. Rev.* **56,** 99–106, 2012.

Williamson, M. S., Lenton, T. M., Shepherd, J. G. and Edwards, N. R.: An efficient numerical terrestrial scheme (ENTS) for Earth system modelling, Ecol. Modell., 198(3–4), 362–374, doi:10.1016/j.ecolmodel.2006.05.027, 2006.

Zeng, N.: Glacial-interglacial atmospheric CO2 changes – the Glacial Burial Hypothesis. – Advances in Atmospheric Sciences, 20: 677–693, 2003.

Zhang, Z. S., Nisancioglu, K., Bentsen, M., Tjiputra, T., Bethke, I., Yan, Q., Risebrobakken, B., Andersson, C., and Jansen, E.: Pre-industrial and mid-Pliocene simulations with NorESM-L, Geosci. Model Dev., 5, 523-533, 2012.

Coupled climate-carbon cycle simulation of the Last Glacial Maximum atmospheric CO_2 decrease using a large ensemble of modern plausible parameter sets

Krista M.S. Kemppinen[1], Philip B. Holden[2], Neil R. Edwards[2], Andy Ridgwell[3,4], Andrew D. Friend[1]

[1]Department of Geography, University of Cambridge, Cambridge CB2 3EN, UK
[2]Environment, Earth and Ecosystem Sciences, The Open University, Milton Keynes, MK7 6AA, UK
[3]School of Geographical Sciences, Bristol University, Bristol BS8 1SS, UK
[4]Department of Earth Sciences, University of California, Riverside, California 92521, USA

Correspondence to: Krista M.S. Kemppinen (Krista.Kemppinen@asu.edu)

Abstract. During the Last Glacial Maximum (LGM), atmospheric CO_2 was around 90 ppmv lower than during the preindustrial period. The reasons for this decrease are most often elucidated through factorial experiments testing the impact of individual mechanisms. Due to uncertainty in our understanding of the real system, however, the different models used to conduct the experiments inevitably take on different parameter values, and different structures. In this paper, the objective therefore, is to take an uncertainty-based approach to investigating the LGM CO_2 drop by simulating it with a large ensemble of parameter sets, designed to allow for a wide range of large-scale feedback response strengths. Our aim is not to definitely explain the causes of the CO_2 drop but rather explore the range of possible responses.~~Despite years of research, however, the exact mechanisms leading to the glacial atmospheric CO_2 drop are still not entirely understood. Here, a large (471-member) ensemble of GENIE-1 simulations is used to simulate the equilibrium LGM minus preindustrial atmospheric CO_2 concentration difference (ΔCO_2). The ensemble has previously been weakly constrained with modern observations and was designed to allow for a wide range of large-scale feedback response strengths. Out of the 471 simulations, 315 complete without evidence of numerical instability, and with a ΔCO_2 that centres around -20 ppmv. Roughly a quarter of the 315 runs predict a more significant atmospheric CO_2 drop, between ~30 and 90 ppmv. This range captures the error in the model's process representations and the impact of processes which may be important for ΔCO_2 but are not included in the model. These runs jointly constitute what we refer to as the "plausible glacial atmospheric CO_2 change-filtered (PGACF) ensemble".~~

We find that the LGM CO_2 decrease tends to predominantly be associated with ~~Our analyses suggest that decreasing LGM atmospheric CO_2 tends to be associated with~~ decreasing sea surface temperatures (SSTs), increasing sea ice area, a weakening of the Atlantic Meridional Overturning Circulation (AMOC), a strengthening of the Antarctic Bottom Water (AABW) cell in the Atlantic Ocean, a decreasing ocean biological productivity, an increasing $CaCO_3$ weathering flux, ~~an increasing terrestrial biosphere carbon inventory and~~and an increasing deep-sea $CaCO_3$ burial flux. The majority of our simulations also predict an increase in terrestrial carbon, coupled with a decrease in ocean and increase in lithospheric carbon. ~~The increases in terrestrial~~

~~biosphere carbon are predominantly due to our choice to preserve rather than destroy carbon in ice sheet areas. However, the ensemble soil respiration also tends to decrease significantly more than net photosynthesis, resulting in relatively large increases in non-burial carbon. In a majority of simulations, the terrestrial biosphere carbon increases are also accompanied by decreases in ocean carbon and increases in lithospheric carbon. In total, however, we find there are 5 different ways of achieving a plausible ΔCO_2 in terms of the sign of individual carbon reservoir changes. The PGACF ensemble members also predict both positive and negative changes in global particulate organic carbon (POC) flux, AMOC and AABW cell strengths, and global $CaCO_3$ burial flux.~~

An initial comparison of these dominant changes with observations and paleo-proxies suggests broad agreement. However, a comparison against carbon isotope data would be needed for a more robust assessment.

~~Comparison of the PGACF ensemble results against observations suggests that the simulated LGM physical climate and biogeochemical changes are mostly of the right sign and magnitude or within the range of observational error, except for the change in global deep-sea $CaCO_3$ burial flux – which tends to be overestimated. We note that changing $CaCO_3$ weathering flux is a variable parameter (included to account for variation in both the $CaCO_3$ weathering rate and the un-modelled $CaCO_3$ shallow water deposition flux), and this parameter is strongly associated with changes in global $CaCO_3$ burial rate. The increasing terrestrial carbon inventory is also likely to have contributed to the LGM increase in deep-sea $CaCO_3$ burial flux via the process of carbonate compensation. However, we do not yet rule out either of these processes as causes of ΔCO_2 since missing processes such as Si fertilisation, Si leakage and the effect of decreasing SSTs on $CaCO_3$ production may have introduced a high LGM global $CaCO_3$ burial rate bias. Including these processes would, all else held constant, lower the rain ratio seen by the sediments and result in a decrease in atmospheric CO_2 and increase in ocean carbon. Despite not modelling $\Delta^{14}C_{atm\ (DIC)}$ and $\delta^{13}C_{atm\ (DIC)}$, we also highlight some ways in which our results may potentially be reconciled with these records.~~

1 Introduction

Analyses of Antarctic ice core records suggest that the atmospheric CO_2 concentration at the Last Glacial Maximum (LGM), about 21 kyr ago, was around 190 ppmv, well below the preindustrial atmospheric concentration of around 280 ppmv. The most commonly accepted mechanisms to explain the atmospheric CO_2 decrease include lower sea surface temperatures (Martin et al., 2005; Menviel et al., 2012), iron fertilisation (Bopp et al., 2003; Oka et al., 2011; Jaccard et al., 2013; Ziegler et al., 2013; Martínez-Garcia et al., 2014; Lambert et al., 2015), sea-ice capping of air-sea gas exchange (Stephens and Keeling, 2000; Sun and Matsumoto, 2010; Chikamoto et al., 2012) and ocean circulation/stratification changes (Adkins et al., 2002; Lynch-Stieglitz et al., 2007; Skinner et al., 2010; Lippold et al., 2012; Gebbie, 2014; Skinner et al., 2014; Tiedemann et al., 2015; de la Fuente et al., 2015; Freeman et al., 2015), due to a range of possible mechanisms such as increased brine rejection (Shin et al., 2003; Bouttes et al., 2010, 2011; Zhang et al., 2013; Ballarotta et al., 2014), a shift in/weakening of the westerly wind belt over the Southern Ocean (Toggweiler et al., 2006; Anderson et al., 2009; Völker and Köhler, 2013), stronger westerly winds over the North Atlantic (Muglia and Schmittner, 2015), and a reduced or reversed buoyancy flux from the atmosphere to the ocean surface in the Southern Ocean (Watson and Garabato, 2006; Ferrari et al., 2014). A process that is conversely assumed to have contributed to increasing atmospheric CO_2 is increasing salinity and ocean total dissolved inorganic carbon (DIC) concentration in response to decreasing sea level (Ciais et al., 2013).

A dominant assumption is also that the terrestrial biosphere carbon inventory was reduced (Crowley et al., 1995; Adams and Faure, 1998; Ciais et al., 2012; Peterson et al., 2014), in line with independent estimates of an ocean carbon inventory that was enhanced by several hundred petagrams (Goodwin and Lauderdale, 2013; Sarnthein et al., 2013; Allen et al., 2015; Skinner et al., 2015; Schmittner and Somes, 2016). The decrease in terrestrial carbon is generally attributed to unfavourable climatic conditions for photosynthesis, and the destruction of organic material by moving ice sheets (e.g. Otto et al., 2002; Prentice et al., 2011; Brovkin et al., 2012; O'ishi and Abe-Ouchi, 2013). The hypothesis that there was an increase in terrestrial carbon has, however, also been put forward (e.g. Zeng, 2003; Zimov, 2006), with some studies additionally suggesting little net change (e.g. Brovkin and Ganopolski, 2015). Processes proposed to be responsible for the terrestrial carbon increase include growth in 'inert' or permafrost carbon, slower 'active' soil respiration rates~~slower soil respiration rates~~, continental shelf regrowth, and the preservation rather than destruction of terrestrial biosphere carbon in areas to be covered by the expanding Laurentide and Eurasian ice sheets (Weitemeyer and Buffett, 2006; Franzén and Cropp, 2007; Zeng et al., 2007; Zimov et al., 2009; Zech et al., 2011).

Other mechanisms which may have affected the LGM atmospheric CO_2 change include changes in carbonate weathering rate, through its control on the ocean ALK:DIC ratio and consequently the solubility of CO_2 (Munhoven, 2002; Jones et al., 2002; Foster and Vance, 2006; Vance et al., 2009; Brovkin et al., 2012; Crocket et al., 2012; Lupker et al., 2013; Simmons et al., 2016), decreasing dissolved organic carbon inventory due to a more stratified deep ocean ~~dissolved organic carbon inventory~~ (Ma and Tian, 2014), reduced shallow water carbonate deposition, which has the opposite impact of increased carbonate weathering rates (Opdyke and Walker, 1992; Kleypas et al., 1997; Brovkin et al., 2007), reduced marine bacterial metabolic rate in response to lower ocean temperatures, which acts to decrease the return rate of DIC from the remineralisation of organic material (Matsumoto et al., 2007; Roth et al., 2014), silicic acid leakage, or the leaking out of silicic acid trapped in the Southern Ocean to fuel diatom production, and hence potentially enhancing the uptake of CO_2 (Matsumoto et al., 2002, 2014), Si fertilisation or the fertilization of diatom productivity in response to increased Si inventory (Harrison, 2000; Tréguer and Pondaven, 2000) and increased oceanic PO_4 inventory~~.~~, due to e.g. lower sea level, alleviating the PO_4 limitation on marine production (Tamburini and Follmi, 2009; Wallmann, 2014, 2015).

Mechanisms put forward to explain the LGM atmospheric CO_2 decrease arise from paleo-data and model studies. The latter most often involve factorial experiments, introducing mechanisms one at a time. There is rarely any investigation of the impact of alternative assumptions regarding parameter values or model structure. Here, our aim is conversely to take an uncertainty-based approach to investigating the LGM CO_2 drop by simulating it with a large ensemble of parameter sets designed to allow for a wide range of large-scale feedback response strengths (Holden et al., 2013a). The objective is not to definitely explain the causes of the CO_2 drop but rather explore the range of possible responses. By *responses* we mean physical and biogeochemical changes in the Earth System (e.g. change in global particulate organic carbon export flux) and how these might be linked to ΔCO_2 and to each other, rather than specific mechanisms (e.g. iron fertilisation). In this study, we furthermore seek to simulate the LGM atmospheric CO_2 drop with the simulated CO_2 feeding back to the simulated climate, which is still infrequently done in LGM CO_2 experiments, and the first time it is done with GENIE-1. Moreover, rather than assuming that terrestrial carbon gets destroyed by the LGM ice sheets, we assume that it gets gradually buried. This assumption has not yet been implemented in an equilibrium set-up.

Formatted: English (United States)

~~To investigate the causes of the LGM atmospheric CO_2 drop, this study utilises an ensemble of sets of parameters which are thought to contribute to variability of atmospheric CO_2 on glacial/interglacial timescales. The ensemble is a modified version of the emulator-filtered plausibility-constrained (EFPC) ensemble of Holden et al. (2013a), using the GENIE-1 EMIC, in its coupled climate-carbon cycle configuration. The philosophy behind the design of the ensemble was initially outlined in Holden et al. (2010a): by applying only weak constraints to the ensemble parameters and the modern climate states accepted as plausible, a wide range of large-scale feedback response strengths is allowed for, in an attempt to encompass the range of behaviour exhibited by higher-resolution multi-model ensembles (Holden et al., 2010a; Edwards et al 2011; Holden et al., 2013a). It is recognised, however, that what constitutes an implausible or plausible climate state is somewhat subjective, and that not all sources of model uncertainty, such as the unknown error due to interacting ice sheets and ocean circulation, or the unknown error due to potential ΔCO_2 mechanisms not included in the model (although see below for some estimates), are accounted for.~~

Despite our ensemble varying many of the parameters thought to contribute to variability in glacial-interglacial atmospheric CO_2, not all sources of uncertainty can be captured, and this is reflected in our simulated ΔCO_2 distribution. We estimate that up to ~60 ppmv of ΔCO_2 could be due to processes not included in our model and error in our process representations (see section 2.4 for details). We thus treat simulations with ΔCO_2 between ~-90 and -30 ppmv as "equally plausible", and focus on describing the physical and biogeochemical changes seen in this subset. We also do an initial assessment of how the subset mean and/or dominant (in terms of sign) responses compare against observations and paleo-proxies, including temperature, sea ice, precipitation, AMOC & AABW cell strengths, terrestrial carbon, ocean carbon, particulate organic matter export and deep-sea $CaCO_3$ burial.

Finally, to test the robustness of relationships derived from the analysis of the ensemble subset with ΔCO_2 between ~-90 and -30 ppmv, we briefly compare the physical and biogeochemical changes seen therein with the changes seen in the ensemble with no ΔCO_2 filter, and the ensemble with a more negative ΔCO_2 filter (~-90 to -60 ppmv) (section 2.4). In general, the same dominant relationships between ΔCO_2 and the physical and biogeochemical changes are observed as in the subset with ΔCO_2 between ~-90 and -30 ppmv. In the case of the ensemble subset with ΔCO_2 between -90 and -60 ppmv, we additionally look at what proportion of the total terrestrial carbon change comes from within the ice sheet areas, and from there draw conclusions for the rest of the ensemble.

The paper is organised as follows. The introduction section, Section 1, is followed by Section 2, which describes the model, the ensemble, the simulation set-up and the ensemble subsets to be analysed. Section 3 is the results and discussion section, which includes a brief evaluation of the preindustrial (control) spin-up simulation to verify reproducibility of Holden et al., 2013a. The majority of the section is devoted to the LGM simulation: namely, diagnosis of the physical and biogeochemical changes (including potential causal relationships) seen in the subset with ΔCO_2 between ~-30 and -90 ppmv, and to a lesser extent, the ensemble with both more and less constrained ΔCO_2. Comparison of the first subset against observations and paleo-proxies is also included. Section 4 provides the key conclusions.

2 Methods

2.1 The model

The GENIE-1 configuration is as described in Holden et al. (2013a). The physical model consists of a three-dimensional frictional geostrophic ocean model (GOLDSTEIN) coupled to a thermodynamic/dynamic sea ice model (Edwards and Marsh, 2005; Marsh et al., 2011) and a two-dimensional Energy-Moisture Balance Model (EMBM). Atmospheric tracers are a sub-component of the EMBM, with a simple module (ATCHEM) used to store the concentration of atmospheric gases and their relevant isotopic properties (Lenton et al., 2007). The model land surface physics and terrestrial carbon cycle are represented by ENTS (Williamson et al., 2006). The ocean biogeochemistry model (BIOGEM) is as described in Ridgwell et al. (2007) but includes a representation of iron cycling (Annan and Hargreaves, 2010), and the biological uptake scheme of Doney et al. (2006). The model sediments are represented by SEDGEM (Ridgwell and Hargreaves, 2007). GENIE-1 also includes a land surface weathering model, ROKGEM (Colbourn, 2011), which redistributes prescribed weathering fluxes according to a fixed river-routing scheme. The model is on a 36 x 36 equal-area horizontal grid, with 16 vertical levels in the ocean.

2.2 The ensemble

The GENIE-1 ensemble consists of 471 parameter sets, varying 29 key model parameters over the ranges in Table 1. It derives from the 471-member EFPC ensemble of Holden et al. (2013a), which varies 24 active parameters and 1 dummy parameter (as a check against over-fitting). The parameter values in Holden et al. (2013a) were derived by building emulators of eight preindustrial climate metrics and applying a rejection sampling method known as approximate bayesian computation (ABC) to find parameter sets that the emulators predicted were modern plausible. Two parameters were later added to the EFPC ensemble in Holden et al. (2013b) to describe the un-modelled response of clouds to global average temperature change (OL1), and the uncertain response of photosynthesis to changing atmospheric CO_2 concentration (VPC). We add two further parameters here that represent uncertain processes specific to the LGM. The first (FFX) scales ice-sheet meltwater fluxes to account for uncertainty in un-modelled isostatic depression at the ice-bedrock interface due to ice sheet growth, and for assuming a fixed land-sea mask (Holden et al., 2010b) We vary the parameter in the ensemble to capture the uncertainty in the magnitude of the glacial sea level drop and its effects on the carbon cycle. ~~(Holden et al., 2010b).~~ The second (GWS) scales the global average carbonate preindustrial weathering rates for the LGM, to account for uncertainty in carbonate weathering and un-modelled shallow water carbonate deposition rate changes. For both FFX and GWS, uniform random values were derived using the generation function runif in R.

Table 1. Ensemble parameters. Ranges are from (a) Holden et al. (2013a), (b) Holden et al. (2013b), and (c) Holden et al. (2010b), with the exception of GWS (see main text). The table also precludes the dummy parameter.

Module	Code	Description	Range	Ref.
EMBM	AHD	Atmospheric heat diffusivity (m^2 s^{-1})	1118875 to 4368143	a
	AMD	Atmospheric moisture diffusivity (m^2 s^{-1})	50719 to 2852835	a
	APM	Atlantic-Pacific moisture flux scaling	0.1 to 2.0	a
	OL0	Clear skies OLR reduction (W m^{-2})	2.6 to 10.0	a
	OL1	OLR feedback (W m^{-2} K^{-1})	-0.5 to 0.5	b

GOLDSTEIN	OHD	Isopycnal diffusivity ($m^2\ s^{-1}$)	312 to 5644	A
	OVD	Reference diapycnal diffusivity ($m^2\ s^{-1}$)	0.00002 to 0.0002	a
	OP1	Power law for diapycnal diffusivity depth profile	0.008 to 1.5	a
	ODC	Ocean inverse drag coefficient (days)	0.5 to 5.0	a
	WSF	Wind scale factor	1.0 to 3.0	a
	FFX	Freshwater flux scaling factor	1.0 to 2.0	c
SEA-ICE	SID	Sea ice diffusivity ($m^2\ s^{-1}$)	5671 to 99032	a
ENTS	VFC	Fractional vegetation dependence on vegetation carbon density ($m^2\ kgC^{-1}$)	0.4 to 1.0	a
	VBP	Base rate of photosynthesis ($kgC\ m^{-2}\ yr^{-1}$)	3.0 to 5.5	a
	VRA	Vegetation respiration activation energy ($J\ mol^{-1}$)	24211 to 71926	a
	LLR	Leaf litter rate (yr^{-1})	0.08 to 0.3	a
	SRT	Soil respiration activation temperature (K)	198 to 241	a
	VPC	Photosynthesis half-saturation to CO_2 (ppmv)	30 to 697	b
BIOGEM	PHS	PO_4 half-saturation concentration ($mol\ kg^{-1}$)	5.3e-8 to 9.9e-7	a
	PRP	Initial proportion of POC export as recalcitrant fraction	0.01 to 0.1	a
	PRD	e-folding remineralisation depth of non-recalcitrant POC (m)	106 to 995	a
	RRS	Rain ratio scalar	0.02 to 0.1	a
	TCP	Thermodynamic calcification rate power	0.2 to 2.0	a
	PRC	Initial proportion of $CaCO_3$ export as recalcitrant fraction	0.1 to 1.0	a
	CRD	e-folding remineralisation depth of non-recalcitrant $CaCO_3$ (m)	314 to 2962	a
	FES	Iron solubility	0.001 to 0.01	a
	ASG	Air-sea gas exchange parameter	0.1 to 0.5	a
ROKGEM	GWS	Land-to-ocean bicarbonate flux scaling factor	0.5 to 1.5	n/a

2.3 Experimental set-up of the model

The preindustrial ensemble simulation results were repeated to verify reproducibility of Holden et al. (2013a). ~~The plausibility metrics are summarised in Table 2.~~ The simulations were performed in two stages, each lasting 10 kyr, on the Cambridge High Performance Computing (HPC) Cluster Darwin. The first stage involved spinning up the model with atmospheric CO_2 concentration relaxed to 278 ppmv and a closed biogeochemistry system. This means that there are no sediment-ocean interactions and the model forces the $CaCO_3$ weathering and deep sea sediment burial rates into balance. An initial $CaCO_3$ weathering is initially prescribed but this is subsequently rescaled internally to balance the modelled $CaCO_3$ burial rate and conserve alkalinity~~The $CaCO_3$ weathering flux is diagnosed in the model to balance the modelled $CaCO_3$ burial rate and conserve alkalinity~~. In the second stage, atmospheric CO_2 was allowed to evolve freely, with interacting oceans and sediments, and the $CaCO_3$ weathering rate is set equal to the $CaCO_3$ burial rate diagnosed from the end of stage 1.~~In the second stage, atmospheric CO_2 was allowed to evolve with interacting oceans and sediments, applying a fixed $CaCO_3$ weathering rate~~

~~diagnosed from the end of stage 1~~. To allow the sediments to reach equilibrium as fast as possible, no bioturbation was modelled in either stage 1 or stage 2.

Each parameter set was then applied to LGM simulations. The modelled preindustrial equilibrium states were used as initial conditions and the ensemble members were integrated for 10 kyr, with freely evolving CO_2. These 10 kyr simulations are variously referred to here as the "LGM equilibrium simulation" or "stage 3", and the LGM equilibrium state refers to the end of stage 3 (see S1 for more details).~~, unless otherwise specified~~. ~~Thus, ΔCO_2, for example, corresponds to end of stage 3 minus end of stage 2 atmospheric CO_2 concentration. The ensemble was integrated for another 10 kyr after stage 3 (yielding 20 kyr of LGM climate in total) to simply verify, by analysing a subset of the ensemble, that the sediments (being the slowest component in the model) were in equilibrium by 10 kyr. These next 10 kyr of LGM simulation are referred to as "stage 4".~~ After application to stages 2 and 3, the original 471 ensemble members were filtered to 315 ensemble members to exclude those simulations with a stage 2 atmospheric CO_2 concentration outside of the range 268 to 288 ppmv (c.f. Prentice et al., 2001), which entered a snowball Earth state in stage 3 or which showed evidence of numerical instability (c.f. Holden et al., 2013b).

Boundary conditions applied in the LGM simulations included orbital parameters (Berger, 1978) and aeolian dust deposition fields (Mahowald et al., 2006). The atmospheric CO_2 used in the radiative code is internally generated, rather than prescribed but the radiative forcing from dust, and gases other than CO_2 was neglected. The model also requires a detrital flux field to the sediments, containing contributions from opal and material from non-aeolian sources (Ridgwell and Hargreaves, 2007). ~~The representation of the ice sheets is as described in Holden et al. (2010b), using the terrestrial ice sheet fraction and orography from the ICE-4G reconstruction of Peltier (1994). Rather than initialising the ensemble with the ice sheet extent and orography at 21 kyr BP, the ice sheets are configured to grow from their preindustrial to LGM extent in 1 kyr, at the beginning of the LGM simulation (i.e. years 0-1 kyr) in order to account for the impact of sea level change on ocean tracers. An important assumption is that the preindustrial terrestrial carbon is preserved beneath the LGM ice sheets, though it is allowed to interact with the atmosphere prior to burial. Sensitivity simulations were performed to verify the simulated equilibrium state is insensitive to the choice of timescale of ice-sheet growth.~~ Weathering fluxes from the preindustrial simulation were applied, scaled by GWS.

The representation of the ice sheets is as described in Holden et al. (2010b), using the terrestrial ice sheet fraction and orography from the ICE-4G reconstruction of Peltier (1994). Rather than initialising the ensemble with the ice sheet extent and orography at 21 kyr BP, the ice sheets are configured to grow from their preindustrial to LGM extent in 1 kyr, at the beginning of the LGM simulation (i.e. years 0-1 kyr) in order to account for the impact of sea level change on ocean tracers. Following Holden et al. (2010b), only the Laurentide and Eurasian Ice Sheets are allowed to change from their preindustrial form (accounting for ~ 80% of global ice sheet change), and we also route the freshwater to build the ice sheets from the Atlantic, Pacific and Arctic, assuming modern topography, rather than extracting it uniformly.~~An important assumption is that the preindustrial terrestrial carbon is preserved beneath the LGM ice sheets, though it is allowed to interact with the atmosphere prior to burial. Sensitivity simulations were performed to verify the simulated equilibrium state is insensitive to the choice of timescale of ice-sheet growth.~~

As discussed in the introduction, the preindustrial terrestrial carbon is preserved underneath the LGM ice sheets, and allowed to interact with the atmosphere prior to its burial. To determine how sensitive the burial carbon amount is to the duration of ice sheet build-up, we test the impact of varying the latter from 1000 to 10,000 years for one ensemble member (extending the total simulation length to 11,000 years). Our assumption is that if the difference is negligle, applying the same ensemble member to a transient simulation of the full glacial cycle (and therefore a more realistic ice sheet build-up history) would not have yielded a dramatically different burial carbon inventory. We find that increasing the ice sheet build-up duration indeed changes the burial carbon amount only marginally (~34 PgC). A limitation, however, is that we do not have a way of testing if other ensemble members may be more sensitive. If one expects the sign of their response to be the same, more sensitive here means more carbon, not less, buried underneath the ice sheet.

~~A distinctive feature of the simulations is that the atmospheric CO_2 used in the radiative code is internally generated, rather than prescribed as in e.g. Tagliabue et al. (2009); Bouttes et al. (2011); Brovkin et al. (2012); Brovkin and Ganopolski (2015); Crichton et al. (2016). The radiative forcing from dust, and gases other than CO_2 was neglected.~~

~~An error in the experimental set-up precludes analysis of simulated carbon isotope tracers. We acknowledge that an evaluation of the simulated $\Delta^{14}C_{atm\ (DIC)}$ and $\delta^{13}C_{atm\ (DIC)}$ against observations would have provided useful constraints (see discussion in conclusions section).~~

2.4 Ensemble subsets

Although our ensemble varies many of the parameters thought to contribute to variability in glacial-interglacial atmospheric CO_2, not all sources of uncertainty can be captured. We estimate that up to ~60 ppmv of ΔCO_2 could be due to error in our process representations and processes not included in our model, such as changing marine bacterial metabolic rate, wind speed (via its effect on gas transfer) and Si fertilization. This is not a comprehensive assessment, however, as our model also does not include processes such as the effect of changing winds on ocean circulation (Toggweiler et al., 2006), Si leakage (Matsumoto et al., 2002, 2013, 2014), the effect of decreasing SSTs on $CaCO_3$ production (Iglesias-Rodriguez et al., 2002), or changing oceanic PO_4 inventory (Menviel et al., 2012). We focus our analyses on the subset of the ensemble with ΔCO_2 between ~-90 and -30 ppmv (Table 2), treating each ensemble member in this range as equally plausible. To test the robustness of diagnosed relationships, we also briefly compare the reponse of this subset with the response of the ensemble with no ΔCO_2 filter, and the response of the ensemble with a more negative ΔCO_2 filter. In the latter case, the upper ΔCO_2 limit is set to ~-60 ppmv, roughly equivalent to allowing for an extra atmospheric CO_2 decrease due to changing marine bacterial metabolic rate, wind speed (via its effect on gas transfer) and Si fertilization, between the best and upper estimate of Kohfeld and Ridgwell (2009). The ΔCO_2 distribution in each subset or ensemble is shown in Fig. 1.

Table 2. Ensemble subsets, including ΔCO_2 and number of members in each.

Ensemble	ΔCO_2 range (ppmv)	Number of members
ENS_{315}	-88 to 74	315
ENS_{104}	-88 to -30	104
ENS_{16}	-88 to -59	16

(a) (b)

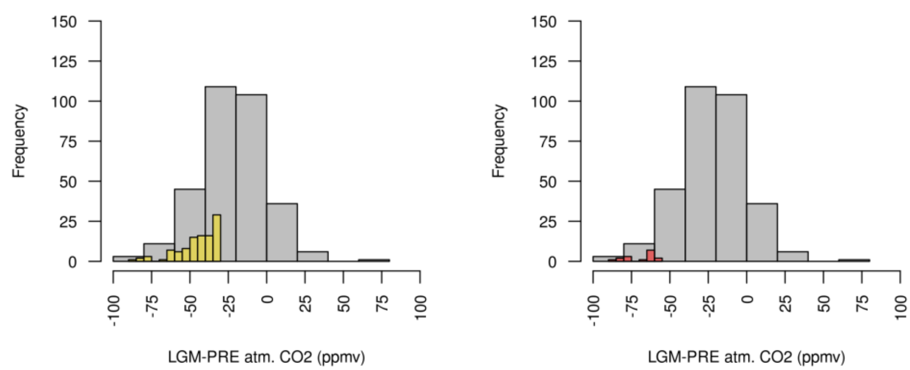

Fig. 1. LGM change in atmospheric CO_2 (a-b) distribution. The ENS_{315} response is shown in grey, the ENS_{104} ensemble response in yellow and the ENS_{16} ensemble response in purple. Unless otherwise specified, the same colour legend applies to all figures in the manuscript.

3 Results and discussion

3.1 Preindustrial simulations

~~3 Preindustrial simulations~~

~~3.1 Ensemble filtering~~

~~After application to stages 2 and 3, the 471-member ("EFPC") ensemble was filtered to 315 simulations, being those with a stage 2 atmospheric~~ $\cancel{CO_2}$ ~~concentration in the range 268 to 288 ppmv (c.f. Prentice et al., 2001), which did not enter a snowball Earth state in stage 3 and which did not evidence numerical instability (c.f. Holden et al., 2013b). These 315 simulations comprise the "EFPC2" ensemble, and form the basis of all the results reported in this study, unless otherwise specified. Individual ensemble members are referred to by their "run IDs", corresponding to the 1000 emulator-filtered parameter sets that were originally applied to GENIE-1 (Holden et al., 2013a).~~

~~3.2 Modern plausibility and other global metrics~~

Comparison of the preindustrial response of ENS_{315} (i.e. the original, non-ΔCO_2 filtered ensemble) against the preindustrial ensemble response of Holden et al., 2013a confirms that the two are very similar. We additionally evaluate ENS_{315} against a few additional preindustrial metrics (see S2) and find responses that can be deemed not uncontroversially implausible, following the design principles for the ensemble, outlined in Holden et al., 2013a.

~~EFPC2 preindustrial atmospheric~~ $\cancel{CO_2}$ ~~has a mean concentration of 278.1 ± 1.3 ppmv (standard deviation). The ensemble mean and range for the eight modern climate plausibility metrics are shown in Table 2, and compared against the results of the 471-member EFPC ensemble (Holden et al., 2013a). Metrics are also reported separately for the annual average global ocean carbon inventory, sea surface temperature and sea ice area, and compared with observations (Table 3). The ensemble mean ocean carbon inventory is close to the 36,000 PgC equilibrium preindustrial ocean carbon inventory predicted by GENIE-1 in Lenton et al. (2006), below reconstructed estimates of ca. 38,000 PgC (Houghton et al., 1990), largely attributable to an underestimated ocean volume at our low resolution (Lenton et al 2006). The ensemble mean SST exceeds observations but the error is still comparable to that associated with previous model predictions (e.g. Kim et al., 2003). The ensemble mean sea ice area (SIA) lies within the range of observed estimates.~~

Formatted: English (United States)

Table 2. The EFPC and EFPC2 ensembles modern climate plausibility metrics. The EFPC2 ensemble values are as reported in Holden et al. (2013a), Table 2. All values are annual averages, except for the Antarctic sea ice area, which is the end-of-year value. The ensemble means are presented as the mean plus minus one standard deviation.

	~~EFPC2 Ensemble mean~~	~~EFPC2 Ensemble range~~	~~EFPC Ensemble mean~~	~~EFPC Ensemble range~~
~~Global SAT (°C)~~	~~13.7 ± 1.1~~	~~11.8 to 16.2~~	~~13.6 ± 1.1~~	~~11.7 to 16.2~~
~~Atlantic overturning stream function maximum (Sv)~~	~~16.4 ± 3.8~~	~~4.5 to 27.3~~	~~17.5 ± 3.2~~	~~10.0 to 25.8~~
~~Atlantic overturning stream function minimum (Sv)~~	~~-4.1 ± 1.0~~	~~-6.8 to -0.8~~	~~-4.1 ± 1.0~~	~~-6.8 to -1.0~~
~~31/12 Antarctic sea ice area (million km^2)~~	~~6.7 ± 2.7~~	~~1.2 to 13~~	~~6.8 ± 2.8~~	~~1.2 to 12.9~~
~~Global VegC (PgC)~~	~~499.9 ± 94.5~~	~~328.6 to 765.5~~	~~492 ± 94~~	~~326 to 762~~
~~Global SoilC (PgC)~~	~~1329.7 ± 279.2~~	~~896.1 to 2353.2~~	~~1351 ± 308~~	~~896 to 2430~~
~~wt% $CaCO_3$~~	~~34.4 ± 7.9~~	~~19.1 to 51.5~~	~~34.1 ± 7.8~~	~~20.0 to 50.0~~
~~Global ocean O_2 (μm kg^{-1})~~	~~164.1 ± 19.3~~	~~121.8 to 217.5~~	~~165 ± 20~~	~~117 to 216~~

Table 3. Preindustrial ocean carbon inventory, sea surface temperature and sea ice area. All values are annual averages.

	~~Ensemble mean~~	~~Ensemble range~~	~~Observations~~
~~Global ocean carbon inventory (PgC)~~	~~36056.2 ± 252.4~~	~~35280.5 to 36655.7~~	~~38000~~ ~~Houghton et al. (1990)~~
~~Global sea surface temperature (°C)~~	~~18.9 ± 1.2~~	~~16.4 to 21.9~~	~~15.9~~ ~~NCDC, 2015~~

~~Global sea ice area (million km^2)~~	~~23 ± 4.2~~	~~16.3 to 38.6~~	~~19 to 27 Lemke et al. (2007)~~

3.2~~4~~ LGM ~~ensemble simulations~~simulations

Formatted: English (United States)

~~4.1 Atmospheric carbon dioxide~~

~~The ensemble ΔCO_2 distribution is centered around -20 ppmv, with a range of -88 to 74 ppmv, although the ensemble member corresponding to the latter ΔCO_2 is an outlier (Fig. 1). A more negative ΔCO_2, between ~ -90 and -30 ppmv is achieved by 104 ensemble members. This range roughly accommodates the impact of error in the model's process representations and the impact of certain potentially important ΔCO_2 mechanisms that are missing from the model, such as changing marine bacterial metabolic rate, wind speed (via its effect on gas transfer) and Si fertilization (Kohfeld and Ridgwell, 2009). This is not a comprehensive assessment, however, as our model also does not include processes such as the effect of changing winds on ocean circulation (Toggweiler et al., 2006), Si leakage (Matsumoto et al., 2002, 2013, 2014), the effect of decreasing SSTs on $CaCO_3$ production (Iglesias-Rodriguez et al., 2002), or changing oceanic PO_4 inventory (Menviel et al., 2012). The fact that it is difficult for our model to achieve a ΔCO_2 of ~-90 ppmv without the missing processes is a significant result because of our extensive exploration of model uncertainty when building the model ensemble. Our assumption moving forward is that the role of processes which *are* included in the model add linearly to the missing ones and that our ~ −30 to −90 ppmv ΔCO_2 therefore represents a "plausible" glacial atmospheric CO_2 change. Rather than trying to identify the "best" parameter set in this "plausible glacial atmospheric CO_2 change-filtered (PGACF) ensemble" (Table 4), we investigate what the emergent model output relationships are and what magnitude and direction responses can be observed. This is to avoid focusing on a candidate parameter with potentially the wrong balance of processes. We also compare the behaviour of the PGACF ensemble (with a mean ΔCO_2 of -45±13 ppmv) with that of the EFPC2 ensemble to better understand the emergent relationships. Moreoever, we identify which members in the PGACF ensemble predict ΔCO_2 from the highly negative end of the ensemble range to help diagnose any significant differences in behaviour along the plausible ΔCO_2 spectrum. The lower ΔCO_2 limit for this subset of the PGACF ensemble is ~ -60 ppmv, roughly equivalent to allowing for an extra atmospheric CO_2 decrease due to changing marine bacterial metabolic rate, wind speed (via its effect on gas transfer) and Si fertilization between the best and upper estimate of Kohfeld and Ridgwell (2009). The ensemble members in the subset are referred to collectively as the "PGACF-16" ensemble (Table 4), with the numeral denoting the number of ensemble members.~~

~~We also note here that we have apparently succeeded in reproducing one of the most remarkable properties of the 800-kyear temporal record of CO_2, namely the nearly constant lower bound across different glacial states. There is a significant caveat, however, which is that 47 of the 471 LGM states subsequently diverge to an unrealistic snowball glaciation response to LGM forcing through feedback mechanisms, probably involving low CO_2, that have to be inferred to be unrealistically strong in this context. These simulations have to be rejected, thus it is difficult to draw any firm conclusions regarding the dynamical controls that maintain the constancy of the lower CO_2 bound in the real system.~~

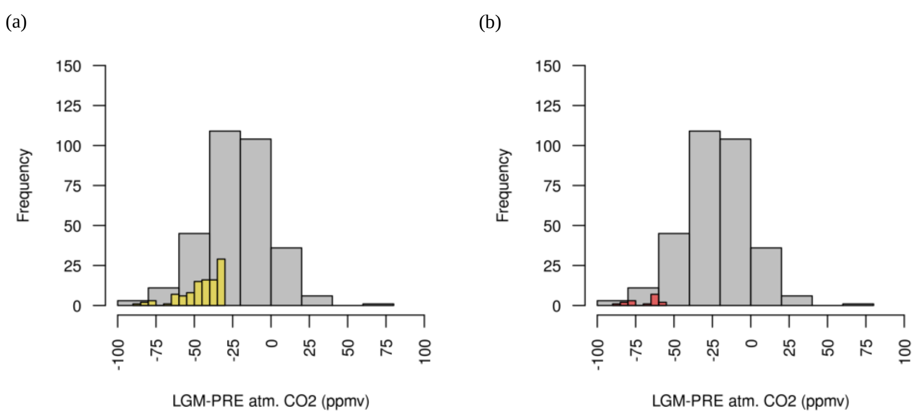

Fig. 1. LGM change in atmospheric CO_2 (a-b) distribution. The EFPC2 ensemble response is shown in grey, the PGACF ensemble response in yellow and the PGACF-16 ensemble response in purple. Unless otherwise specified, the same colour legend applies to all figures in the manuscript.

Table 4. The different ensembles and their ΔCO_2. As discussed in the main text, the EPFC ensemble is the EFPC ensemble of Holden et al. (2013a), which is weakly constrained by modern climate, but includes four additional parameters (that have no effect on modern climate). The EFPC2 ensemble is the same ensemble as EFPC but excludes ensemble members with preindustrial atmospheric CO_2 concentration outside of 268 to 288 ppmv, which entered a snowball Earth state in the LGM simulation, or which evidenced numerical instability. The PGACF is the subset of the EFPC2 ensemble with ΔCO_2 between ~-30 and -90 ppmv, while PGCAF-16 represents those PGCAF ensemble members (16 in total) with ΔCO_2 no higher than ~-60 ppmv.

~~Ensembles~~	~~ΔCO_2 range (ppmv)~~	~~Number of members~~	~~Details~~
~~EFPC~~	~~n/a~~	~~471~~	~~Derived from Holden et al. (2013a)~~
~~EFPC2~~	~~-88 to 74~~	~~315~~	~~Subset of the EFPC ensemble~~
~~PGACF~~	~~-88 to -30~~	~~104~~	~~Subset of the EPFC2 ensemble~~
~~PGACF-16~~	~~-88 to -59~~	~~16~~	~~Subset of the PGACF ensemble~~

3.2.1 ~~4.2~~ Climate, sea level and ocean circulation

Temperature

The ENS_{104} mean LGM surface air temperature (SAT) anomaly (ΔSAT) is -4.6 $\pm$ 1.7, and the range is -2.5 to -10.4 °C. The mean is close to the observed ΔSAT of -4 $\pm$ 1 °C (Annan and Hargreaves, 2013), and the range roughly equivalent to the range of previous model-based estimates (Kim et al., 2003; Masson-Delmotte et al., 2006; Schneider von Deimling et al., 2006; Braconnot et al., 2007; Holden et al., 2010a; Brady et al., 2013). ~~The LGM SAT anomaly (ΔSAT) in the PGACF ensemble varies between -2.5 and -10.4 °C, with a mean of -4.6 $\pm$ 1.7 °C, close to the observed ΔSAT of -4 $\pm$ 1 °C (Annan and Hargreaves, 2013).~~ The ENS_{104} mean LGM SST anomaly (ΔSST) is -1.8 ± 0.8 °C, and the range is -4.5 and -0.7 °C. The mean is again close to an observational data-constrained model estimate (Schmittner et al. (2011), and within the range of estimates inferred from proxy data (MARGO Project Members 2009 in Masson-Delmotte et al., 2013). ~~The LGM SST anomaly (ΔSST) varies between -4.5 and -0.7 °C, with a mean of -1.8 ± 0.8 °C, also close to the -1.7 °C observational data-constrained model~~

~~estimate of Schmittner et al. (2011), and within the -0.7°C to -2.7°C range inferred from proxy data (MARGO Project Members 2009 in Masson-Delmotte et al., 2013).~~ There is a positive correlation between ΔSAT and ΔCO_2 (r = 0.75, 0.05 significance level hereforth), most likely reflecting the radiative impact of atmospheric CO_2 on SAT, as well as the effect of changing SAT on ΔCO_2. As suggested above, decreasing SST may contribute to decreasing CO_2 via the CO_2 solubility temperature dependence. Changing SAT may also affect ΔCO_2 via its effects on sea ice, ocean circulation, terrestrial and marine productivity (see below). The positive correlation is reproduced in ENS_{315} (r = 0.74), and ΔSAT and ΔSST tend to be less negative in ENS_{315} than in ENS_{104} (Fig. 2). In ENS_{16}, ΔSAT and ΔSST are from the extreme or at least lower end of the ENS_{104} range.~~Compared to the EFPC2 ensemble, both the PGACF ensemble ΔSAT and ΔSST tend to be more negative (Fig. 2). There is also a positive correlation between ΔSAT and ΔCO_2 in the PGACF and EFPC2 ensembles (r = 0.75 and 0.74), reflecting the radiative impact of atmospheric CO_2 on SAT, and also potentially the effect of changing SAT on ΔCO_2. As suggested above, decreasing SST may contribute to decreasing CO_2 via the CO_2 solubility temperature dependence. Changing SAT may also affect ΔCO_2 via its effects on sea ice, ocean circulation, terrestrial and marine productivity (see below). In the PGACF-16 ensemble, ΔSAT and ΔSST are from the extreme or at least lower end of the PGACF ensemble range and mostly well below observations. It is thus possible that the contribution of individual temperature-dependent processes to ΔCO_2 may have been distorted in the PGACF-16 ensemble.~~

The ENS_{104} mean ΔSAT and ΔSST spatial distributions are shown in Fig. 3. In line with observations (Annan and Hargreaves, 2013), the largest SAT decreases (> 10 °C) are simulated over the Laurentide and Eurasian Ice Sheets. The equator to pole temperature gradient is also broadly reproduced. The largest SST decreases (≥ 4 °C) are found in the North Atlantic and northeast Pacific, with more limited cooling (≤ -2 °C) in the tropics and polar regions, again consistent with observations. The largest SST decreases ought to, however, also be found in the southern hemisphere mid-latitudes whereas the simulate cooling is more moderate.

~~The PGACF ensemble mean ΔSAT spatial distribution is shown in Fig. 3, and in line with observations (Annan and Hargreaves, 2013), the largest LGM decreases (> 10 °C) are found in North America, coinciding with the Laurentide ice sheet, and in the eastern Atlantic/ northwestern Eurasia region, coinciding with the Eurasian ice sheet. The maximum observed SAT decrease, however, is -20 °C, compared to just -16 °C in the ensemble mean. The simulated temperature changes in the North Pacific range between -4 and -7 °C, roughly consistent with the observed -2 to -8 °C changes. At low latitudes conversely, the Pacific, Atlantic and Indian Ocean SAT decreases in the Northern Hemisphere tend to be larger than in the Southern Hemisphere whereas observations show no such divide. The ensemble mean also does not capture the somewhat larger temperature decreases over low latitude land areas (2 to 4 °C) compared to low latitude ocean areas (1 to 2 °C). Another discrepancy is the underestimation of southern high latitudes SAT decreases, with simulated ΔSATs ranging between -4 and -7 °C, compared to between -4 and -12 °C in observations. At least a fraction of the discrepancy is likely caused by the underestimation of LGM SH sea ice (see below), and which has previously been attributed to excessive atmospheric heat diffusion in GENIE-1 (Lenton~~

~~et al., 2006; Lunt et al., 2006). This is conversely not an issue in the preindustrial ensemble simulations as winter SH sea ice area was used as a constraint during the modern plausibility filtering process (Table 2).~~

~~The PGACF ensemble mean spatial distribution of ΔSST is also shown in Fig. 3, and exhibits the largest decreases (≥ 4 °C) in the North Atlantic and northeast Pacific. The smallest (< 1°C) decreases are conversely found in the polar regions, with ΔSST ranging between -2 and -3 °C in the tropics. These patterns are roughly consistent with the observations (Annan and Hargreaves, 2013) which show ΔSSTs of mostly ≤ -2 °C and ≤ -1 °C in the tropics and polar regions respectively. However, while the ensemble mean polar ΔSSTs are consistently negative, the observed polar ΔSSTs include SST increases of up to 2 °C. The latter can also be observed in the northernmost North Atlantic. In the North Pacific, the ensemble mean ΔSSTs are somewhat underestimated, particularly in the west, with the observed ΔSSTs ranging between -2 and -8 °C. The only exception is the Central Pacific, around 60 °N, where SST increases of up to 1 °C can be found in observations. Cooling across the southern mid-latitudes is more severely underestimated, with simulated ΔSSTs ranging between -2 and -3 °C compared to between -2 to -8 °C in observations.~~

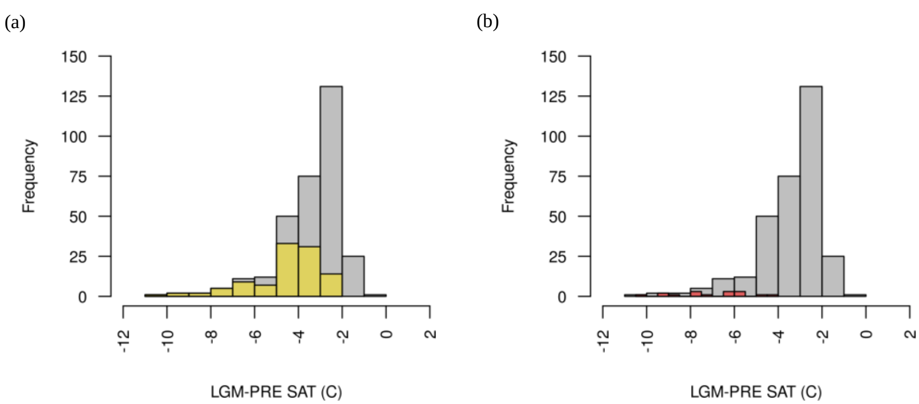

(c)

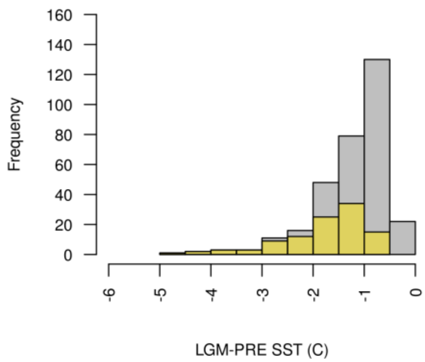

(d)

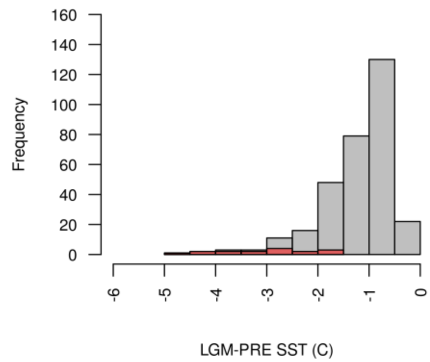

Fig. 2. LGM change in surface air temperature (a-b) and sea surface temperature (c-d) distributions.

(a)

(b)

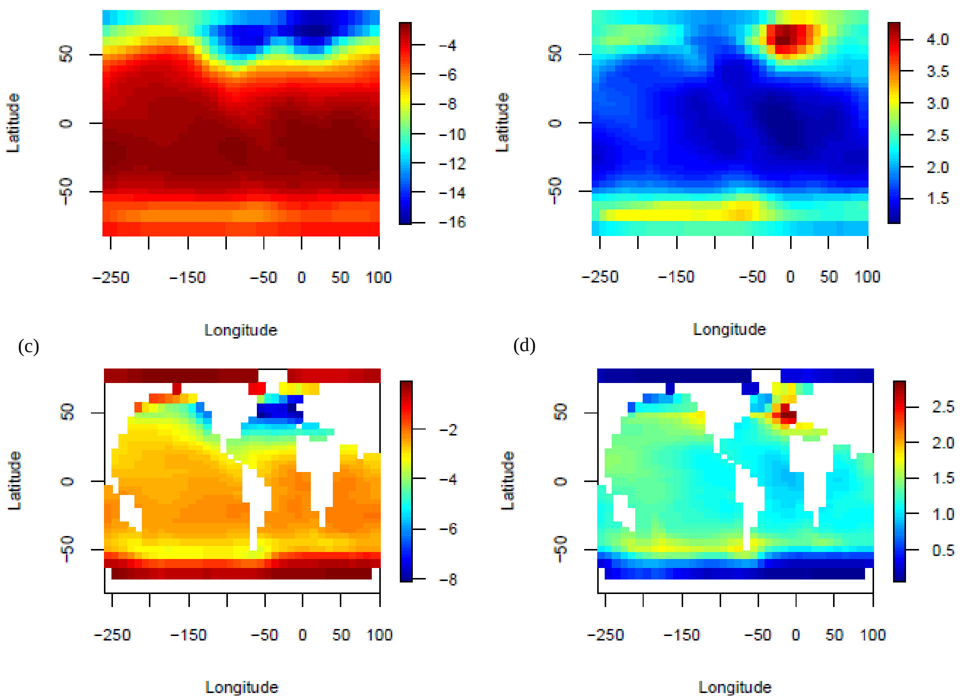

Fig. 3. LGM change in surface air temperature (a-b) and sea surface temperature (c-d) (°C) ENS$_{104}$ ~~PGACF ensemble~~ mean (left) and standard deviation (right).

Sea level

The ENS_{104} mean percentage increase in LGM salinity (%S) (and DIC, ALK, PO_4, etc) due to decreasing sea level is 2.84 $\pm$ 0.62 and the range is 2 to 4. ~~The percentage increase in LGM salinity (%S) (and DIC, ALK, PO_4, etc) due to decreasing sea level in the PGACF ensemble varies between 2 and 4, with a mean of 2.84 $\pm$ 0.62.~~ There is no significant relationship between %S and ΔCO_2, and the distribution of %S is similar in ENS_{104} than in both ENS_{315} and ENS_{16} (Fig. 4). There is, however, a weak positive correlation between %S and ΔCO_2 in ENS_{315} (r = 0.17).~~Its distribution is similar to that found in the EFPC2 and the PGACF-16 ensembles (Fig. 4). Thereis also no significant relationship between %S and ΔCO_2 in the PGACF ensemble, although there is a weak positive one (r = 0.17) in the EFPC2 ensemble.~~

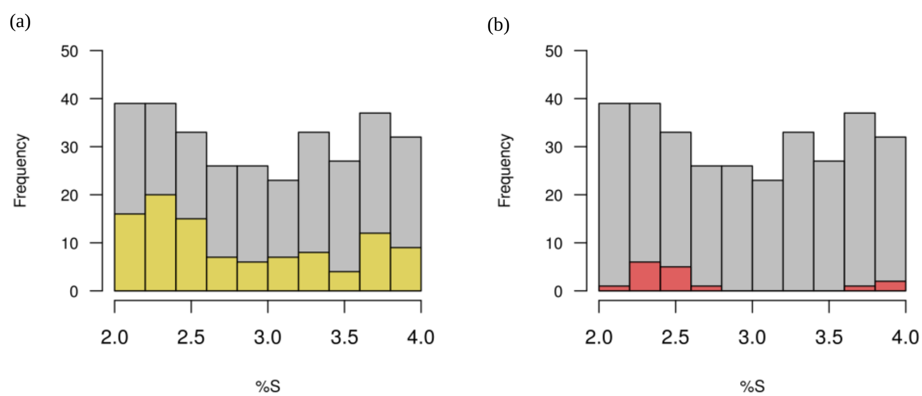

Fig. 4. Percentage increase in LGM salinity due to decreasing seal level (a-b) distribution.

Sea ice

The ENS_{104} mean LGM global annual sea ice area anomaly (ΔSIA) is 18.6 $\pm$ 7.4 million km^2, and the range is 9.9 to 44 million km^2. ~~The PGACF ensemble LGM global annual sea ice area anomaly (ΔSIA) has a mean of 18.6 $\pm$ 7.4 million km^2, and a range of 9.9 to 44 million km^2. The ΔSIA in the PGACF ensemble tends to be higher than in *the EFPC2 ensemble*, and smaller than in the PGACF-16 ensemble (Fig. 5).~~ There is a negative correlation between ΔSIA and ΔSAT (r = -0.97) and between ΔSIA and ΔCO_2 (r = -0.74).~~There is also a negative correlation between ΔSIA and both ΔSAT (r = -0.97 and -0.96) and ΔCO_2 (r = -0.74 and -0.74) in both the PGACF and EFPC2 ensembles~~. The negative correlation between ΔSIA and ΔCO_2 likely reflects the impact of changing atmospheric CO_2 on ΔSIA but may also include a smaller contribution from changing sea ice area to ΔCO_2. Increasing LGM sea ice area may have for instance reduced the outgassing of CO_2 from the ocean, particularly in the Southern Ocean via sea ice capping, and reduced the net ocean-atmosphere CO_2 flux by decreasing the AMOC strength (see below). The negative correlation between ΔSIA and ΔSAT, and between ΔSIA and ΔCO_2, is reproduced in ENS_{315} (r = -0.96 and r = -0.74 respectively). ΔSIA in ENS_{104} also tends to be higher than in ENS_{315}, and smaller than in ENS_{16} (Fig. 5).

As shown in Fig. 6, fractional sea ice cover increases in all regions where sea ice is present in preindustrial simulations, although the largest increases take place in the North Atlantic.

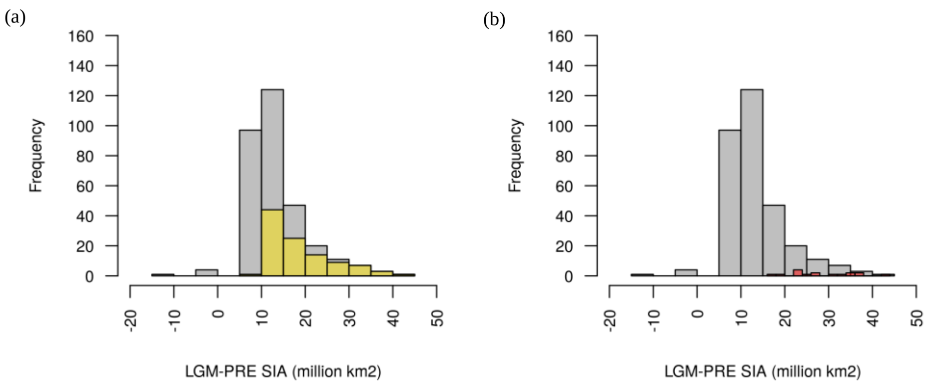

Fig. 5. LGM change in global sea ice area (a-b) distribution.

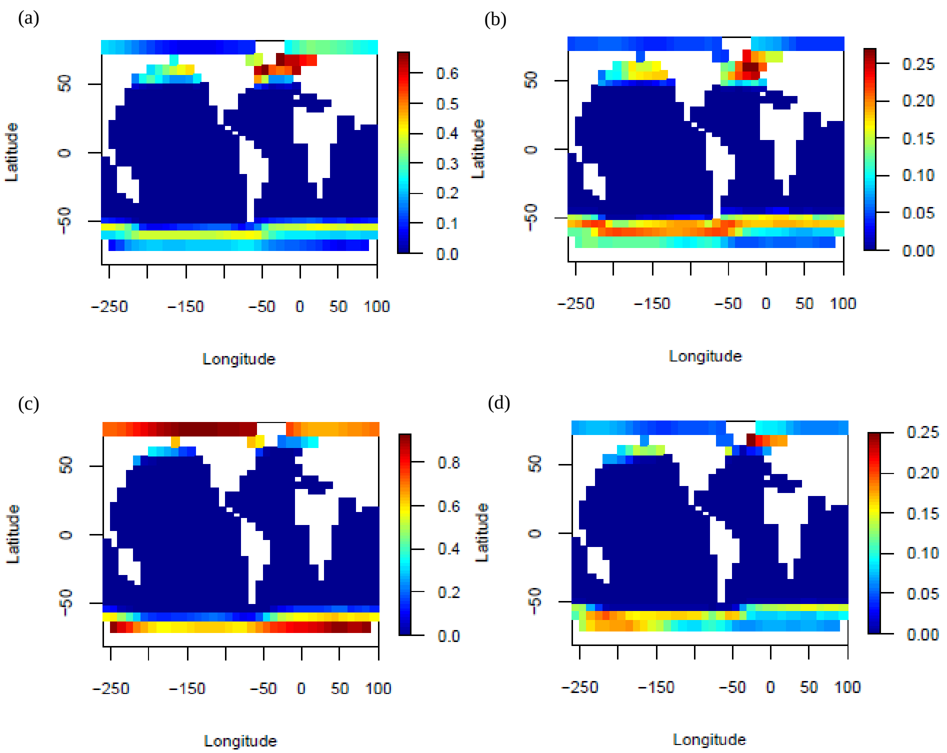

Fig. 6. LGM-PRE (a-b) and PRE (c-d) fractional sea ice cover ENS$_{104}$~~PGACF ensemble~~ means (left) and standard deviations (right).

Precipitation

The ENS_{104} mean spatial distribution of the ~~The spatial distribution of the PGACF ensemble mean~~ LGM precipitation rate anomaly (ΔPP) is shown in Fig. 7. The LGM changes are mostly negative but regions of positive ΔPP do exist, notably over Siberia and Australia. The largest LGM precipitation decreases (> 1.5 mm day $^{-1}$, with a maximum of 2.25 mm day $^{-1}$) are found over northern North America, and from around the eastern North Atlantic to northwest Asia, coinciding with the location of the Laurentide and Eurasian Ice Sheets (and the largest increases in fractional sea ice cover) respectively. Relatively large precipitation decreases (> 0.75 mm day $^{-1}$) are also simulated across China, equatorial Africa and other regions of enhanced fractional sea ice cover. Comparison against a pollen-based precipitation reconstruction (Bartlein et al., 2011 in Alder and Hostetler, 2015) suggest that the simulated precipitation changes over Europe and equatorial Africa are of the right direction, while precipitation changes over western Siberia at least ought to be negative. The sign of the precipitation changes over North America is mostly consistent with observations, which record negative changes over most of the continent. However, positive changes, which are also observed, are not captured. ~~The changes are roughly consistent with pollen-based precipitation reconstructions (Bartlein et al., 2011 in Alder and Hostetler, 2015) which suggest that precipitation decreased by ~ 0.27 to 1.1 mm day $^{-1}$ in northern Europe/northwest Asia, and by ≥ ~1.1 mm day $^{-1}$ (with a maximum of 3.4 mm day $^{-1}$) in northwest and eastern North America. The observations additionally point toward increased precipitation in the Great Basin region but this is not captured by the ensemble mean potentially because the precipitation change may be caused by a displacement of the track of the westerlies by the Laurentide Ice Sheet, and the current model does not allow for such dynamical changes (Bartlein et al., 2011). In the observations also, precipitation decreases in the 0.27 to 1.1 mm day $^{-1}$ range extend to southern Europe and to the Middle East, where the ensemble mean conversely predicts precipitation decreases no larger than ~ 0.5 mm day $^{-1}$ and precipitation increases of up to ~ 0.1 mm day $^{-1}$ respectively. Precipitation decreases in the 0.27 to 1.1 mm day $^{-1}$ range are also observed in equatorial Africa where the ensemble mean predicts somewhat comparable changes (-0.75 mm day $^{-1}$). The main exception is the rainforest region where observations suggest precipitation increased by up to 1.1 mm day $^{-1}$. Relatively large precipitation decreases, of around 1 mm day $^{-1}$, are further simulated for the Tibetan plateau region, for which there is no observational data, and for mid-latitude east Asia, for which there is just one observation, in Japan. The latter suggests a precipitation decrease of 2.4 mm day $^{-1}$ (Bartlein et al., 2011, supplementary information). A potentially more significant discrepancy is the simulated precipitation increases of~~

~~up to 0.1 mm day $^{-1}$ in continental Siberia, where observations conversely indicate precipitation *decreases* in the 0.07 to 1.1 mm day $^{-1}$ range. In Beringia also, precipitation decreases by > 0.5 mm day $^{-1}$ in the ensemble mean but exhibits both increases and decreases of up to ~ 1.1 mm day $^{-1}$ in the observations.~~ Although not shown here, comparison of the ENS_{104}~~PGACF ensemble~~ mean against the ENS_{315}~~EFPC2 ensemble~~ mean suggests that the precipitation patterns in the two are very similar, but the decreases generally tend to be higher in the ENS_{104}~~PGACF ensemble~~ mean. The precipitation decreases in the latter conversely tend to be smaller than in ENS_{16}~~the PGACF-16 ensemble~~.

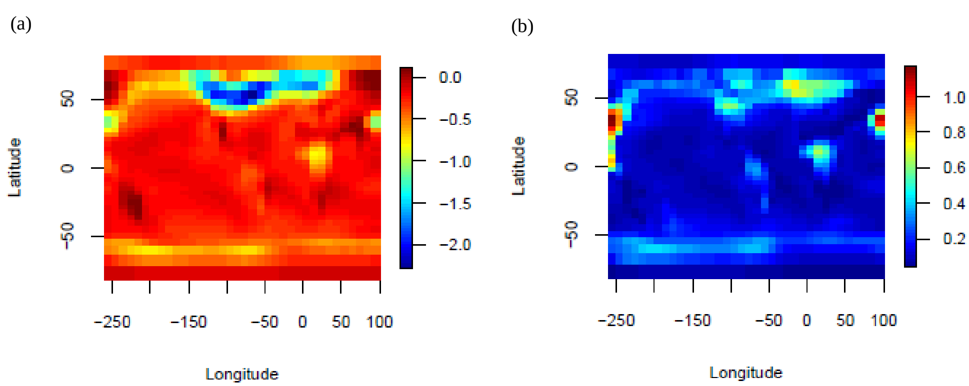

Fig. 7. LGM change in precipitation rate (mm day^{-1}) ENS_{104}~~PGACF~~ mean (a) and standard deviation (b).

Ocean circulation

The ENS_{104} mean LGM AMOC strength anomaly ($\Delta\psi_{max}$) is -2.8 ± 2.8 Sv, and the range is -8 to 4.7 Sv (Fig. 8). These estimates are at the low end of the $\Delta\psi_{max}$ predicted by 9 PMIP2 (Weber et al., 2007) and 8 PMIP3 (Muglia and Schmittner, 2015) coupled model simulations. However, they do not include the more negative $\Delta\psi_{max}$ predicted by Völker and Köhler

(2013) for instance. ~~The PGACF ensemble LGM AMOC strength anomaly ($\Delta\psi_{max}$) has a mean of -2.8 ± 2.8 Sv and a range of -8 to 4.7 Sv (Fig. 8), which is at the low end of the $\Delta\psi_{max}$ predicted by 9 PMIP2 (Weber et al., 2007) and 8 PMIP3 (Muglia and Schmittner, 2015) coupled model simulations ([-6.2, 7.3 Sv] and [1.8, 10.4] respectively). It does not, however, include the more negative $\Delta\psi_{max}$ predicted by Völker and Köhler (2013) for instance ($\Delta\psi_{max}$ = -11.6 Sv).~~ The ENS_{104} mean LGM-PRE AABW cell strength in the Atlantic Ocean ($\Delta\psi_{min}$) is 0.1 ± 1.2 Sv, which here represents an LGM decrease in cell strength as we keep the original (negative) sign for anticlockwise flow of Antarctic water. A negative $\Delta\psi_{min}$ conversely represents an LGM increase in cell strength. The range of $\Delta\psi_{min}$ is -4.3 to 4.3 Sv, roughly comparable to the range of $\Delta\psi_{min}$ predicted in Weber et al. (2007) (see also Muglia and Schmittner, 2015), but excluding the much larger ψ_{min} increase predicted by Kim et al. (2003) for example.~~The LGM-PRE AABW cell strength in the Atlantic Ocean ($\Delta\psi_{min}$) PGACF ensemble mean is 0.1 ± 1.2 Sv, which represents an LGM decrease in cell strength as the latter is negative to denote the anticlockwise flow of Antarctic water. A negative $\Delta\psi_{min}$ here conversely always represents an LGM increase in cell strength unless otherwise specified. The total range of $\Delta\psi_{min}$ is from -4.3 to 4.3 Sv, roughly comparable to the range of $\Delta\psi_{min}$ (-3.4 to 3.5 Sv) predicted in Weber et al. (2007) (see also Muglia and Schmittner, 2015), but excluding the much larger ψ_{min} increase (14 Sv) predicted by Kim et al. (2003) for example~~. ~~Out of the 104 simulations in the PGACF ensemble, one ensemble member predicts no formation of AABW (LGM ψ_{min} = 0).~~ The northern limits of the ENS_{104} mean LGM AMOC and AABW cells are roughly at the same latitudes as in the preindustrial simulations (Fig. 9). ~~The northern limits of the PGCAF ensemble mean LGM AMOC and AABW cells (where ψ again approaches 0 Sv) are roughly the same latitude as in the preindustrial simulations (Fig. 9).~~ The maximum depth reached by the ensemble mean AMOC base is also similar to preindustrial. Observations (Lynch-Stieglitz et al., 2007; Lippold et al., 2012; Gebbie, 2014; Böhm et al., 2015), conversely, suggest that the LGM AMOC shoaled to < 2 km, raising its base depth by 2500 and 600 m at the north and south end of the return flow respectively. The LGM AABW, in turn, is thought to have filled the deep Atlantic below 2 km, reaching as far north as 65 °N, which is ca. 25 degrees north of its modern northern limit (Oppo et al., 2015).

Although not show here, the ENS_{16}~~PGACF-16~~ ensemble members tend to exhibit a shoaling of the AMOC and enhanced penetration of AABW. With regard to $\Delta\psi_{max}$ and $\Delta\psi_{min}$, these tend to be more negative (i.e. weaker AMOC and stronger AABW) than in ENS_{104}~~the PGACF-16~~. The $\Delta\psi_{max}$ and $\Delta\psi_{min}$ in ENS_{315} ~~the EFPC2 ensemble~~ tend to conversely be more positive. In ENS_{104}, we also find a positive relationship between $\Delta\psi_{max}$ and ΔCO_2 (r = 0.57) and a negative relationship between $\Delta\psi_{min}$ and ΔCO_2 (r = -0.42). The relationships are reproduced in ENS_{315} (r = 0.59 and r = -0.36 respectively). We additionally find, in both ENS_{104} and ENS_{315}, negative correlations between $\Delta\psi_{max}$ and $\Delta\psi_{min}$ (r = -0.62 and -0.63), $\Delta\psi_{min}$ and ΔSAT (r = -0.4 and -0.4) and $\Delta\psi_{max}$ and ΔSIA (r = -0.62 and -0.66), as well as positive correlations between $\Delta\psi_{max}$ and ΔSAT (r = 0.68 and 0.66), and $\Delta\psi_{min}$ and ΔSIA (r = 0.37 and 0.42). ~~Analyses of the PGACF and EFPC2 ensembles also reveals a positive relationship between $\Delta\psi_{max}$ and ΔCO_2 (r = 0.57 and 0.59), and a negative relationship between $\Delta\psi_{min}$ and ΔCO_2 (r = -0.42 and -0.36). There is, moreover, a negative correlation between $\Delta\psi_{max}$ and $\Delta\psi_{min}$ (r = -0.62 and -0.63), a~~

~~positive correlation between $\Delta\psi_{max}$ and ΔSAT (r = 0.68 and 0.66), a negative correlation between $\Delta\psi_{min}$ and ΔSAT (r = -0.4 and -0.4), a negative correlation between $\Delta\psi_{max}$ and ΔSIA (r = -0.62 and -0.66), and a positive correlation between $\Delta\psi_{min}$ and ΔSIA (r = 0.37 and 0.42).~~

Based on these relationships, we hypothesise that increasing LGM AABW strength led to an expansion of the AABW cell, with the latter restricting the AMOC to lower depths, and reducing its overturning rate (e.g. Shin et al., 2003). The increase in AABW strength was likely driven by increases in sea ice enhancing brine rejection. Sea ice increases in the North Atlantic may have additionally weakened the AMOC cell by locally reducing deep convection.

~~Based on these relationships, we hypothesise that increasing LGM AABW (AMOC) strength led to an expansion of the AABW (AMOC) cell, with the latter restricting the AMOC (AABW) to lower depths (higher latitudes), and reducing its overturning rate (e.g. Shin et al., 2003). Increasing sea ice may have also contributed to increasing ψ_{min} and decreasing ψ_{max} by increasing SH brine rejection and reducing North Atlantic deep convection respectively.~~

The relationships between $\Delta\psi_{max}$, $\Delta\psi_{min}$ and ΔCO_2 are also consistent with increasing ψ_{min} (decreasing ψ_{max}) contributing to decreasing atmospheric CO_2. The replacement of NADW by AABW in the North Atlantic would have for instance led to a dissolution of deep sea sediment $CaCO_3$ due to AABW having a lower bottom water CO_3^{2-} concentration than NADW (see e.g. Yu et al., 2014). The increased $CaCO_3$ dissolution flux in turn raises the whole ocean alkalinity, lowering the atmospheric CO_2. Enhanced AABW production would have also caused the deep ocean to become more stratified, allowing more DIC to accumulate at depth, and promoting further $CaCO_3$ dissolution. A decrease in NADW formation on its own may have moreover lowered atmospheric CO_2 by reducing the outgassing of CO_2 at the ocean surface and the burial rate of deep sea $CaCO_3$ through the concomitant increase in deep sea DIC accumulation.Further investigation is, however, required to confirm these causal relationships.

~~The relationships between $\Delta\psi_{max}$, $\Delta\psi_{min}$ and ΔCO_2 may in turn suggest that increasing ψ_{min}(decreasing ψ_{max}) contributed to decreasing atmospheric CO_2. The replacement of NADW by AABW in the North Atlantic would have for instance led to a dissolution of deep sea sediment $CaCO_3$ due to AABW having a lower bottom water CO_3^{2-}concentration than NADW. The increased $CaCO_3$ dissolution flux in turn raises the whole ocean alkalinity, lowering the atmospheric CO_2. Enhanced AABW production would have also caused the deep ocean to become more stratified, allowing more DIC to accumulate at depth, and promoting further $CaCO_3$ dissolution. A decrease in NADW formation on its own may have moreover lowered atmospheric CO_2 by reducing the outgassing of CO_2 at the ocean surface and the burial rate of deep sea $CaCO_3$ through the concomitant increase in deep sea DIC accumulation. Further investigation is, however, required to verify these causal relationships. An alternative, or more likely complementary, explanation for the correlation between $\Delta\psi_{max}$ and ΔCO_2 for instance is that decreasing CO_2 leads to decreasing ψ_{max}, and increasing ψ_{min} by increasing the amount of sea ice.~~

(a)

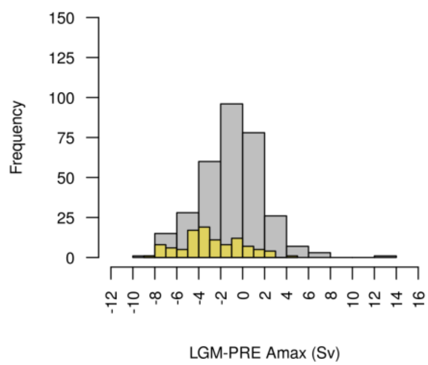
Frequency
150
125
100
75
50
25
0
-12 -10 -8 -6 -4 -2 0 2 4 6 8 10 12 14 16
LGM-PRE Amax (Sv)

(b)

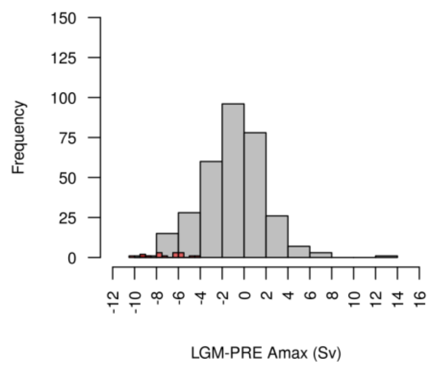
Frequency
150
125
100
75
50
25
0
-12 -10 -8 -6 -4 -2 0 2 4 6 8 10 12 14 16
LGM-PRE Amax (Sv)

(c) (d)

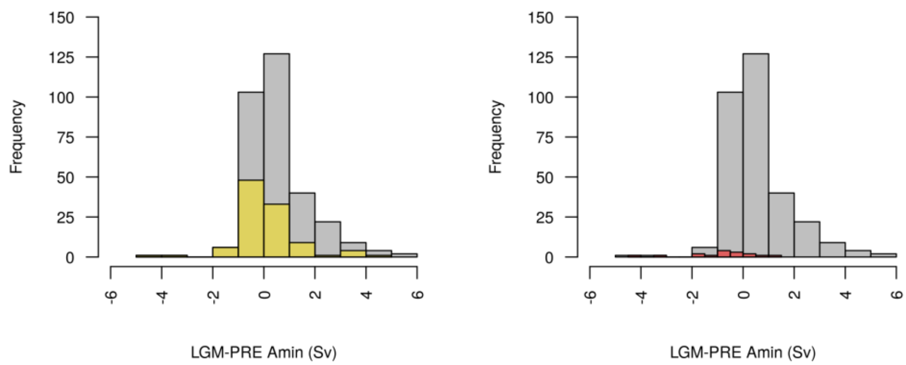

Fig. 8. LGM change in ψ_{max} (a-b) and ψ_{min} (c-d) distributions.

(a) (b)

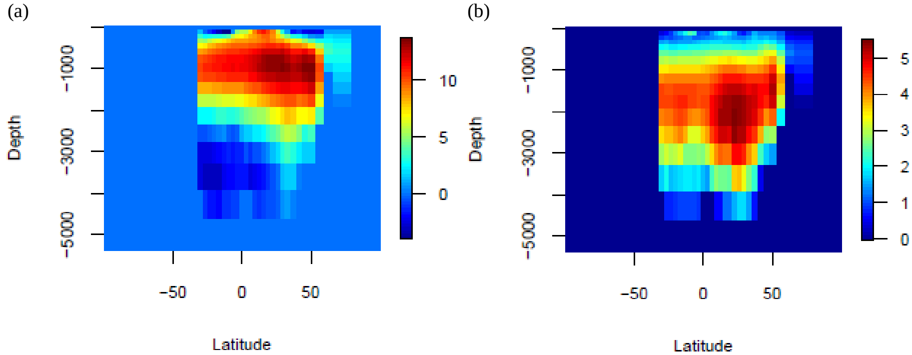

(c) (d)

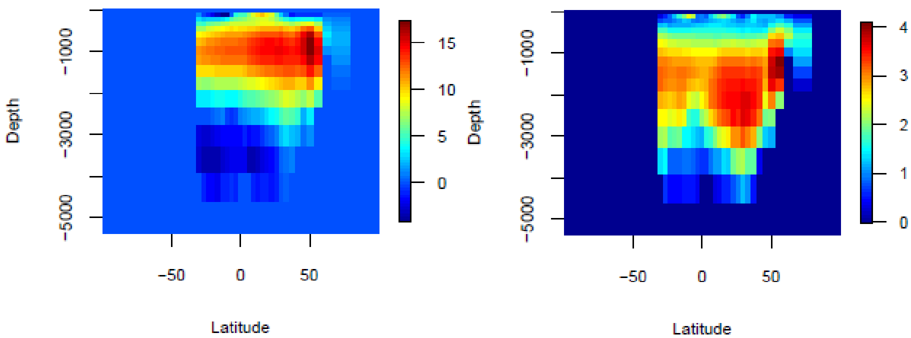

Fig. 9. LGM (a-b) and PRE (c-d) Atlantic overturning stream functions (Sv) ENS_{104}~~PGACF ensemble~~ means (left) and standard deviations (right).

3.2.2~~4.3~~ Terrestrial biosphere, ocean and lithospheric carbon

Most of the ensemble members in the PGACF ensemble predict an LGM increase in terrestrial biosphere (ΔTerrC), and lithospheric[1] (ΔLithC) carbon inventory and a decrease in ocean carbon inventory (ΔOceanC) (Fig. 10). The remaining ensemble members predict one of four other scenarios of carbon partitioning, with the second most common scenario (11% of ensemble members) being increasing terrestrial carbon and decreasing ocean and lithospheric carbon. Similar patterns can also be observed in ENS_{315} and ENS_{16} (Table 3). A likely explanation for scenario 1 is that the growth of biosphere carbon on land (see below) causes a flux of CO_2 from the atmosphere to the land, leading to immediate outgassing of CO_2 from the ocean to remove the atmospheric pCO_2 difference. The CO_2 outgassing also leads to an increase in surface $[CO_3^{2-}]$ and subsequently deep ocean $[CO_3^{2-}]$, which reduces $CaCO_3$ dissolution (and increases lithospheric carbon). The increase in $CaCO_3$ burial in turn decreases $[CO_3^{2-}]$ and increases $[CO_2]$, which is communicated back to the

[1] The ΔLithC stems from changes in the deep-sea $CaCO_3$ burial flux and/or $CaCO_3$ weathering/shallow water deposition flux and was initially calculated to ensure that carbon was being conserved over the LGM simulation.

surface, with a resultant increase in atmospheric CO_2 (Kohfeld and Ridgwell, 2009). The above explanation is of course only part of the explanation for this dominant carbon partitioning scenario, with physical mechanisms also expected to play a role, in addition to any changes in ocean productivity and changes in land carbonate weathering (see below).

~~The same trends are also observed in the EFPC2 and PGACF-16 ensembles. More specifically, the EFPC2 predicts there are 7 different scenarios of carbon partitioning between the terrestrial biosphere, ocean and lithospheric carbon reservoirs (Table 5). The dominant scenario, namely an increase in terrestrial biosphere and lithospheric carbon inventory, and a decrease in ocean carbon inventory, includes roughly 89% of ensemble members. In the PGACF and PFACF-16 ensembles, the proportions are 79 and 63% respectively. The second most common scenario is an increase in terrestrial biospere and ocean carbon, and a decrease in lithospheric carbon, comprising 5% of EPFC2 ensemble members, and 11% and 19% of PGACF and PGACF-16 ensemble members respectively. The third most common scenario is an increase in terrestrial biosphere carbon and a decrease in ocean and lithospheric carbon, comprising 3, 8 and 13% of members in the EFPC2, PGACF and PGACF-16 ensembles respectively.~~

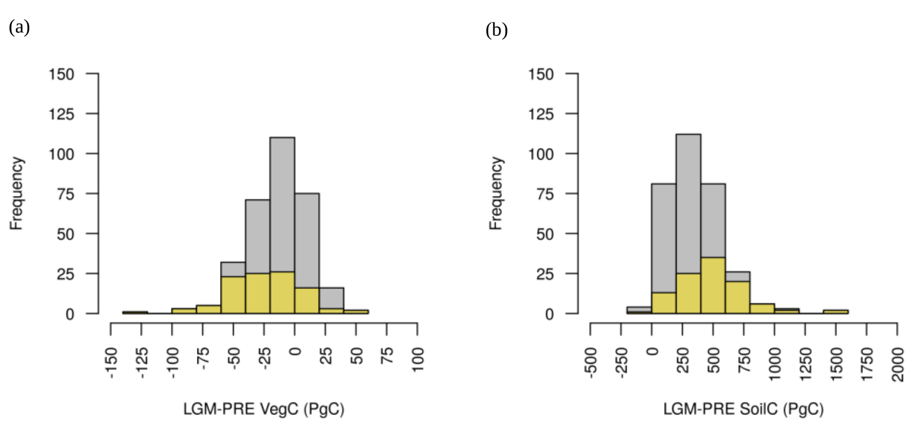

(c)

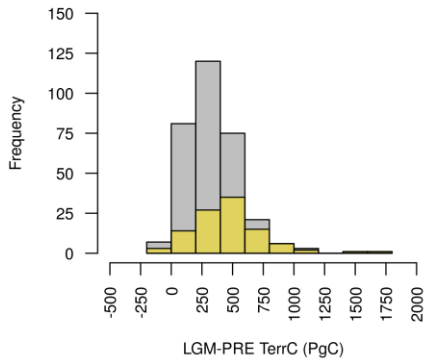

(d)

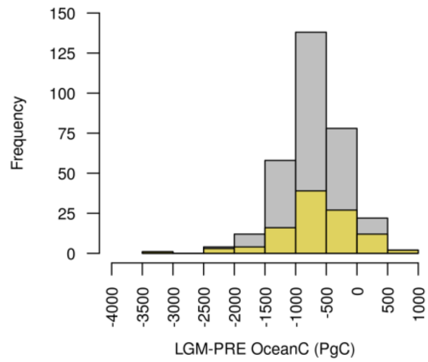

(e)

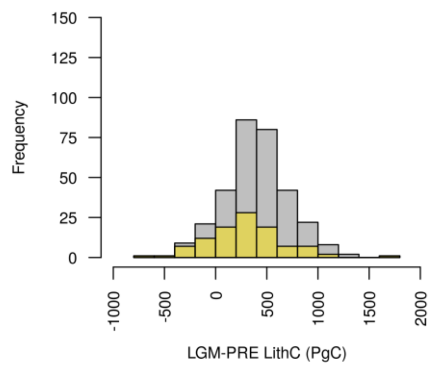

Fig. 10. LGM change in vegetation (a), soil (b), terrestrial (vegetation + soil) (c), ocean (d) and lithospheric (e) carbon inventory distributions.

Table 3. LGM-PRE carbon partitioning scenarios in ENS_{315}, ENS_{104} and ENS_{16}.

Scenarios			ENS_{315} Total counts	ENS_{315} (% of total)	ENS_{104} Total counts	ENS_{104} (% of total)	ENS_{16} Total counts	ENS_{16} (% of total)
1. ΔTerrC(+)	ΔOceanC(-)	ΔLithC(+)	279	(89)	82	(79)	10	(63)
2. ΔTerrC(+)	ΔOceanC(+)	ΔLithC(-)	16	(5)	11	(11)	3	(19)
3. ΔTerrC(+)	ΔOceanC(-)	ΔLithC(-)	11	(3)	8	(8)	2	(13)
4. ΔTerrC(-)	ΔOceanC(+)	ΔLithC(+)	1	(1)	1	(1)	0	(0)
5. ΔTerrC(-)	ΔOceanC(+)	ΔLithC(-)	5	(2)	2	(1)	1	(6)
6. ΔTerrC(-)	ΔOceanC(-)	ΔLithC(+)	1	(1)	0	(0)	0	(0)
7. ΔTerrC(+)	ΔOceanC(+)	ΔLithC(+)	2	(1)	0	(0)	0	(0)

Table 5. LGM-PRE carbon partitioning scenarios in the EFPC2 (n=315), PGACF (n=104) and PGACF-16 (n=16) ensembles.

~~Scenarios~~			~~N=315~~ ~~Total counts~~	~~(% of total)~~	~~N=104~~		~~N=16~~	
~~1. ΔTerrC(+)~~	~~ΔLithC(+)~~	~~ΔOceanC(-)~~	~~279~~	~~(89)~~	~~82~~	~~(79)~~	~~10~~	~~(63)~~
~~2. ΔTerrC(+)~~	~~ΔOceanC(+)~~	~~ΔLithC(-)~~	~~16~~	~~(5)~~	~~11~~	~~(11)~~	~~3~~	~~(19)~~
~~3. ΔTerrC(+)~~	~~ΔLithC(-)~~	~~ΔOceanC(-)~~	~~11~~	~~(3)~~	~~8~~	~~(8)~~	~~2~~	~~(13)~~
~~4. ΔTerrC(-)~~	~~ΔOceanC(+)~~	~~ΔLithC(+)~~	~~1~~	~~(1)~~	~~1~~	~~(1)~~	~~0~~	~~(0)~~
~~5. ΔTerrC(-)~~	~~ΔLithC(-)~~	~~ΔOceanC(+)~~	~~5~~	~~(2)~~	~~2~~	~~(1)~~	~~1~~	~~(6)~~
~~6. ΔTerrC(-)~~	~~ΔOceanC(-)~~	~~ΔLithC(+)~~	~~1~~	~~(1)~~	~~0~~	~~(0)~~	~~0~~	~~(0)~~
~~7. ΔTerrC(+)~~	~~ΔLithC(+)~~	~~ΔOceanC(+)~~	~~2~~	~~(1)~~	~~0~~	~~(0)~~	~~0~~	~~(0)~~

The ENS_{104} mean ΔTerrC, ΔOceanC and ΔLithC, the signs of which are consistent with scenario 1, are reported in Table 4, alongside previous estimates from observational data- and model-based studies. From here we can see that the mean ΔTerrC is only aligned with a handful of estimates and no studies so far report a negative ΔOceanC. Instead, ΔOceanC is estimated to be positive, primarily based on carbon isotope data. The loss of hundreds of petagrams of carbon from the ocean in response to terrestrial carbon growth has, however, been previously proposed (e.g. Zimov et al., 2006). Moreover, if we assume that 90% of the atmospheric CO_2 perturbation caused by the increase in terrestrial biosphere carbon reported in Table 4 gets removed by the ocean and sediments, the change in ocean carbon would be negative, even after adding the remaining carbon to be lost from the atmosphere to the ocean. We discuss what these results would likely mean for carbon isotope data in section 3.2.6.

~~As shown in Table 6, a positive ΔTerrC and a negative ΔOceanC are only consistent with a handful of observational data- and model- based studies. In the absence of other reservoir changes, a flux of CO_2 from the atmosphere to the land (or vice-versa) will lead to immediate outgassing of CO_2 from (uptake by) the ocean to remove the atmospheric pCO_2 difference. Carbonate compensation of the increased terrestrial carbon storage will also result in an increased deep sea $CaCO_3$ burial flux, and surface ocean pCO_2, leading to an increase in lithospheric carbon and atmospheric CO_2, and a further decrease in ocean carbon. Here, at least another part of the ensemble changes in lithospheric carbon will have been driven by changes in the land to ocean bicarbonate flux since the latter is prescribed in the simulations. There is also a positive correlation between $\Delta\psi_{max}$ and ΔLithC in both the PGACF and EFPC2 ensembles (r = 0.25 and r = 0.32), which potentially suggests that reducing the AMOC strength indeed leads to a decrease in deep sea $CaCO_3$ burial rate, as suggested above.~~

~~The PGACF ensemble mean ΔTerrC is of the same sign and order of magnitude as the ΔTerrC predicted by Zimov et al. (2006, 2009), Zech et al. (2011) and Zeng (2003, 2007). ΔOceanC is not directly calculated in these studies and is instead typically assumed to have decreased by several hundred PgC as a result of the terrestrial biosphere carbon gain.~~

The positive ΔTerrC studies in Table 4 attribute the increase in terrestrial biosphere carbon to different factors: Zimov et al., 2009 and Zech et al., 2011 predict large increases in permafrost carbon while Zeng et al., 2003 ignores permafrost and instead attributes most of the glacial terrestrial carbon increase to ice sheet burial carbon. Another contributor is the storage of carbon on exposed continental shelves. Here, neither this carbon accumulation mechanism nor that of peat growth (absent also in Zeng, 2003), are included in our model. As discussed above, permafrost growth is also not represented explicitly but there is an attempt to capture the very slow rates of soil decomposition characteristic of permafrost (Williamson et al., 2006). Similarly to Zeng (2003), the model gradually buries carbon in LGM ice sheet areas. Analysis of ENS_{16} suggests that during the 1000 years of LGM ice sheet build-up, the terrestrial carbon inventory in the areas to be occupied by the ice sheets increases by between 6 and 444 PgC, yielding LGM ice-sheet carbon inventories (or "burial" carbon inventories) between 318 and 1341 PgC (Table 5). This increase accounts for less than half of the total LGM change in terrestrial carbon (i.e. ΔTerrC) in the majority of simulations. However, if this "extra" carbon (accumulated in response to climate forcings), and the carbon already present in the ice sheet areas at the end of the preindustrial spin-up, were to have been destroyed rather than preserved, ΔTerrC would be negative in all but 3 simulations, as opposed to positive in all but one simulation (Table 5).

~~The previous positive ΔTerrC studies attribute the increase in terrestrial biosphere carbon to different factors: Zimov, N.S. and Zech. R, predict large increases in permafrost carbon while Zeng, N. ignores permafrost and instead attributes most of the glacial terrestrial carbon increase to ice sheet burial carbon. Another contributor is the storage of carbon on exposed continental shelves. Here, neither this carbon accumulation mechanism nor that of peat growth (absent also in Zeng, 2003), are included in our model. As discussed above, permafrost growth is also not represented explicitly but there is an attempt to capture the very slow rates of soil decomposition characteristic of permafrost (Williamson et al., 2006). Similarly to Zeng (2003), the model gradually buries carbon in LGM ice sheet areas.~~

Table 4. $\Delta\mathrm{TerrC}$, $\Delta\mathrm{OceanC}$ and $\Delta\mathrm{LithC}$ (PgC) in this study (ENS_{104} mean, standard deviation and range) and previous studies. ~~**Table 6. ΔTerrC, ΔOceanC and ΔLithC (PgC) in this study (PGACF ensemble mean, standard deviation and range) and previous studies.**~~ PE14 = Peterson et al. (2014), OA13 = O'ishi and Abe-Ouchi (2013), C12 = Ciais et al. (2012), Z03 = Zeng (2003), SA13 = Sarnthein et al. (2013), BG15 = Brovkin and Ganopolski (2015), PR11= Prentice et al. (2011), SK15 = Skinner et al. (2015), SS16 = Schmittner and Somes (2016), GL13 = Goodwin and Lauderdale (2013), A15 = Allen et al. (2015), CR95 = Crowley et al. (1995), AF98 = Adams and Faure (1998), BR12 =

	This study	Previous studies	Ref.	Details
$\Delta\mathrm{TerrC}$	467.5±286.5 [-51.6,1603.8]	[-1160, 530]	CR95	Pollen database
		-1500	AF98	Ecological data
		[-694, -550]	PR11	Simulation with LPX
		-600	BR12	Simulation with CLIMBER-2
		-597	OA13	Simulation with MIROC-LPJ
		-511	PE14	Benthic foraminiferal δ^{13}C records
		-330	C12	Benthic foraminiferal, ice core and terrestrial δ^{13}C records + simulation with LPJ land ecosystem model
		0	BG15	Simulation with CLIMBER-2 (+ permafrost, peat, glacial burial carbon)
		547	Z03	Simulation with a coupled atmosphere-land-ocean-carbon model
		[200, 400]	ZE11	Soil carbon measurements
		$<$1000	ZI09	Soil carbon measurements
$\Delta\mathrm{OceanC}$	-664±626.9 [-3187.7, 662.4]	[730, 980]	SA13	Ocean radiocarbon records
		687	SK15	Ocean radiocarbon records
		654	A15	Ocean $[\mathrm{CO}_3^{2-}]$ reconstructions + benthic foraminiferal δ^{13}C records
		[570, 970]	GL13	Ocean $[\mathrm{CO}_3^{2-}]$ reconstructions
		520	C12	Benthic foraminiferal, ice core and terrestrial δ^{13}C records + simulation with LPJ land ecosystem model
		[510,670]	SS16	Simulation with MOBI 1.5 coupled to Uvic

ΔLithC	292.5±373.9 [-654.9,1700.9]	n/a	n/a	n/a

Most of the increase in ice sheet carbon is due to soil carbon, with vegetation carbon decreasing in all but one simulation. The range of carbon inventory changes includes the 116 PgC increase in ice sheet carbon, and consequent total burial carbon inventory (431 PgC), estimated by Zeng (2003). It would also allow for an additional 250-550 PgC (Franzen, 1994) from increased glacial peat accumulation to be buried under the ice sheets, as suggested by Zeng (2003). No observational data-based estimates of the LGM burial carbon inventory are available since there is so far only limited evidence for organic material being preserved by ice during glaciations (Franzen, 1994 and references in Weitemeyer and Buffett, and Zeng, 2007). Outside of the ice sheets, increases in terrestrial carbon inventory are mostly due to soil carbon, which increases in all simulations. Vegetation carbon, conversely, decreases in the majority of simulations. The range of non-ice sheet carbon changes includes the 198 PgC increase in non-burial non-shelf terrestrial carbon predicted by Zeng (2003) as a result of reduced soil respiration. Here, the increase in terrestrial biosphere carbon both inside and outside of the ice sheet areas, are presumed to reflect the decrease in soil respiration rate due to colder SATs exceeding the decrease in net photosynthesis (i.e. total photosynthesis-respiration) rate due to lower CO_2, SAT and precipitation, as they are mainly driven by soil carbon increases. In most previous model- and observational data-based studies it is conversely suggested that the reduced photosynthesis effect due to climate and CO_2 changes outcompetes the reduced respiration effect on a global scale. In O'ishi and Abe-Ouchi (2013) for example, the terrestrial carbon that would be gained if ice sheet carbon was preserved rather than destroyed (383 PgC) is smaller than the amount of carbon that is lost in response to the LGM climate and CO_2 changes (502 PgC).

Although not evaluated directly, it is likely that similar ice sheet/non-ice sheet terrestrial carbon proportions than in ENS_{16} are found in ENS_{104} and ENS_{315} because of the similar climate change distributions in all three instances (see earlier sections). Although not shown here, the spatial distribution of ΔTerrC in ENS_{16} is also similar to that of the ENS_{104} (and ENS_{315}) mean. The spatial distribution of ΔTerrC in ENS_{104} is shown in Fig. 11 and compared against observations. ~~Analysis of the PGACF-16 ensemble members' terrestrial carbon reservoirs suggests that if the preindustrial ice sheet carbon inventory (the terrestrial biosphere carbon in grid cells to be buried by the LGM ice sheets) were to be destroyed instead of preserved at the LGM, the ΔTerrC would be negative in all but 3 simulations (Tables 7 and 8). During the 1000 years of LGM ice sheet build-up, the ice sheet carbon increases by between 6 and 444 PgC, yielding LGM ice-sheet carbon inventories (or "burial" carbon inventories) between 318 and 1341 PgC (Table 8), and accounting for less than half of the total LGM change in terrestrial carbon (i.e. ΔTerrC) in all but one simulation (EM 442). Most of the ice sheet carbon increase is due to soil carbon, with vegetation carbon decreasing in all but one simulation (EM 871). The range of carbon~~

~~inventory changes includes the 116 PgC increase in ice sheet carbon, and consequent total burial carbon inventory (431 PgC), estimated by Zeng (2003). It would also allow for an additional 250-550 PgC (Franzen, 1994) from increased glacial peat accumulation to be buried under the ice sheets, as suggested by Zeng (2003). No observational data-based estimates of the LGM burial carbon inventory are available since there is so far only limited evidence for organic material being preserved by ice during glaciations (Franzen, 1994 and references in Weitemeyer and Buffett, and Zeng, 2007). Outside of the ice sheets, the terrestrial carbon inventory increases in all but one simulation (EM 219), by between 111 and 1089 PgC. This is mostly due to soil carbon, which increases in all simulations. The vegetation carbon, conversely, decreases in all but three simulations (EM 837, EM 863 and EM 837). The range of non-ice sheet carbon changes includes the 198 PgC increase in non-burial non-shelf terrestrial carbon predicted by Zeng (2003) as a result of reduced soil respiration.~~

~~The ensemble LGM terrestrial biosphere carbon increases both inside and outside of the ice sheet areas are presumed to reflect the decrease in soil respiration rate due to colder SATs exceeding the decrease in net photosynthesis (i.e. total photosynthesis-respiration) rate due to lower CO_2, SAT and precipitation, as they are mainly driven by soil carbon increases. In most previous model- and observational data-based studies it is conversely suggested that the reduced photosynthesis effect due to climate and CO_2 changes outcompetes the reduced respiration effect on a global scale. In O'ishi and Abe-Ouchi (2013) for example, the terrestrial carbon that would be gained if ice sheet carbon was preserved rather than destroyed (383 PgC) is smaller than the amount of carbon that is lost in response to the LGM climate and CO_2 changes (502 PgC). Although not evaluated directly, it is likely that similar ice sheet/non-ice sheet terrestrial carbon proportions to those in the PGACF-16 are found in the PGACF and EFPC2 ensembles because of the similar climate change distributions exhibited in all three instances. The spatial distribution of $\Delta TerrC$ in the PGACF ensemble (described below) is also characteristic of that found in the PGACF-16 and EFPC2 ensembles.~~

The largest increases in terrestrial carbon ($\geq$ 20 kgC m^{-2}) are found in North America and Europe/western Asia, both within and south of the Laurentide and Eurasian ice sheet margins (Fig. 11). Regions with smaller but still relatively large ($\geq$ 10 kgC m^{-2}) increases include the Andes and Patagonia regions, the southern tip of the African continent, eastern north Siberia and the grid cells just south of the Tibetan plateau. The largest LGM decreases in terrestrial carbon ($\geq$ 10 kgC m^{-2}) conversely tend to be found in northwest North America, Beringia and the Tibetan plateau region. Other regions with relatively large ($\geq$ 5 kgC m^{-2}) decreases include equatorial Africa and the deserts in central Asia. Everywhere else the LGM terrestrial carbon density increases by between 0 and 10 kgC m^{-2}. Comparison against paleoecological reconstruction studies (Crowley et al., 1995) suggests that the simulated terrestrial carbon changes within the Laurentide and Eurasian ice sheet areas are of the wrong sign, except in northwest North America, since these studies assume the complete destruction of vegetation and soils in ice sheet areas. Discrepancies between the ENS_{104} and observations further arise from the rainforest regions, where the ensemble mean predicts terrestrial biosphere carbon density changes between -5 and 10 kgC m^{-2}, well above observed changes of ~ -23 kgC m^{-2}. It is important to note, however, that as suggested in Zeng (2007), the rate of decomposition of soil carbon at the LGM may have been slower than assumed in pollen data-based studies. The largest increases in terrestrial carbon density (~ 40 kgC m^{-2}) produced by the ensemble mean are comparable to those found in areas with permafrost growth (Zimov et al., 2006). However, the peaks are potentially misplaced, being located within and south of the Laurentide and Eurasian ice sheet covered areas, rather than in eastern Siberia and Alaska. Alternatively, terrestrial carbon increases in eastern Siberia and Alaska are simply underestimated in the ensemble mean and large increases in terrestrial carbon indeed took place within the ice sheet areas during glacial periods.

The highly negative LGM terrestrial carbon changes in northwest North America and adjacent Beringia are likely caused by precipitation decreasing comparatively more than SAT, and causing the decrease in photosynthesis to exceed the decrease in soil respiration. However, it is also noteworthy that, although not shown here, the regions with the largest decreases in terrestrial carbon density, namely northwest North America, Beringia and the Tibetan plateau area, are also the regions with the largest terrestrial carbon densities in the preindustrial simulations. We further, note that in the preindustrial ENS_{315} mean, the Tibetan soil carbon peak is overestimated and the North American soil carbon peak misplaced, compared to observations. We attribute the first discrepancy to the lack of soil weathering in the model and the inclusion of land use effects in the observational data-based estimate (Holden et al., 2013b; Williamson et al., 2006). The second discrepancy is attributed to the lack of explicit representation of permafrost and the absence of moisture control on soil respiration.

~~The largest PGCAF ensemble mean LGM increases (≥ 20 kgC m^{-2}) in total terrestrial carbon are found in North America and Europe/western Asia, both within and south of the Laurentide and Eurasian ice sheet margins (Fig. 11). Regions with smaller but still relatively large (≥ 10 kgC m^{-2}) increases include the Andes and Patagonia regions, the southern tip of the African continent, eastern north Siberia and the grid cells just south of the Tibetan plateau. The largest LGM decreases in terrestrial carbon (≥ 10 kgC m^{-2}) conversely tend to be found in northwest North America, Beringia and the Tibetan plateau region. Other regions with relatively large (≥ 5 kgC m^{-2}) decreases include equatorial Africa and the deserts in central Asia. Everywhere else the LGM terrestrial carbon density increases by between 0 and 10 kgC m^{-2}. Comparison against paleoecological reconstruction studies (Crowley et al., 1995) suggests that the simulated terrestrial carbon changes within the Laurentide and Eurasian ice sheet areas are of the wrong sign, except in northwest North America, since these studies assume the complete destruction of vegetation and soils in ice sheet areas. Discrepancies between the PGACF ensemble mean and observations further arise from the rainforest regions, where the ensemble mean predicts terrestrial biosphere carbon density changes between -5 and 10 kgC m^{-2}, well above observed changes of ~ -23 kgC m^{-2}. It is important to note, however, that as suggested in Zeng (2007), the rate of decomposition of soil carbon at the LGM may have been slower than assumed in pollen data-based studies. The largest increases in terrestrial carbon density (~ 40 kgC m^{-2}) produced by the ensemble mean are comparable to those found in areas with permafrost growth (Zimov et al., 2006). However, the peaks are potentially misplaced, being located within and south of the Laurentide and Eurasian ice sheet covered areas, rather than in eastern Siberia and Alaska. Alternatively, terrestrial carbon increases in eastern Siberia and Alaska are simply~~

~~underestimated in the ensemble mean and large increases in terrestrial carbon indeed took place within the ice sheet areas during glacial periods. The highly negative LGM terrestrial carbon changes in northwest North America and adjacent Beringia are likely caused by precipitation decreasing comparatively more than SAT, and causing the decrease in photosynthesis to exceed the decrease in soil respiration. However, it is also noteworthy that, although not shown here, the regions with the largest decreases in terrestrial carbon density, namely northwest North America, Beringia and the Tibetan plateau area, are also the regions with the largest terrestrial carbon densities in the preindustrial simulations.~~

Table 5. Ice sheet and non-ice sheet terrestrial carbon stocks. Columns 2 and 5 show the amount of carbon stored in ice sheet areas during the preindustrial and LGM periods respectively. Column 3 is the difference between the two inventories. Column 4 is the change in ice sheet carbon expressed as percentage of the total LGM terrestrial carbon change. Column 6 is the LGM change in carbon outside of the ice sheets.

EM	PRE ice sheet	LGM-PRE ice sheet	% LGM-PRE Total land	LGM Burial	LGM-PRE non-ice sheet
442	456	117	51	573	111
873	896	444	29	1341	1089
511	677	262	32	939	567
99	372	33	20	405	130
871	404	149	26	553	425
786	502	131	21	633	486
107	540	86	22	626	310
701	549	161	36	710	283
801	707	275	39	982	423
219	312	6	16	318	-34
694	389	95	30	484	227
623	697	181	36	879	319
522	713	210	28	923	531
863	408	73	16	480	380
478	573	165	41	739	233
837	784	395	33	1179	796

Table 7. Preindustrial ice sheet carbon (PgC) and contribution (%) to preindustrial total land (i.e. vegetation + soil), vegetation and soil carbon (PgC) in each PGACF-16 ensemble member (EM).

~~EM~~	~~Ice-sheet~~	~~% Total Land~~	~~% Vegetation~~	~~% Soil~~
~~442~~	~~456~~	~~24~~	~~14~~	~~28~~
~~873~~	~~896~~	~~35~~	~~20~~	~~40~~
~~511~~	~~677~~	~~27~~	~~14~~	~~31~~
~~99~~	~~372~~	~~22~~	~~13~~	~~25~~
~~871~~	~~404~~	~~23~~	~~15~~	~~28~~
~~786~~	~~502~~	~~26~~	~~15~~	~~30~~
~~107~~	~~540~~	~~33~~	~~18~~	~~36~~
~~701~~	~~549~~	~~28~~	~~16~~	~~33~~
~~801~~	~~707~~	~~35~~	~~19~~	~~40~~
~~219~~	~~312~~	~~21~~	~~14~~	~~24~~
~~694~~	~~389~~	~~25~~	~~14~~	~~29~~
~~623~~	~~697~~	~~32~~	~~16~~	~~36~~
~~522~~	~~713~~	~~37~~	~~18~~	~~42~~
~~863~~	~~408~~	~~24~~	~~16~~	~~28~~
~~478~~	~~573~~	~~31~~	~~16~~	~~35~~
~~837~~	~~784~~	~~47~~	~~31~~	~~53~~

Table 8. LGM ice sheet carbon change and contribution (%) to the total LGM terrestrial carbon change (i.e. ΔTerrC) in each PGACF-16 ensemble member (EM). Also shown is the amount of carbon (in PgC) buried underneath the ice sheets during the LGM and the LGM non-ice sheet carbon change. All units are PgC.

~~EM~~	~~LGM-PRE ice sheet~~	~~% LGM-PRE Total land~~	~~LGM Burial~~	~~LGM-PRE non-ice sheet~~
~~442~~	~~117~~	~~51~~	~~573~~	~~111~~
~~873~~	~~444~~	~~29~~	~~1341~~	~~1089~~
~~511~~	~~262~~	~~32~~	~~939~~	~~567~~
~~99~~	~~33~~	~~20~~	~~405~~	~~130~~
~~871~~	~~149~~	~~26~~	~~553~~	~~425~~

~~786~~	~~131~~	~~21~~	~~633~~	~~486~~
~~107~~	~~86~~	~~22~~	~~626~~	~~310~~
~~701~~	~~161~~	~~36~~	~~710~~	~~283~~
~~801~~	~~275~~	~~39~~	~~982~~	~~423~~
~~219~~	~~6~~	~~16~~	~~318~~	~~-34~~
~~694~~	~~95~~	~~30~~	~~484~~	~~227~~
~~623~~	~~181~~	~~36~~	~~879~~	~~319~~
~~522~~	~~210~~	~~28~~	~~923~~	~~531~~
~~863~~	~~73~~	~~16~~	~~480~~	~~380~~
~~478~~	~~165~~	~~41~~	~~739~~	~~233~~
~~837~~	~~395~~	~~33~~	~~1179~~	~~796~~

(a)

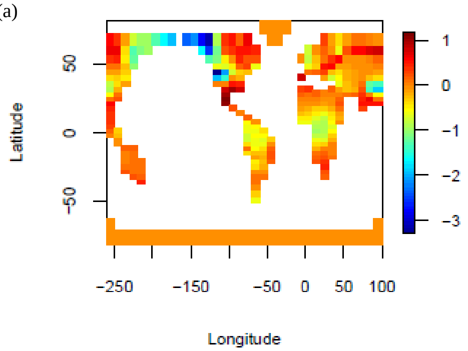

(b)

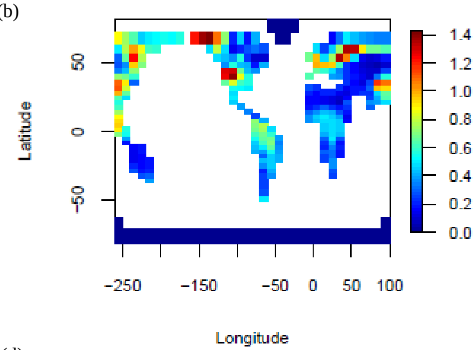

(c)

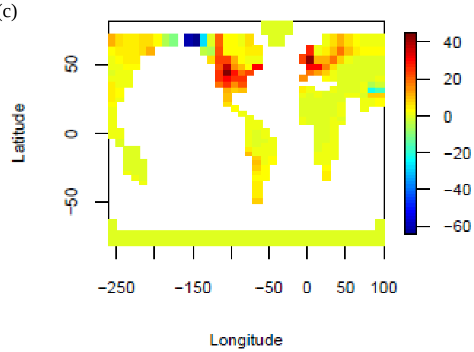

(d)

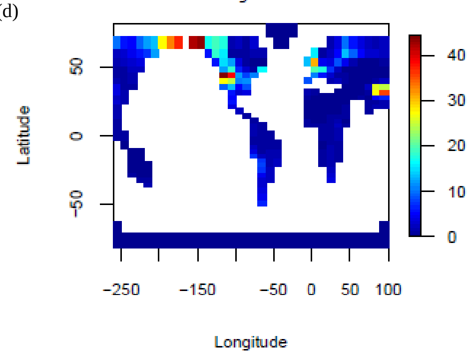

(e) (f)

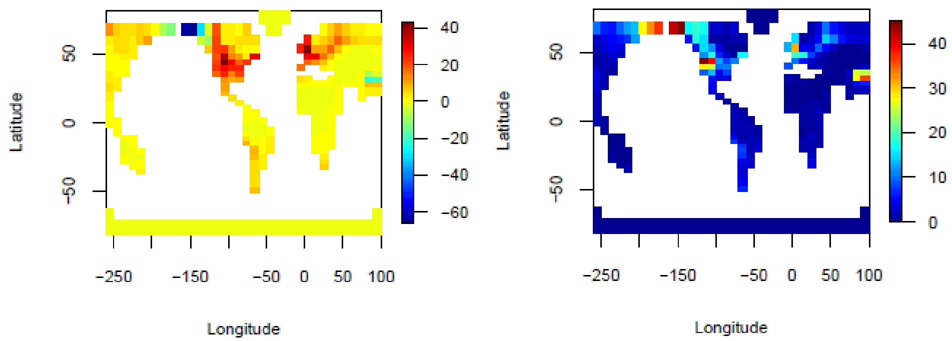

Fig. 11. LGM vegetation (a-b), soil (c-d) and total terrestrial carbon changes (e-f) ENS_{104}~~PGACF ensemble~~ mean (left) and standard deviation (right). Units are kgC m^{-2}.

3.2.3~~4.4~~ Ocean primary productivity

The ENS_{104} mean LGM total POC export flux anomaly (ΔPOC_{exp}) is -0.19 $\pm$ 1 PgC yr^{-1} and the range is -2.57 to 2.56 PgC yr^{-1}, roughly consistent with previous model-based estimates (e.g. Brovkin et al., 2002; Bopp et al., 2003; Brovkin et al., 2007; Chikamoto et al., 2012; Palastanga et al., 2013; Schmittner and Somes, 2016; Buchanan et al., 2016) (Fig. 12). ~~The PGACF ensemble LGM total POC export flux change (ΔPOC_{exp}) has a mean of -0.19 $\pm$ 1 PgC yr^{-1} and varies between -2.57 and 2.56 PgC yr^{-1}, roughly within the range of previous model-based estimates (e.g. Brovkin et al., 2002; Bopp et al., 2003; Brovkin et al., 2007; Chikamoto et al., 2012; Palastanga et al., 2013; Schmittner and Somes, 2016; Buchanan et al., 2016) (Fig. 12).~~

The POC flux decreases in ENS_{315} and ENS_{16} tend to be smaller and larger respectively. ΔPOC_{exp} is positively correlated with $\Delta\psi_{max}$ (r = 0.72 and 0.79) and negatively correlated with $\Delta\psi_{min}$ (r = -0.62 and -0.58) in both ENS_{104} and ENS_{315}. The correlations potentially suggest that decreasing AMOC strength and increasing AABW production lead to decreasing POC export. One possible mechanism is enhanced deep ocean stratification due to increasing AABW formation leading to not only more efficient trapping of DIC at depth (see above), but also nutrients and therefore reduced availability in the euphotic zone. All else held constant, a weaker and shallower AMOC cell would also inhibit the transfer of nutrients from the deep ocean to the surface. A negative correlation can additionally be found between ΔPOC_{exp} and ΔSIA (r = -0.55 and -0.6), probably because no primary production occurs beneath the sea ice surface and increasing sea ice area at the LGM therefore leads to decreasing POC export flux. This would also explain the largest ENS_{104} mean decreases in POC export flux coinciding with increases in sea ice fraction (Fig. 13).

~~The POC flux decreases in the EFPC2 and PGACF-16 ensembles tend to be smaller and larger respectively. The ΔPOC_{exp} is also positively correlated with $\Delta\psi_{max}$ (r = 0.72 and 0.79) and negatively correlated with $\Delta\psi_{min}$ (r = -0.62 and -0.58) in both the PGACF and the EFPC2 ensembles. The correlations potentially suggest that decreasing AMOC strength and increasing AABW production lead to decreasing POC export. One possible mechanism is enhanced deep ocean stratification due to increasing AABW formation leading to more efficient trapping of nutrients at depth and hence reduced availability in the euphotic zone. All else held constant, a weaker and shallower AMOC cell would also inhibit the transfer of nutrients from the deep ocean to the surface. A negative correlation can additionally be found between ΔPOC_{exp} and ΔSIA (r = -0.55 and -0.6), probably because no primary production occurs beneath the sea ice surface and increasing sea ice area at the LGM therefore leads to decreasing POC export flux. This would also explain the largest PGACF ensemble mean decreases in POC export flux coinciding with increases in sea ice fraction (Fig. 13).~~

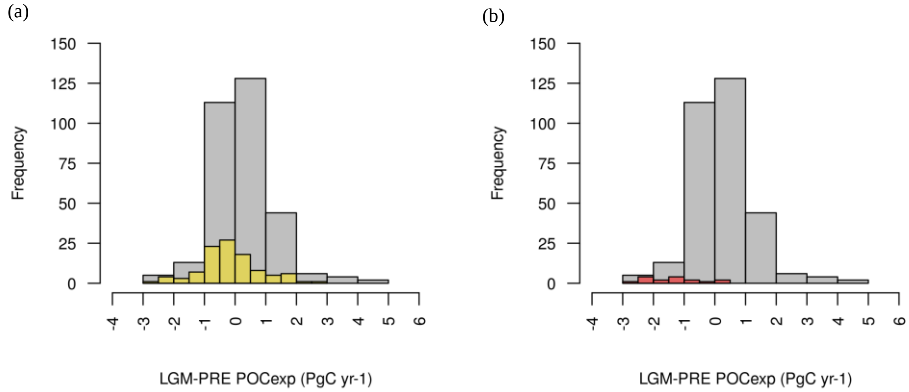

Fig. 12. LGM change in POC export flux (a-b) distributions.

(a) (b)

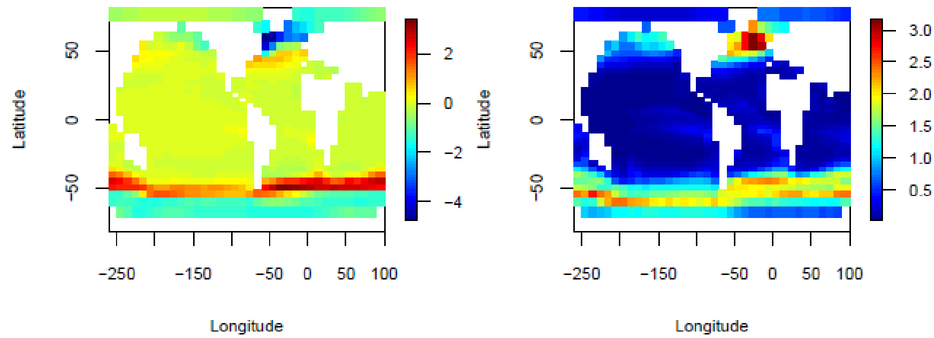

Fig. 13. LGM surface POC export flux change (molC m^{-2} yr^{-1}) ENS$_{104}$ ~~PGACF ensemble~~ mean (a) and standard deviation (b).

The largest LGM PGACF ensemble *increases* in POC export flux conversely occur at around 50 °S, roughly in front of the Antarctic sea ice margins. Increases in POC export are also simulated close to the North Pacific and Atlantic sea ice margins, as well as in the eastern equatorial Pacific and the southwest Atlantic upwelling region. The sea ice margin POC export flux increases are likely caused by the advection of unutilised nutrients from underneath the sea ice. However, they may additionally be caused by the enhanced iron availability from the increased supply of aeolian dust, particularly in the Southern Ocean and North Pacific since these are strongly limited by iron (Ridgwell et al., 2007). Iron fertilization may also explain the increases in POC export flux in the eastern equatorial Pacific and in the southwest Atlantic upwelling region. Comparison against observations suggests that the ensemble mean POC flux changes immediately north, and south of the Antarctic sea ice margins align with observations of increased and reduced marine productivity in the Subantarctic (~45 to 60 °N) and Southern Ocean respectively (Kohfeld et al., 2005; Kohfeld et al., 2013; Jaccard et al., 2013; Martínez-García et al., 2014). The simulated decreases in export flux in the Arctic and subarctic Atlantic (i.e. above ca. 50 °N), and the increases in export flux immediately south of 50°N are also in agreement with previous reconstructions (Kohfeld et al., 2005; Radi and de Vernal, 2008).

The mostly lower LGM export fluxes at the equator and in the South Atlantic are conversely inconsistent with the observational data of Kohfeld et al., (2005). The decreases may be caused by the increases in productivity in HNLC regions reducing the phosphate (the other limiting nutrient in GENIE-1 besides iron) availability for photosynthesis in other regions. They may additionally be due to the model not simulating enhanced nutrient inventories in response to enhanced weathering or reduced shallower water deposition of organic matter. The model also does not vary wind speed which may have resulted in stronger tropical upwelling in the Atlantic at the LGM. The evidence is more ambiguous (or missing) for the Pacific (Jaccard et al., 2010; Kohfeld and Chase, 2011; Kohfeld et al., 2005; Costa et al., 2016) and Indian Oceans (Kohfeld et al., 2005; Singh et al., 2011) and is therefore not discussed in more detail here.~~The evidence for the North Pacific is somewhat ambiguous. Jaccard et al. (2010) suggest there was a decrease in productivity in the subarctic western Pacific (at around 50 °N) while Kohfeld and Chase (2011) suggest that there was a decrease in productivity in the coastal northwest Pacific but also that the export fluxes in the open ocean may have been higher. The evidence for the equatorial Pacific is also mixed, with Kohfeld et al. (2005) suggesting that the export fluxes were higher during the LGM while Costa et al. (2016) suggest that productivity was reduced around the centre of the region. Ocean productivity data for the South Pacific appears to still be rather limited. In the Indian ocean, Kohfeld et al. (2005) suggest that LGM POC export fluxes were higher rather than lower, as in the PGACF ensemble mean, particularly in the equatorial region. Singh et al. (2011) conversely suggest that the fluxes were lower.~~

3.2.4~~4.5~~ Carbonate weathering and shallow water deposition

The ENS_{104} mean glacial weathering factor (GWS) is 1.16 $\pm$ 0.24 (corresponding to a percentage change in the land to ocean bicarbonate flux (%LOC) of 38.67), and the range is 0.52 to 1.5 (corresponding to a %LOC between -49.33 and 50). (Fig. 14). The GWS in ENS_{104} tends to be larger than in ENS_{315} and smaller than in ENS_{16}. There is also a negative correlation between GWS and ΔCO_2 (r = -0.52) in ENS_{315}, suggesting that increasing the input of bicarbonate to the ocean leads to a decrease in CO_2 by raising the inventories of ALK and DIC in a 2:1 ratio. In ENS_{104}, however, r is below the 0.05 significance level, suggesting that it is less important.

~~The PGACF ensemble glacial weathering factor (GWS) has a mean of 1.16~~ $\cancel{\pm}$ ~~0.24 (corresponding to a percentage change in the land to ocean bicarbonate flux (%LOC) of 38.67), and a range of 0.52 to 1.5 (corresponding to a %LOC between -49.33 and 50), roughly covering the range of prescribed glacial weathering changes in EFPC2 (Fig. 14). Compared to the EFPC2 ensemble, however, the GWS in the PGACF ensemble tends to be larger, while conversely tending to be smaller than in the PGACF-16 ensemble. There is also a negative correlation between GWS and~~ $\cancel{\Delta CO_2}$ ~~(r = -0.52) in the EFPC2 ensemble, suggesting that increasing the input of bicarbonate to the ocean leads to a decrease in~~ $\cancel{CO_2}$ ~~by raising the inventories of ALK and DIC in a 2:1 ratio. The total effect of varying GWS over its full range is ~ 40 ppmv (Fig. 15). In the PGACF ensemble, however, r is below the 0.05 significance level, suggesting that it is less important.~~

(a) (b)

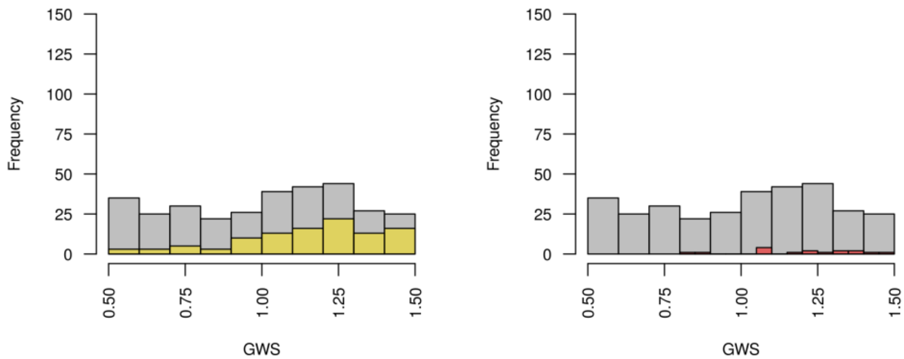

Fig. 14. GWS (a-b) distributions.

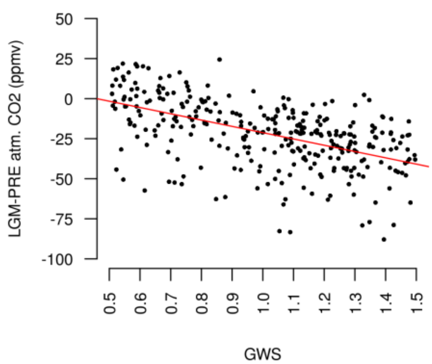

Fig. 15. Scatterplot of LGM change in atmospheric CO_2 versus GWS in the EFPC2 ensemble.

3.2.5~~4.6~~ Deep-sea carbonate burial

The ENS_{104} mean global deep-sea $CaCO_3$ burial flux anomaly ($\Delta CaCO3_{bur}$) is 0.036 $\pm$ 0.045 PgC yr^{-1} and the range is -0.098 to 0.139 PgC yr^{-1} (Fig. 15). The mean value is ca. 3 times larger than the observed value (Catubig et al., 1998), although the latter still falls within the range of simulated values. $\Delta CaCO3_{bur}$ in ENS_{104} tends to be higher than in ENS_{315}, and lower than in ENS_{16}. It is strongly determined by GWS, as suggested by the positive correlation (r = 0.88 and 0.9) between the two, in both ENS_{104} and ENS_{315}. Increasing %LOC should indeed cause the $CaCO_3$ burial flux to increase as increasing ALK means the deep ocean CO_3^{2-} will eventually increase, causing the saturation horizon to fall and allowing $CaCO_3$ to accumulate over greater areas (which are now exposed to undersaturated waters) (Sigman and Boyle, 2000). The input of ALK to the surface ocean will also increase the rate of $CaCO_3$ export production (which will in turn increase the sediment deposition flux of $CaCO_3$) since as discussed in Chikamoto et al. (2008), the latter is proportional to the production rate of POC (which is equal to the POC export flux), together with the sea surface saturation state with respect to $CaCO_3$, in GENIE-1. There is indeed also a positive correlation between %LOC and the global change in $CaCO_3$ export (r = 0.27 and 0.4), and between the latter and $\Delta CaCO3_{bur}$ (r = 0.34 and 0.45) in both ENS_{104} and ENS_{315}.

~~The PGACF ensemble global deep sea sediment $CaCO_3$ burial flux anomaly ($\Delta CaCO3_{bur}$) has a mean of 0.036 $\pm$ 0.045 PgC yr^{-1}, and a range of -0.098 to 0.139 PgC yr^{-1} (Fig. 16). The ensemble mean value is ca. 3 times larger than the observed value (Catubig et al., 1998), although the latter still falls within the range of simulated values. The $\Delta CaCO3_{bur}$ in the PGACF ensemble tend to be higher than in the EFPC2 ensemble, and lower than in PGACF-16 ensemble. It is strongly determined by GWS, as suggested by the positive correlation (r = 0.88 and 0.9) between the two, in both the PGACF and the EFPC2 ensembles. Increasing %LOC should indeed cause the $CaCO_3$ burial flux to increase as increasing ALK means the deep ocean CO_3^{2-} will eventually increase, causing the saturation horizon to fall and allowing $CaCO_3$ to accumulate over greater areas (which are now exposed to undersaturated waters) (Sigman and Boyle, 2000). The input of ALK to the surface ocean will also increase the rate of $CaCO_3$ export production (which will in turn increase the sediment deposition flux of $CaCO_3$) since as discussed in Chikamoto et al. (2008), the latter is proportional to the production rate of POC (which is equal to the POC export flux), together with the sea surface saturation state with respect to $CaCO_3$, in GENIE-1. There is indeed also a positive correlation between %LOC and the global change in $CaCO_3$ export (r = 0.27 and 0.4), and between the latter and $\Delta CaCO3_{bur}$ (r = 0.34 and 0.45) in both the PGACF and the EFPC2 ensembles.~~

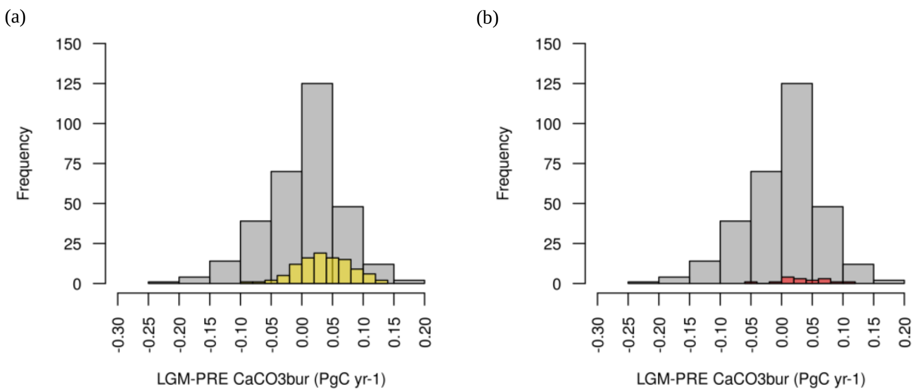

Fig. 15~~6~~. LGM change in deep sea sediment $CaCO_3$ burial flux (a-b) distributions.

The ENS_{104} mean spatial distribution of $\Delta CaCO3_{bur}$ is shown in Fig. 16. Relatively large increases in burial flux ($\geq 0.5 \times 10^{-5}$ mol cm^{-2} yr^{-1}) can be found at around 50 °S, in the North Pacific, and to a lesser extent the North Atlantic. In other regions, the burial flux is significantly lower or negative, with the largest losses ($\leq$ -0.5 $\times 10^{-5}$ mol cm^{-2} yr^{-1}) occurring the North Atlantic and arctic regions. The only exception is the western North Atlantic which exhibits a large in burial. A comparison of the results against the reconstructions of Catubig et al., 1998 is somewhat difficult as the coverage is poor but overall $CaCO_3$ burial was higher in the North Atlantic and the Pacific, and lower in the tropical and South Atlantic, and the Indian and Southern Ocean.

~~The PGACF ensemble mean spatial distribution of $\Delta CaCO3_{bur}$ is shown in Fig. 17, with the largest LGM increases in burial flux ($\geq 0.5 \times 10^{-5}$ mol cm^{-2} yr^{-1}) roughly coinciding with the largest increases in POC export flux, at around 50 °S, and in the North Atlantic, particularly around the west coast. Large increases can also be found in the North Pacific, but within rather than immediately south of the sea ice covered area. The largest decreases in burial flux ($\leq$ -0.5 $\times 10^{-5}$ mol cm^{-2} yr^{-1}) are found in the Arctic and North Atlantic, north of the sea ice limits, as well as in the Southern Hemisphere immediately south of the peak increases in burial flux. Comparison against the reconstructions of Catubig et al. (1998) suggests that the mostly negative burial changes in the Pacific Ocean are at odds with the observations, except in the western tropical Pacific. The largest increases in burial flux are also observed in the eastern equatorial Pacific, rather than in the North Pacific, as in the ensemble mean. A possible reason for the discrepancy is the underestimation of increases in productivity (and therefore increases in $CaCO_3$ export flux) in the eastern equatorial Pacific. Other disagreements between~~

~~the ensemble mean and the observations include the large ensemble mean increases in burial flux across the Atlantic, Indian and Pacific basins at around 50 °S, where observations conversely suggest the fluxes were lower, not higher. The simulated increases may be caused by an overestimation of ocean primary productivity (and therefore $CaCO_3$ export), or alternatively, an overestimation of $CaCO_3$ export fluxes only. The latter could be due to the lack of direct mechanism for reducing the surface rain ratio, such as Si fertilization, or the absence of a temperature control on $CaCO_3$ production since the latter may cease with SSTs below 10 °C (Iglesias-Rodriguez et al., 2002 in Brovkin et al., 2007).~~

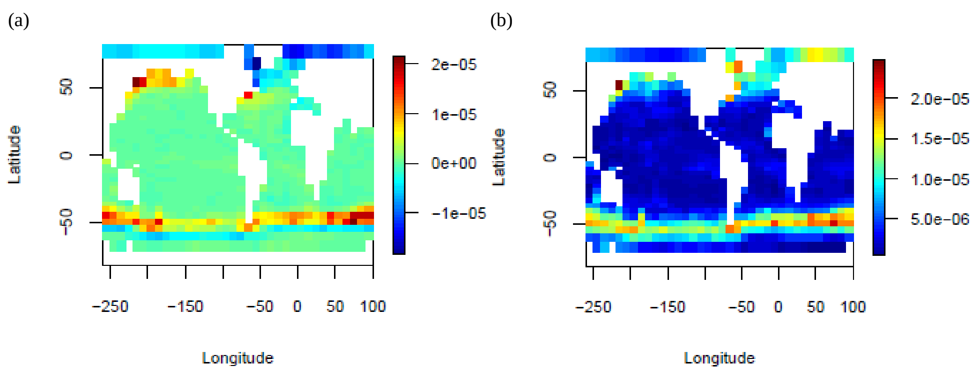

Fig. 16~~8~~. LGM deep sea $CaCO_3$ burial rate change (mol cm^{-2} yr^{-1}) ENS_{104} ~~PGACF ensemble~~ mean (a) and standard deviation (b).

3.2.6 Other paleo proxies

To further evaluate the sign and magnitude of our simulated LGM changes, and in particular ΔTerrC, a key future test would be to add carbon isotopes into GENIE-1's terrestrial biosphere carbon module and re-run the ENS_{104} LGM simulations with $\Delta^{14}C_{atm\ (DIC)}$ and $\delta^{13}C_{atm\ (DIC)}$ spun up. As shown in Table 4, a frequent argument for a lower glacial terrestrial carbon inventory is the reconstructed mean glacial ocean $\delta^{13}C$ value of ca. 0.35‰ lower than present due to the fact that plants discriminate against ^{13}C during photosynthesis. In our simulations conversely, it follows that the increase in glacial terrestrial carbon inventory would have resulted in an *increase* in ocean $\delta^{13}C$. However, other processes such as reduced marine productivity, lower SSTs (Schmitt et al., 2012) and greater sea ice area (Stephen and Keeling, 2000) may have counteracted at least some of this increase. Increasing LGM $CaCO_3$ weathering flux would have conversely raised ocean $\delta^{13}C$ although our model does not account for changes in the organic carbon weathering flux, which if increased would result in a decrease in $\delta^{13}C$. Wallmann (2014) attribute most of the observed LGM ocean $\delta^{13}C$ decrease to enhanced weathering and reduced deposition of organic carbon at continental margins due to lower sea levels. Menviel et al. (2015) have also shown that weaker surface winds can contribute to a lower ocean $\delta^{13}C$ while these are held fixed in our model. It has further been argued that enhanced glacial carbonate ion concentrations may have reduced the $\delta^{13}C$ in foraminera shells without altering mean ocean $\delta^{13}C$ (Lea et al., 1999).

As discussed in Zeng (2003) the glacial increase in terrestrial carbon inventory may also potentially explain transient trends in the glacial-interglacial atmospheric $\delta^{13}C$ record, such as the increase in atmospheric $\delta^{13}C$ over the glaciation, and the decrease of about 0.3 ‰ at the beginning of the deglaciation (Smith et al., 1999). Another feature of the deglacial record, namely the rise in $\delta^{13}C_{atm}$ between ca. 12 and 7 kyr BP, is in turn attributed to increasing SSTs and terrestrial biosphere regrowth on previously ice-covered areas. A more common explanation for the deglacial $\delta^{13}C_{atm}$ variation, which resembles the letter W, is conversely that the beginning of the pattern was caused by the release of old carbon from the deep ocean while the end of the pattern was largely due to terrestrial biosphere regrowth. The middle section of the W, characterised by subdued variation in $\delta^{13}C_{atm}$, is attributed to abrupt climate changes (Schmitt et al., 2012). More recently, however, it has also been suggested that the deglacial decrease in $\delta^{13}C_{atm}$ at ca. 17.5 kyr BP may be caused at least partly by the demise of iron-stimulated Southern Ocean biological productivity (Fischer et al., 2015) and the release of carbon from thawing permafrost (Crichton et al., 2016). A better test, therefore, would be for the ENS_{104} ensemble members to not only simulate LGM-PRE $\delta^{13}C_{atm}$ but also the transient changes in $\delta^{13}C_{atm}$ over the deglaciation. A further test would be to compare the simulated spatial distribution of $\delta^{13}C$ with observations (e.g. Menviel et al., 2017).

Another frequent but more indirect argument for a lower glacial terrestrial carbon inventory is the deglacial drop in atmospheric $\Delta^{14}C$, which is typically attributed to the release of old ocean carbon accumulated over the previous glacial period. Zeng (2007) and others (e.g. Zech, 2012) conversely propose that it is caused by the release of very old, and therefore ^{14}C-depleted, carbon from the terrestrial biosphere. More recent higher resolution records of deglacial $\Delta^{14}C$ and atmospheric CO_2 (e.g. Durand et al., 2013 in Köhler et al., 2014; Marcott et al., 2014) have, however, so far not been discussed by the enhanced glacial terrestrial carbon inventory studies. Another challenge is that a terrestrial biosphere-induced early deglacial decrease in atmospheric $\Delta^{14}C$ would have also led to a decrease in ocean $\Delta^{14}C$ and this is yet to be reconciled with ocean $\Delta^{14}C$ data. Studies so far have suggested there was a decrease in deep ocean $\Delta^{14}C$ during the glaciation, corresponding to an increase in ventilation age, and an increase in deep ocean $\Delta^{14}C$ at deglaciation, corresponding to a decrease in ventilation age, and also coinciding with the decrease in atmospheric $\Delta^{14}C$ (Hughen et al., 2006; Skinner et al., 2010; Skinner et al., 2015; de la Fuente et al., 2015; Freeman et al., 2015). With a reduced deep ocean ventilation at the LGM, it is assumed that the carbon sequestration capacity of the ocean was enhanced, and that the magnitude and spread of these changes resulted in a global increase rather than decrease in ocean carbon.

A potential limitation, however, with the use of ocean $\Delta^{14}C$ to infer larger LGM ocean carbon inventory pools is the presence of $\Delta^{14}C_{DIC}$ which indicate no change in ventilation age, or conversely an increase (Broecker and Barker, 2007; Broecker and Clark, 2010; Cléroux et al., 2010; Lund et al., 2011), and processes besides water mass aging which may have contributed to decreasing glacial $\Delta^{14}C_{DIC}$ such as decreasing atmospheric ^{14}C production rate, increased weathering of ^{14}C-depleted $CaCO_3$, input of ^{14}C-depleted carbon from the mantle and inaccurate estimation of surface ocean reservoir age (Broecker and Barker, 2007; Lund et al., 2011; Wagner and Hendy, 2015). The feasibility of a large extremely ^{14}C-depleted deep ocean carbon reservoir has also been contested in terms of atmospheric CO_2, deep ocean oxygen (namely the absence of large-scale anoxia) and $CaCO_3$ depth constraints (Hain et al., 2011), and from a dynamical standpoint (Broecker and Clark, 2010). Another strong future test would therefore be for ENS_{104} to simulate spatially resolved LGM ocean $\Delta^{14}C$, as well as the changes in atmospheric $\Delta^{14}C$ over the deglaciation.

Finally, we have shown that decreasing LGM atmospheric CO_2 in our ensemble tends to be accompanied by decreasing POC export production, which all else held constant would result in an increase in deep ocean oxygenation – a feature which we have not assessed. Proxy records to date conversely tend to indicate that there was a decrease, not an increase, in deep ocean oxygen concentration (Jaccard et al., 2016). When observed over sufficiently large areas, the latter supports the presence of an enhanced ocean carbon inventory as deoxygenation can be explained by reduced ocean ventilation (the sole input of oxygen is from the ocean surface) (Wagner and Hendy, 2015). As discussed above, the reduced ventilation is in turn assumed to have led to the accumulation of a significant amount of DIC in the ocean interior. Thus, explaining the lower deep ocean oxygen concentrations without having to reduce ocean ventilation as extensively as suggested by previous studies would as a minimum likely require LGM export production to have increased rather than decreased (assuming the enhanced POC export production does not automatically result in an increase in glacial ocean carbon inventory). Alternatively, it may be possible to increase deep ocean oxygen consumption by increasing organic matter at depth but keeping the surface POC export flux constant. This would require adding processes such as increasing remineralisation depth with decreasing ocean temperature and increasing ballasting into our model (Kohfeld and Ridgwell, 2009; Menviel et al., 2012). We also note that including missing processes affecting the ocean biological pump such as increased oceanic PO_4 inventory could potentially result in a net increase in LGM POC export, helping lower oxygen concentrations. However, this would then make reconciliation of our positive $\Delta TerrC$ with the observed negative LGM ocean $\delta^{13}C$ more difficult.

4~~5~~ Conclusions

We have used an uncertainty-based approach to investigating the LGM atmospheric CO_2 drop by simulating it with a large ensemble of parameter sets, designed to allow for a wide range of large-scale feedback response strengths. Our objective was not to definitely explain the causes of the CO_2 drop but rather explore the range of possible responses. Our investigation also involved simulating the CO_2 drop with the simulated CO_2 feeding back to the simulated climate, which is still relatively rare in LGM atmospheric CO_2 experiments, and the first time it is done with GENIE-1. Moreover, rather than assuming that terrestrial carbon gets destroyed by the LGM ice sheets, we allowed for its gradual burial. This assumption had not yet been implemented in an equilibrium set-up.

~~We have described the application, to preindustrial and LGM equilibrium simulations, of an ensemble of sets of model parameters which are thought to contribute to variability of atmospheric CO_2 on glacial/interglacial timescales. The ensemble (denoted EFPC2) was weakly constrained in Holden et al. (2013a) with eight preindustrial/modern metrics of the atmosphere, ocean, sea ice, terrestrial carbon, ocean biogeochemistry and ocean sediments, and were designed to allow for a wide range of large-scale feedback response strengths. The simulations were forced with orbital parameters, 2-D fields of orography and ice sheet fraction as well as oceanic dust deposition fields. The atmospheric CO_2 for the radiative code was generated internally. In the LGM simulations, a range of $CaCO_3$ weathering flux changes was prescribed in an attempt to take into account uncertainty in the observed weathering and shallow water deposition fluxes of $CaCO_3$. Changing sea level was also included as a variable parameter in order to capture the uncertainty in the magnitude of the sea level drop and its effects on the carbon cycle. The terrestrial biosphere carbon in ice sheet areas was, furthermore, configured to be preserved rather than destroyed, and to interact with the atmosphere prior to its burial.~~

~~The EFPC2 ensemble preindustrial global SAT, ψ_{max}, ψ_{min}, SIA_{SHW}, VegC, SoilC, wt% $CaCO_3$ and global ocean O_2 were compared against the results of Holden et al. (2013a) to verify reproducibility. The evaluation of the ensemble mean response against observations of ocean temperature, salinity, dissolved PO_4, dissolved O_2, alkalinity and DIC in Holden et al., 2013a was conversely not repeated. The ensemble results were also compared against new metrics, namely OceanC, SST, SIA to verify plausibility. In line with previous GENIE-1 studies, the ensemble mean OceanC was underestimated due to constraints on the model ocean volume. However, for ensemble mean SIA and SST, it was found that the values were in agreement with observations and had an error of comparable magnitude to that found in previous model studies respectively.~~

Despite our ensemble varying many of the parameters thought to contribute to variability in glacial-interglacial atmospheric CO_2, not all sources of uncertainty could be captured, and this was reflected in our simulated ΔCO_2 distribution. We estimated that up to ~60 ppmv of ΔCO_2 could be attributed to processes not included in our model and error in our process representations. As a result, we treated simulations with ΔCO_2 between ~-90 and -30 ppmv as "equally plausible", and focused on describing the physical and biogeochemical changes seen in this subset, as well as their linkages to ΔCO_2. We found the range of responses to be large, including the presence of five different ways of achieving a plausible ΔCO_2 in terms of the sign of individual carbon reservoir changes. However, several dominant changes could be detected. Namely: the LGM atmospheric CO_2 decrease tended to predominantly be associated with decreasing SSTs, increasing sea ice area, a weakening of the AMOC, a strengthening of the AABW cell in the Atlantic Ocean, a decreasing ocean biological productivity, an increasing $CaCO_3$

weathering flux and an increasing deep-sea $CaCO_3$ burial flux. The majority of our simulations also predicted an increase in terrestrial carbon, coupled with a decrease in ocean and an increase in lithospheric carbon. The increase in terrestrial carbon, which is uncommon in LGM simulations, was attributed to our choice to preserve rather than destroy ice sheet carbon, as well as the fact that the latter increased rather than decreased in response to climate forcings. If most of the carbon that was present in ice sheet areas at the end of the preindustrial runs had been lost to climate forcings, it would not matter much whether the remaining stocks had been destroyed or preserved. From the literature, it is not clear how much of the carbon in ice sheet areas is thought to have been lost strictly in response to ice sheet "bulldozing" versus climate impacts.

~~Analysis of the LGM-PRE results revealed a centering of the EFPC2 ensemble~~ $\cancel{\Delta CO_2}$ ~~around -20 ppmv and a simulated~~ $\cancel{\Delta CO_2}$ ~~between ~-90 and -30 ppmv in roughly a third of ensemble members. This range was deemed to capture the impact of error in the model's process representations and the impact of a few potentially important missing processes (acknowledging that a larger number of processes have previously been proposed). The fact that our model struggled to achieve a~~ $\cancel{\Delta CO_2}$ ~~of ~ -90 ppmv was argued to be significant because of the extensive exploration of model uncertainty that underpinned the building of our model ensemble. To move forward, we assumed that the impact of processes included in the model added linearly to the missing ones and that the ~ −30 to −90 ppmv~~ $\cancel{\Delta CO_2}$ ~~therefore represented a plausible glacial atmospheric~~ $\cancel{CO_2}$ ~~change (the PGACF ensemble). Rather than trying to determine the best parameter set within the PGACF ensemble, we explored the magnitude and direction of responses across the ensemble, to identify the emergent model output relationships. We also examined these across larger (EFPC2 ensemble: -88 to 74 ppmv) and smaller (PGACF-16: -88 to -59 ppmv)~~ $\cancel{\Delta CO_2}$ ~~ranges, to check against sample size artefacts and to determine whether processes' behaviour might vary across the~~ $\cancel{\Delta CO_2}$ ~~spectrum. The focus on a larger number of parameter sets was to prevent us from proposing a~~ $\cancel{\Delta CO_2}$ ~~solution with potentially the wrong balance of processes.~~

~~The ensemble members in the PGACF-16 ensemble, with~~ $\cancel{\Delta CO_2}$ ~~closer to observation than in the PGACF ensemble, were found to be associated, for the most part, with extreme cooling, which may have affected other parts of the model's behaviour. At the same time, however, our analyses revealed that the behaviour of the PGACF-16 ensemble tended to be consistent with that of the PGACF ensemble. The behaviour of the latter also aligned with that of the EFCP2 ensemble. In the PGACF ensemble, decreasing atmospheric~~ $\cancel{CO_2}$ ~~tended to be associated with decreasing SSTs, increasing sea ice area, a weakening of the AMOC, a strengthening of the AABW cell, a decreasing ocean biological productivity, an increasing land to ocean bicarbonate flux, an increasing terrestrial biosphere carbon inventory and an increasing deep-sea~~ $\cancel{CaCO_3}$ ~~burial flux. The majority of ensemble members were also found to not only predict an increase in terrestrial biosphere carbon but a decrease in ocean carbon and an increase in lithospheric carbon. In total, however, there were five different ways of achieving a plausible~~ $\cancel{\Delta CO_2}$ ~~in terms of the sign of individual carbon reservoir changes. The PGACF ensemble also predicted both positive and negative changes in global POC flux, AMOC and AABW cell strengths, and global~~ $\cancel{CaCO_3}$ ~~burial flux. The bidirectional change in global~~ $\cancel{CaCO_3}$ ~~burial flux is likely to be a consequence of prescribing both increases and decreases in the land to~~

~~ocean bicarbonate flux, as our analysis suggests the two are strongly correlated. The bidirectionality in AMOC/AABW strength change in turn suggests a non-linear response to the climate forcings, and may involve atmosphere, ocean and sea ice processes.~~

~~The predominantly positive ΔTerr in our ensemble was attributed primarily to the burial of ice sheet carbon. However, it was also shown that in the ensemble soil respiration tends to decrease significantly more than net photosynthesis, resulting in a relatively large increase in non-burial carbon. Assuming 90% of the terrestrial biosphere carbon induced atmospheric CO_2 perturbation gets removed by the oceans and the sediments (e.g. Zeng, 2003; Joos et al., 2004; Kohfeld and Ridgwell, 2009; Zech, 2012), the ΔCO_2 due to the PGACF ensemble mean ΔTerrC is -22 ppmv. Assuming a SST sensitivity of ca. 10 ppmv/°C (e.g. Menviel et al., 2012; Martin et al., 2005) in turn suggests a ΔCO_2 due to ΔSST of -18 ppmv. Their total effect would account for most of the simulated ΔCO_2. Taking into account the impact of decreasing sea level, however, would raise the atmospheric CO_2, as would decreasing POC export as less CO_2 is now being stored in ocean biota. A process which conversely will have further decreased atmospheric CO_2 is increasing $CaCO_3$ weathering (/decreasing $CaCO_3$ shallow water deposition), particularly since our regression analyses suggest an impact of around 40 ppmv when varying GWS over its full range.~~

An initial comparison of the dominant changes with observations and paleo-proxies suggested broad agreement. However, a comparison against carbon isotope data would be needed to more robustly determine agreement between our model results and empirical data. Another useful future research endeavour would be to investigate the relationships between the simulated changes and ensemble parameters, in order to help isolate the individual mechanisms that directly, or indirectly, cause atmospheric CO_2 to change.

~~To determine how realistic the aforementioned LGM changes are, the PGACF ensemble mean response was evaluated against observations of physical climate, ocean circulation, terrestrial biosphere carbon, and ocean and sediment biogeochemistry. Naturally some discrepancies were expected due to the differing ΔCO_2 between our ensemble and ice core records. The sign and magnitude of the global temperature responses, however, were aligned with observations. Our evaluation of the PGACF ensemble mean precipitation changes also suggested that the model reproduces certain key features such as the strong LGM decreases in precipitation around the North Atlantic region but fails to reproduce certain other features that are seemingly related to the model atmosphere's tendency to produce precipitation that is too evenly distributed and limited inter-basin moisture transport. A potential consequence of the latter at least is the overestimation of vegetation carbon density in Siberia, assuming that moisture is a limiting factor.~~

~~Due to the range of observed LGM AMOC and AABW cell strength responses, it was not possible to evaluate the model AMOC and AABW cell strength responses with great accuracy. It was conversely possible to evaluate the model AMOC cell's position as most data-based studies agree that the latter was shallower and that AABW penetrated further north. Despite the PGACF ensemble mean decrease in ψ_{max}, there was no apparent change in the position of the AMOC cell, potentially because of the concomitant decrease in ψ_{min} (stronger AABW cell). In the PGACF-16 ensemble, however the decreases in ψ_{min}~~

~~tended to be greater than in the PGACF ensemble and associated with a shoaling of the AMOC cell and enhanced penetration of AABW into the Atlantic. The agreement between the PGACF ensemble mean LGM terrestrial biosphere carbon change spatial distribution and observations was found to largely depend on the observations used and the amount of error attributed to these. As such, we consider our LGM terrestrial biosphere carbon change spatial distribution to not be implausible. With regard to LGM POC export flux changes, observations generally agree on the pattern of change in the Southern Ocean, and this was reproduced by the PGACF ensemble mean. However, there is uncertainty with regard to the sign of the LGM global POC export flux change. The general consensus with regard to the LGM global $CaCO_3$ burial flux change is conversely that it was very small. Deep ocean $[CO_3^{2-}]$ reconstructions also reveal LGM and Late Holocene (0-5 kyr BP) global mean deep ocean $[CO_3^{2-}]$ that are roughly similar (Yu et al., 2014). In contrast, the PGACF ensemble was found to predict a relatively large mean LGM global $CaCO_3$ burial flux increase. A potential cause of the discrepancy is our range of permissible $CaCO_3$ weathering/shallow water deposition flux changes. Increased terrestrial biosphere carbon inventories may have also contributed since they lead to an increase in $CaCO_3$ burial flux via the process of carbonate compensation. However, we do not yet rule out either of these processes as causes of ΔCO_2 since a high LGM global $CaCO_3$ burial rate bias may have been introduced by processes missing from the model, such as Si fertilisation, Si leakage and the effect of decreasing SSTs on $CaCO_3$ production. The impact of these processes would be to decrease the rain ratio at the sea bed, leading to a decrease in atmospheric CO_2 and increase in ocean carbon inventory. Wallmann (2014) also shows that changes in global $CaCO_3$ burial flux over the last ~ 100 kyr BP can be roughly reproduced without invoking a decrease in terrestrial carbon stocks, although their model does simulate an increase in DIC stock and an increase, not a decrease in POC export flux.~~

~~To further evaluate the sign and magnitude of our simulated LGM changes, and in particular ΔTerrC, a key future test would be to add carbon isotopes into GENIE-1's terrestrial biosphere carbon module and re-run the PGACF LGM simulations with $\Delta^{14}C_{atm\,(DIC)}$ and $\delta^{13}C_{atm\,(DIC)}$ spun up. As shown in Table 6, a frequent argument for a lower glacial terrestrial carbon inventory is the reconstructed mean glacial ocean $\delta^{13}C$ value of ca. 0.35‰ lower than present due to the fact that plants discriminate against ^{13}C during photosynthesis. In our simulations conversely, it follows that the increase in glacial terrestrial carbon inventory would have resulted in an *increase* in ocean $\delta^{13}C$. However, other processes such as reduced marine productivity, lower SSTs (Schmitt et al., 2012) and greater sea ice area (Stephen and Keeling, 2000) may have counteracted at least some of this increase. Increasing LGM $CaCO_3$ weathering flux would have conversely raised ocean $\delta^{13}C$ although our model does not account for changes in the organic carbon weathering flux, which if increased would result in a decrease in $\delta^{13}C$. Wallmann (2014) attribute most of the observed LGM ocean $\delta^{13}C$ decrease to enhanced weathering and reduced deposition of organic carbon at continental margins due to lower sea levels. Menviel et al. (2015) have also shown that weaker surface winds can contribute to a lower ocean $\delta^{13}C$ while these are held fixed in our model. It has further been argued that enhanced glacial carbonate ion concentrations may have reduced the $\delta^{13}C$ in foraminera shells without altering mean ocean $\delta^{13}C$ (Lea et al., 1999).~~

~~As discussed in Zeng (2003) the glacial increase in terrestrial carbon inventory may also potentially explain the increase in atmospheric $\delta^{13}C$ over the glaciation, as well the decrease of about 0.3 ‰ at the beginning of the deglaciation (Smith et al., 1999). Another feature of the deglacial record, namely the rise in $\delta^{13}C_{atm}$ between ca. 12 and 7 kyr BP, is in turn attributed to increasing SSTs and terrestrial biosphere regrowth on previously ice-covered areas. A more common explanation for the deglacial $\delta^{13}C_{atm}$ variation, which resembles the letter W, is conversely that the beginning of the pattern was caused by the release of old carbon from the deep ocean while the end of the pattern was largely due to terrestrial biosphere regrowth. The middle section of the W, characterised by subdued variation in $\delta^{13}C_{atm}$, is attributed to abrupt climate changes (Schmitt et al., 2012). More recently, however, it has also been suggested that the deglacial decrease in $\delta^{13}C_{atm}$ at ca. 17.5 kyr BP may be caused at least partly by the demise of iron-stimulated Southern Ocean biological productivity (Fischer et al., 2015) and the release of carbon from thawing permafrost (Crichton et al., 2016). A better test, therefore, would be for our PGACF ensemble members to not only simulate LGM-PRE $\delta^{13}C_{atm}$ but also the transient changes in $\delta^{13}C_{atm}$ over the deglaciation.~~

~~Another frequent but more indirect argument for a lower glacial terrestrial carbon inventory is the deglacial drop in atmospheric $\Delta^{14}C$, which is typically attributed to the release of old ocean carbon accumulated over the previous glacial period. Zeng (2007) and others (e.g. Zech, 2012) conversely propose that it is caused by the release of very old, and therefore ^{14}C-depleted, carbon from the terrestrial biosphere. More recent higher resolution records of deglacial $\Delta^{14}C$ and atmospheric CO_2 (e.g. Durand et al., 2013 in Köhler et al., 2014; Marcott et al., 2014) have, however, so far not been discussed by the enhanced glacial terrestrial carbon inventory studies. Another challenge is that the early deglacial decrease in atmospheric $\Delta^{14}C$ would have also led to a decrease in ocean $\Delta^{14}C$ and this is yet to be reconciled with ocean $\Delta^{14}C$ data. Studies so far have suggested there was a decrease in deep ocean $\Delta^{14}C$ during the glaciation, corresponding to an increase in ventilation age, and an increase in deep ocean $\Delta^{14}C$ at deglaciation, corresponding to a decrease in ventilation age, and also coinciding with the decrease in atmospheric $\Delta^{14}C$ (Hughen et al., 2006; Skinner et al., 2010; Skinner et al., 2015; de la Fuente et al., 2015; Freeman et al., 2015). With a reduced deep ocean ventilation at the LGM, it is assumed that the carbon sequestration capacity of the ocean was enhanced, and that the magnitude and spread of these changes resulted in a global increase rather than decrease in ocean carbon.~~

~~A potential limitation, however, with the use of ocean $\Delta^{14}C$ to infer larger LGM ocean carbon inventory pools is the presence of $\Delta^{14}C_{DIC}$ which indicate no change in ventilation age, or conversely an increase (Broecker and Barker, 2007; Broecker and Clark, 2010; Cléroux et al., 2010; Lund et al., 2011), and processes besides water mass aging which may have contributed to decreasing glacial $\Delta^{14}C_{DIC}$ such as decreasing atmospheric ^{14}C production rate, increased weathering of ^{14}C-depleted $CaCO_3$, input of ^{14}C-depleted carbon from the mantle and inaccurate estimation of surface ocean reservoir age (Broecker and Barker, 2007; Lund et al., 2011; Wagner and Hendy, 2015). The feasibility of a large extremely ^{14}C-depleted deep ocean carbon reservoir has also been contested in terms of atmospheric CO_2, deep ocean oxygen (namely the absence of large-scale anoxia)~~

~~and $CaCO_3$ depth constraints (Hain et al., 2011), and from a dynamical standpoint (Broecker and Clark, 2010). Another strong future test would therefore for our PGACF ensemble to simulate spatially resolved LGM ocean $\Delta^{14}C$, as well as the changes in atmospheric $\Delta^{14}C$ over the deglaciation.~~

~~Finally, we have shown that decreasing LGM atmospheric CO_2 in our ensemble tends to be accompanied by decreasing POC export production, which all else held constant would result in an increase in deep ocean oxygenation – a feature which we have not assessed. Proxy records to date conversely tend to indicate that there was a decrease, not an increase, in deep ocean oxygen concentration (Jaccard et al., 2016). When observed over sufficiently large areas, the latter supports the presence of an enhanced ocean carbon inventory as deoxygenation can be explained by reduced ocean ventilation (the sole input of oxygen is from the ocean surface) (Wagner and Hendy, 2015). As discussed above, the reduced ventilation is in turn assumed to have led to the accumulation of a significant amount of DIC in the ocean interior. Thus, explaining the lower deep ocean oxygen concentrations without having to reduce ocean ventilation as extensively as suggested by previous studies would as a minimum likely require LGM export production to have increased rather than decreased (assuming the enhanced POC export production does not automatically result in an increase in glacial ocean carbon inventory). Alternatively, it may be possible to increase deep ocean oxygen consumption by increasing organic matter at depth but keeping the surface POC export flux constant. This would require adding processes such as increasing remineralisation depth with decreasing ocean temperature and increasing ballasting into our model (Kohfeld and Ridgwell, 2009; Menviel et al., 2012). We also note that including missing processes affecting the ocean biological pump such as increased oceanic PO_4 inventory could potentially result in a net increase in LGM POC export, helping lower oxygen concentrations. However, this would then make reconciliation of our positive ΔTerrC with the observed negative LGM ocean $\delta^{13}C$ more difficult.~~

Acknowledgements

This work made use of the Darwin Supercomputer of the University of Cambridge High Performance Computing Service (HPCS). K.M.S. Kemppinen thanks staff at HPCS for their technical support, and Antara Banerjee and Alex Archibald for help with R This manuscript was greatly improved by comments from an anonymous reviewer.

References

Adams, J. M. and Faure, H.: A new estimate of changing carbon storage on land since the last glacial maximum, based on global land ecosystem reconstruction, Glob. Planet. Change, 16–17, 3–24, doi:10.1016/S0921-8181(98)00003-4, 1998.

Adkins, J. F., Mcintyre, K. and Schrag, D. P.: The Salinity, Temperature, and d18O of the Glacial Deep Ocean, Science, 298(November), 1769–1773, doi:10.1126/science.1076252, 2002.

Alder, J. R. and Hostetler, S. W.: Global climate simulations at 3000-year intervals for the last 21 000 years with the GENMOM coupled atmosphere-ocean model, Clim. Past, 11(3), 449–471, doi:10.5194/cp-11-449-2015, 2015.

Allen, K. A., Sikes, E. L., Hönisch, B., Elmore, A. C., Guilderson, T. P., Rosenthal, Y. and Anderson, R. F.: Southwest Pacific deep water carbonate chemistry linked to high southern latitude climate and atmospheric CO2 during the Last Glacial Termination, Quat. Sci. Rev., 122, 180–191, doi:10.1016/j.quascirev.2015.05.007, 2015.

Anderson, R. F., Ali, S., Bradtmiller, L. I., Nielsen, S. H. H., Fleisher, M. Q., Anderson, B. E. and Burckle, L. H.: Wind-Driven Upwelling in the Southern Ocean and the Deglacial Rise in Atmospheric CO2, Science, 323(5920), 1443–1448, doi:10.1126/science.1167441, 2009.

Annan, J. D. and Hargreaves, J. C.: A new global reconstruction of temperature changes at the Last Glacial Maximum, Clim. Past, 9(1), 367–376, doi:10.5194/cp-9-367-2013, 2013.Annan, J. D. and Hargreaves, J. C.: Efficient identification of ocean thermodynamics in a physical/biogeochemical ocean model with an iterative Importance Sampling method, Ocean Model., 32(3–4), 205–215, doi:10.1016/j.ocemod.2010.02.003, 2010.

Ballarotta, M., Falahat, S., Brodeau, L. and Döös, K.: On the glacial and interglacial thermohaline circulation and the associated transports of heat and freshwater, Ocean Sci., 10(6), 907–921, doi:10.5194/os-10-907-2014, 2014.

Bartlein, P. J., Harrison, S. P., Brewer, S., Connor, S., Davis, B. A. S., Gajewski, K., Guiot, J., Harrison-Prentice, T. I., Henderson, A., Peyron, O., Prentice, I. C., Scholze, M., Seppä, H., Shuman, B., Sugita, S., Thompson, R. S., Viau, A. E., Williams, J. and Wu, H.: Pollen-based continental climate reconstructions at 6 and 21 ka: A global synthesis, Clim. Dyn., 37(3), 775–802, doi:10.1007/s00382-010-0904-1, 2011.

Berger, A.: Long-term variations of daily insolation and quaternary climatic changes, J. Atmos. Sci. 35(12), 2362–2367, 1978.

Böhm, E., Lippold, J., Gutjahr, M., Frank, M., Blaser, P., Antz, B., Fohlmeister, J., Frank, N., Andersen, M. B. and Deininger, M.: Strong and deep Atlantic meridional overturning circulation during the last glacial cycle, Nature, 517(7534), 73–76, doi:10.1038/nature14059, 2015.

Bopp, L., Kohfeld, K. E., Le Quéré, C. and Aumont, O.: Dust impact on marine biota and atmospheric CO2 during glacial periods, Paleoceanography, 18(2), 1046, dio:10.1029/2002PA000810, doi:10.1029/2002PA000810, 2003.

Bouttes, N., Paillard, D. and Roche, D. M.: Impact of brine-induced stratification on the glacial carbon cycle, Clim. Past, 6(5), 575–589, doi:10.5194/cp-6-575-2010, 2010.

Bouttes, N., Paillard, D., Roche, D. M., Brovkin, V. and Bopp, L.: Last Glacial Maximum CO2 and δ13C successfully reconciled, Geophys. Res. Lett., 38(2), Citation No. L02705, doi:10.1029/2010gl044499, 2011.

Broecker, W. and Barker, S.: A 190‰ drop in atmosphere's Δ14C during the "Mystery Interval" (17.5 to 14.5 kyr), Earth Planet. Sci. Lett., 256(1–2), 90–99, doi:10.1016/j.epsl.2007.01.015, 2007.

Broecker, W. and Clark, E.: Search for a glacial-age 14C-depleted ocean reservoir, Geophys. Res. Lett., 37(13), doi:10.1029/2010GL043969, 2010.

Brovkin, V. and Ganopolski, A.: The role of the terrestrial biosphere in CLIMBER-2 simulations of the last glacial CO2 cycles. Nova Act Lc NF, 121, 43-47, 2015.

Brovkin, V., Hofmann, M., Bendtsen, J. and Ganopolski, A.: Ocean biology could control atmospheric delta C-13 during glacial-interglacial cycle, Geochemistry Geophys. Geosystems, 3, 22, doi:1027\r10.1029/2001gc000270, 2002.

Brovkin, V., Ganopolski, A., Archer, D. and Rahmstorf, S.: Lowering of glacial atmospheric CO2 in response to changes on oceanic circulation and marine biogeochemistry, Paleoceanography, 22(4), doi:10.1029/2006PA001380, 2007.

Brovkin, V., Ganopolski, A., Archer, D. and Munhoven, G.: Glacial CO 2 cycle as a succession of key physical and biogeochemical processes, Clim. Past, 8(1), 251–264, doi:10.5194/cp-8-251-2012, 2012.

Buchanan, P. J., Matear, R. J., Lenton, A., Phipps, S. J., Chase, Z. and Etheridge, D.: The simulated climate of the Last Glacial Maximum and insights into the global carbon cycle, Clim. Past Discuss., 11(2), 1–45, doi:10.5194/cp-2016-73, 2016.

Catubig, N. R., Archer, D. E., Francois, R., DeMenocal, P., Howard, W. and Yu, E. F.: Global deep-sea burial rate of calcium carbonate during the Last Glacial Maximum, Paleoceanography, 13(3), 298–310, doi:10.1029/98PA00609, 1998.

Chikamoto, M. O., Matsumoto, K. and Ridgwell, A.: Response of deep-sea CaCO3 sedimentation to Atlantic meridional overturning circulation shutdown, J. Geophys. Res. Biogeosciences, 113(3), doi:10.1029/2007JG000669, 2008.

Chikamoto, M. O., Abe-Ouchi, A., Oka, A., Ohgaito, R. and Timmermann, A.: Quantifying the ocean’s role in glacial CO2 reductions, Clim. Past, 8(2), 545–563, doi:10.5194/cp-8-545-2012, 2012.

Ciais, P., Tagliabue, A., Cuntz, M., Bopp, L., Scholze, M., Hoffmann, G., Lourantou, A., Harrison, S. P., Prentice, I. C., Kelley, D. I., Koven, C. and Piao, S. L.: Large inert carbon pool in the terrestrial biosphere during the Last Glacial Maximum, Nat. Geosci., 5(1), 74–79, doi:10.1038/ngeo1324, 2012.

Ciais, P., Sabine, C., Bala, G., Bopp, L., Brovkin, V., Canadell, J., Chhabra, A., DeFries, R., Galloway, J., Heimann, M., Jones, C., Quéré, C. Le, Myneni, R. B., Piao, S. and Thornton, P.: The physical science basis. Contribution of working group I to the fifth assessment report of the intergovernmental panel on climate change, Chang. IPCC Clim., 465–570, doi:10.1017/CBO9781107415324.015, 2013.

Cléroux, C., deMenocal, P. and Guilderson, T.: Deglacial radiocarbon history of tropical Atlantic thermocline waters: Absence of CO2 reservoir purging signal, Quat. Sci. Rev., 30(15–16), 1875–1882, doi:10.1016/j.quascirev.2011.04.015, 2011.

Colbourn, G.: Weathering effects on the carbon cycle in an Earth System Model, Ph.D. thesis, School of Environmental Sciences, University of East Anglia, United Kingdom, 2011.

Costa, K. M., McManus, J. F., Anderson, R. F., Ren, H., Sigman, D. M., Winckler, G., Fleisher, M. Q., Marcantonio, F. and Ravelo, A. C.: No iron fertilization in the equatorial Pacific Ocean during the last ice age, Nature, 529(7587), 519–522, doi:10.1038/nature16453, 2016.

Crichton, K. A., Bouttes, N., Roche, D. M., Chappellaz, J. and Krinner, G.: Permafrost carbon as a missing link to explain CO 2 changes during the last deglaciation, Nat. Geosci., 9(9), 683–686, doi:10.1038/ngeo2793, 2016.

Crocket, K.C., Vance, D., Foster, G.L., Richards, D.A. and Tranter, M.:Continental weathering fluxes during the last glacial/interglacial cycle: insights from the marine sedimentary Pb isotope record at Orphan Knoll, NW Atlantic, Quaternary Sci Rev 38: 89-99. Doi: 10.1016/j.quascirev.2012.02.004, 2012.

Crowley, T. J.: Ice Age terrestrial carbon changes revisited, Global Biogeochem. Cycles, 9(3), 377–389, doi:10.1029/95GB01107, 1995.

De La Fuente, M., Skinner, L., Calvo, E., Pelejero, C. and Cacho, I.: Increased reservoir ages and poorly ventilated deep waters inferred in the glacial Eastern Equatorial Pacific, Nat. Commun., 6, doi:10.1038/ncomms8420, 2015.

Doney, S. C., Lindsay, K., Fung, I. and John, J.: Natural variability in a stable, 1000-yr global coupled climate-carbon cycle simulation, J. Clim., 19(13), 3033–3054, doi:10.1175/JCLI3783.1, 2006.

Durand, N., Deschamps, P., Bard, E., Hamelin, B., Camoin, G., Thomas, A. L., Henderson, G. M., Yokoyama, Y. and Matsuzaki, H.: Comparison of 14C and U-Th Ages in Corals from IODP #310 Cores Offshore Tahiti, Radiocarbon, 55(4), 1947–1974, doi:10.2458/azu_js_rc.v55i2.16134, 2013.

~~Edwards, N. R., Cameron, D. and Rougier, J.: Precalibrating an intermediate complexity climate model, Clim. Dyn., 37(7–8), 1469–1482, doi:10.1007/s00382-010-0921-0, 2011.~~

Edwards, N. R. and Marsh, R.: Uncertainties due to transport-parameter sensitivity in an efficient 3-D ocean-climate model, Clim. Dyn., 24(4), 415–433, doi:10.1007/s00382-004-0508-8, 2005.

Ferrari, R., Jansen, M. F., Adkins, J. F., Burke, A., Stewart, A. L. and Thompson, A. F.: Antarctic sea ice control on ocean circulation in present and glacial climates, Proc. Natl. Acad. Sci., 111(24), 8753–8758, doi:10.1073/pnas.1323922111, 2014.

Fischer, H. , Schmitt, J. , Schneider, R. , Eggleston, S. , Joos, F. , Bauska, T. K. , Marcott, S. A. , Brook, E. J. , Köhler, P. and Chappellaz, J.: Latest Insights into Past Carbon Cycle Changes from CO2 and δ13Catm , Nova Act Lc, 121 (408), 59-63, 2015.

Foster, G. L. and Vance, D.: Negligible glacial-interglacial variation in continental chemical weathering rates, Nature, 444(7121), 918–921, doi:10.1038/nature05365, 2006.

Franzen, L. G.: Are wetlands the key to the ice-age cycle enigma, Ambio, 23(4), 300–308, 1994.

Franzén, L.G. and Cropp, R.A.: The Peatland/ice age Hypothesis revised, adding a possible glacial pulse trigger. Geogr. Ann., 89 A (4): 301–330, 2007.

Freeman, E., Skinner, L. C., Tisserand, A., Dokken, T., Timmermann, A., Menviel, L. and Friedrich, T.: An Atlantic-Pacific ventilation seesaw across the last deglaciation, Earth Planet. Sci. Lett., 424, 237–244, doi:10.1016/j.epsl.2015.05.032, 2015.

Gebbie, G.: How much did Glacial North Atlantic Water shoal?, Paleoceanography, 29(3), 190–209, doi:10.1002/2013PA002557, 2014.

Goodwin, P. and Lauderdale, J. M.: Carbonate ion concentrations, ocean carbon storage, and atmospheric CO 2, Global Biogeochem. Cycles, 27(3), 882–893, doi:10.1002/gbc.20078, 2013.

Hain, M. P., Sigman, D. M. and Haug, G. H.: Shortcomings of the isolated abyssal reservoir model for deglacial radiocarbon changes in the mid-depth Indo-Pacific Ocean, Geophys. Res. Lett., 38(4), doi:10.1029/2010GL046158, 2011.

Harrison, K. G.: Role of increased marine silica input on paleo-pCO<inf>2</inf> levels, Paleoceanography, 15(3), 292–298, doi:10.1029/1999PA000427, 2000.

Holden, P. B., Edwards, N. R., Oliver, K. I. C., Lenton, T. M. and Wilkinson, R. D.: A probabilistic calibration of climate sensitivity and terrestrial carbon change in GENIE-1, Clim. Dyn., 35(5), 785–806, doi:10.1007/s00382-009-0630-8, 2010a.

Holden, P. B., Edwards, N. R., Wolff, E. W., Lang, N. J., Singarayer, J. S., Valdes, P. J. and Stocker, T. F.: Interhemispheric coupling, the West Antarctic Ice Sheet and warm Antarctic interglacials, Clim. Past, 6(4), 431–443, doi:10.5194/cp-6-431-2010, 2010b.

Holden, P. B., Edwards, N. R., Müller, S. A., Oliver, K. I. C., Death, R. M. and Ridgwell, A.: Controls on the spatial distribution of oceanic δ13CDIC, Biogeosciences, 10(3), 1815–1833, doi:10.5194/bg-10-1815-2013, 2013a.

Holden, P. B., Edwards, N. R., Gerten, D. and Schaphoff, S.: A model-based constraint on CO2 fertilisation, Biogeosciences, 10(1), 339–355, doi:10.5194/bg-10-339-2013, 2013b.

Houghton, J. T., Jenkins, G. J., Ephraums, J. J.: Climate Change. The IPCC Scientitific Assessment. Cambridge University Press, Cambridge, 1990.

Hughen, K., Southon, J., Lehman, S., Bertrand, C. and Turnbull, J.: Marine-derived 14C calibration and activity record for the past 50,000 years updated from the Cariaco Basin, Quat. Sci. Rev., 25(23–24), 3216–3227, doi:10.1016/j.quascirev.2006.03.014, 2006.

Iglesias-Rodríguez, M. D., Brown, C. W., Doney, S. C., Kleypas, J., Kolber, D., Kolber, Z., Hayes, P. K. and Falkowski, P. G.: Representing key phytoplankton functional groups in ocean carbon cycle models: Coccolithophorids, Global Biogeochem. Cycles, 16(4), 47-1-47–20, doi:10.1029/2001GB001454, 2002.

Jaccard, S. L., Galbraith, E. D., Sigman, D. M. and Haug, G. H.: A pervasive link between Antarctic ice core and subarctic Pacific sediment records over the past 800 kyrs, Quat. Sci. Rev., 29(1–2), 206–212, doi:10.1016/j.quascirev.2009.10.007, 2010.

Jaccard, S. L., Hayes, C. T., Martinez-Garcia, A., Hodell, D. A., Anderson, R. F., Sigman, D. M. and Haug, G. H.: Two Modes of Change in Southern Ocean Productivity Over the Past Million Years, Science, 339(6126), 1419–1423, doi:10.1126/science.1227545, 2013.

Jaccard, S. L., Galbraith, E. D., Martínez-Garciá, A. and Anderson, R. F.: Covariation of deep Southern Ocean oxygenation and atmospheric CO2 through the last ice age, Nature, 530(7589), 207–210, doi:10.1038/nature16514, 2016.

Jones, I. W., Munhoven, G., Tranter, M., Huybrechts, P. and Sharp, M. J.: Modelled glacial and non-glacial HCO3−, Si and Ge fluxes since the LGM: Little potential for impact on atmospheric CO2concentrations and a potential proxy of continental chemical erosion, the marine Ge/Si ratio, Glob. Planet. Change, 33(1–2), 139–153, doi:10.1016/S0921-8181(02)00067-X, 2002.

Joos, F., Gerber, S., Prentice, I. C., Otto-Bliesner, B. L. and Valdes, P. J.: Transient simulations of Holocene atmospheric carbon dioxide and terrestrial carbon since the Last Glacial Maximum, Global Biogeochem. Cycles, 18(2), doi:10.1029/2003GB002156, 2004.

Kim, S.-J., Flato, G. and Boer, G.: A coupled climate model simulation of the Last Glacial Maximum, Part 2: approach to equilibrium, Clim. Dyn., 20(6), 635–661, doi:10.1007/s00382-002-0292-2, 2003.

Kleypas, J. A.: Modeled estimates of global reef habitat and carbonate production since the last glacial maximum, Paleoceanography, 12(4), 533–545, doi:10.1029/97PA01134, 1997.

Kohfeld, K. E.: Role of Marine Biology in Glacial-Interglacial CO2 Cycles, Science, 308(5718), 74–78, doi:10.1126/science.1105375, 2005.

Kohfeld, K. E. and Chase, Z.: Controls on deglacial changes in biogenic fluxes in the North Pacific Ocean, Quat. Sci. Rev., 30(23–24), 3350–3363, doi:10.1016/j.quascirev.2011.08.007, 2011.

Kohfeld, K. E. and Ridgwell, A.: Glacial-Interglacial Variability in Atmospheric CO2, Surf. Ocean. Atmos. Process., 251–286, doi:10.1029/2008GM000845, 2009.

Kohfeld, K. E., Graham, R. M., de Boer, A. M., Sime, L. C., Wolff, E. W., Le Quéré, C. and Bopp, L.: Southern Hemisphere westerly wind changes during the Last Glacial Maximum: Paleo-data synthesis, Quat. Sci. Rev., 68, 76–95, doi:10.1016/j.quascirev.2013.01.017, 2013.

Köhler, P., Knorr, G. and Bard, E.: Permafrost thawing as a possible source of abrupt carbon release at the onset of the Bølling/Allerød, Nat. Commun., 5, doi:10.1038/ncomms6520, 2014.

Lambert, F., Tagliabue, A., Shaffer, G., Lamy, F., Winckler, G., Farias, L., Gallardo, L. and De Pol-Holz, R.: Dust fluxes and iron fertilization in Holocene and Last Glacial Maximum climates, Geophys. Res. Lett., 42(14), 6014–6023, doi:10.1002/2015GL064250, 2015.

Lea, D. W., Bijma, J., Spero, H. J. and Archer, D.: Implications of a Carbonate Ion Effect on Shell Carbon and Oxygen Isotopes for Glacial Ocean Conditions, Use Proxies Paleoceanogr. Examples from South Atl., 513–522, 1999.

Lenton, T. M., Williamson, M. S., Edwards, N. R., Marsh, R., Price, A. R., Ridgwell, A. J., Shepherd, J. G. and Cox, S. J.: Millennial timescale carbon cycle and climate change in an efficient Earth system model, Clim. Dyn., 26(7–8), 687–711, doi:10.1007/s00382-006-0109-9, 2006.

Lenton, T. M., Marsh, R., Price, A. R., Lunt, D. J., Aksenov, Y., Annan, J. D., Cooper-Chadwick, T., Cox, S. J., Edwards, N. R., Goswami, S., Hargreaves, J. C., Harris, P. P., Jiao, Z., Livina, V. N., Payne, A. J., Rutt, I. C., Shepherd, J. G., Valdes, P. J., Williams, G., Williamson, M. S. and Yool, A.: Effects of atmospheric dynamics and ocean resolution on bi-stability of the thermohaline circulation examined using the Grid ENabled Integrated Earth system modelling (GENIE) framework, Clim. Dyn., 29(6), 591–613, doi:10.1007/s00382-007-0254-9, 2007.

Lippold, J., Luo, Y., Francois, R., Allen, S. E., Gherardi, J., Pichat, S., Hickey, B. and Schulz, H.: Strength and geometry of the glacial Atlantic Meridional Overturning Circulation, Nat. Geosci., 5(11), 813–816, doi:10.1038/ngeo1608, 2012.

Lund, D. C., Mix, A. C. and Southon, J.: Increased ventilation age of the deep northeast Pacific Ocean during the last deglaciation, Nat. Geosci., 4(11), 771–774, doi:10.1038/ngeo1272, 2011.

~~Lunt, D. J., Williamson, M. S., Valdes, P. J., Lenton, T. M. and Marsh, R.: Comparing transient, accelerated, and equilibrium simulations of the last 30 000 years with the GENIE-1 model, Clim. Past, 2, 221–235, doi:10.5194/cp-2-221-2006, 2006.~~

Lupker, M., France-Lanord, C., Galy, V., Lavé, J. and Kudrass, H.: Increasing chemical weathering in the Himalayan system since the Last Glacial Maximum, Earth Planet. Sci. Lett., 365, 243–252, doi:10.1016/j.epsl.2013.01.038, 2013.

Lynch-Stieglitz, J., Adkins, J. F., Curry, W. B., Dokken, T., Hall, I. R., Herguera, J. C., Hirschi, J. J.-M., Ivanova, E. V, Kissel, C., Marchal, O., Marchitto, T. M., McCave, I. N., McManus, J. F., Mulitza, S., Ninnemann, U., Peeters, F., Yu, E.-F. and

Zahn, R.: Atlantic meridional overturning circulation during the Last Glacial Maximum., Science, 316(5821), 66–69, doi:10.1126/science.1137127, 2007.

Ma, W. and Tian, J.: Modeling the contribution of dissolved organic carbon to carbon sequestration during the last glacial maximum, Geo-Marine Lett., 34(5), doi:10.1007/s00367-014-0378-y, 2014.

Mahowald, N. M., Muhs, D. R., Levis, S., Rasch, P. J., Yoshioka, M., Zender, C. S. and Luo, C.: Change in atmospheric mineral aerosols in response to climate: Last glacial period, preindustrial, modern, and doubled carbon dioxide climates, J. Geophys. Res. Atmos., 111(10), doi:10.1029/2005JD006653, 2006.

Marcott, S. A., Bauska, T. K., Buizert, C., Steig, E. J., Rosen, J. L., Cuffey, K. M., Fudge, T. J., Severinghaus, J. P., Ahn, J., Kalk, M. L., McConnell, J. R., Sowers, T., Taylor, K. C., White, J. W. C. and Brook, E. J.: Centennial-scale changes in the global carbon cycle during the last deglaciation, Nature, 514(7524), 616–619, doi:10.1038/nature13799, 2014.

Marsh, R., Muller, S. A., Yool, A., and Edwards, N. R.: Incorporation of the C-GOLDSTEIN efficient climate model into the GENIE framework: “eb go gs” configurations of GENIE, Geosci. Model Dev., 4, 957–992, doi:10.5194/gmd-4-957-2011, 2011.

Martin, P., Archer, D. and Lea, D. W.: Role of deep sea temperature in the carbon cycle during the last glacial, Paleoceanography, 20(2), 1–10, doi:10.1029/2003PA000914, 2005.

Martinez-Garcia, A., Sigman, D. M., Ren, H., Anderson, R. F., Straub, M., Hodell, D. A., Jaccard, S. L., Eglinton, T. I. and Haug, G. H.: Iron Fertilization of the Subantarctic Ocean During the Last Ice Age, Science, 343(6177), 1347–1350, doi:10.1126/science.1246848, 2014.

Masson-Delmotte, V., Kageyama, M., Braconnot, P., Charbit, S., Krinner, G., Ritz, C., Guilyardi, E., Jouzel, J., Abe-Ouchi, A., Crucifix, M., Gladstone, R. M., Hewitt, C. D., Kitoh, A., LeGrande, A. N., Marti, O., Merkel, U., Motoi, T., Ohgaito, R., Otto-Bliesner, B., Peltier, W. R., Ross, I., Valdes, P. J., Vettoretti, G., Weber, S. L., Wolk, F. and Yu, Y.: Past and future polar amplification of climate change: Climate model intercomparisons and ice-core constraints, Clim. Dyn., 26(5), 513–529, doi:10.1007/s00382-005-0081-9, 2006.

Matsumoto, K., Sarmiento, J. L. and Brzezinski, M. A.: Silicic acid leakage from the Southern Ocean: A possible explanation for glacial atmospheric *p* CO_2, Global Biogeochem. Cycles, 16(3), 5-1-5–23, doi:10.1029/2001GB001442, 2002.

Matsumoto, K., Hashioka, T. and Yamanaka, Y.: Effect of temperature-dependent organic carbon decay on atmospheric pCO2, J. Geophys. Res. Biogeosciences, 112(2), doi:10.1029/2006JG000187, 2007.

Matsumoto, K., Tokos, K., Huston, A. and Joy-Warren, H.: MESMO 2: A mechanistic marine silica cycle and coupling to a simple terrestrial scheme, Geosci. Model Dev., 6(2), 477–494, doi:10.5194/gmd-6-477-2013, 2013.

Matsumoto, K., Chase, Z. and Kohfeld, K.: Different mechanisms of silicic acid leakage and their biogeochemical consequences, Paleoceanography, 29(3), 238–254, doi:10.1002/2013PA002588, 2014.

Menviel, L., Joos, F. and Ritz, S. P.: Simulating atmospheric CO 2, 13C and the marine carbon cycle during the Last Glacial-Interglacial cycle: Possible role for a deepening of the mean remineralization depth and an increase in the oceanic nutrient inventory, Quat. Sci. Rev., 56, 46–68, doi:10.1016/j.quascirev.2012.09.012, 2012.

Menviel, L., Mouchet, A., Meissner, K. J., Joos, F. and England, M. H.: Impact of oceanic circulation changes on atmospheric δ13CO2, Global Biogeochem. Cycles, 29(11), 1944–1961, doi:10.1002/2015GB005207, 2015.

Muglia, J. and Schmittner, A.: Glacial Atlantic overturning increased by wind stress in climate models, Geophys. Res. Lett., 42(22), 9862–9869, doi:10.1002/2015GL064583, 2015.

Munhoven, G.: Glacial - Interglacial changes of continental weathering: Estimates of the related CO2 and HCO3- flux variations and their uncertainties, Glob. Planet. Change, 33(1–2), 155–176, doi:10.1016/S0921-8181(02)00068-1, 2002.

O'Ishi, R. and Abe-Ouchi, A.: Influence of dynamic vegetation on climate change and terrestrial carbon storage in the Last Glacial Maximum, Clim. Past, 9(4), 1571–1587, doi:10.5194/cp-9-1571-2013, 2013.

Oka, A., Abe-Ouchi, A., Chikamoto, M. O. and Ide, T.: Mechanisms controlling export production at the LGM: Effects of changes in oceanic physical fields and atmospheric dust deposition, Global Biogeochem. Cycles, 25, doi:10.1029/2009GB003628, 2011.

Opdyke, B. N. and Walker, J. C. G.: Return of the coral reef hypothesis: basin to shelf partitioning of CaCO3 and its effect on atmospheric CO2, Geology, 20(8), 733–736, doi:10.1130/0091-7613(1992)020<0733:ROTCRH>2.3.CO, 1992.

Oppo, D. W., Curry, W. B. and McManus, J. F.: What do benthic δ13C and δ18O data tell us about Atlantic circulation during Heinrich Stadial 1?, Paleoceanography, 30(4), 353–368, doi:10.1002/2014PA002667, 2015.

Otto, D., Rasse, D., Kaplan, J., Warnant, P. and François, L.: Biospheric carbon stocks reconstructed at the Last Glacial Maximum: Comparison between general circulation models using prescribed and computed sea surface temperatures, Glob. Planet. Change, 33(1–2), 117–138, doi:10.1016/S0921-8181(02)00066-8, 2002.

Palastanga, V., Slomp, C. P. and Heinze, C.: Glacial-interglacial variability in ocean oxygen and phosphorus in a global biogeochemical model, Biogeosciences, 10(2), 945–958, doi:10.5194/bg-10-945-2013, 2013.

Peltier, W. R.: Ice age paleotopography., Science, 265(5169), 195–201, doi:10.1126/science.265.5169.195, 1994.

Peterson, C. D., Lisiecki, L. E. and Stern, J. V.: Deglacial whole-ocean δ13C change estimated from 480 benthic foraminiferal records, Paleoceanography, 29(6), 549–563, doi:10.1002/2013PA002552, 2014.

Prentice, I., Farquhar, G. and Fasham, M.: The carbon cycle and atmospheric carbon dioxide, Clim. Chang. 2001 Sci. Basis, 183–237, doi:10.1256/004316502320517344, 2001.

Prentice, I., Harrison, S. and Bartlein, P.: Global vegetation and terrestrial carbon cycle changes after the last ice age, New Phytol., 189(4), 988–998, doi:10.1111/j.1469-8137.2010.03620.x, 2011.

Radi, T. and de Vernal, A.: Last glacial maximum (LGM) primary productivity in the northern North Atlantic Ocean, Can. J. Earth Sci., 45, 1299–1316, doi:Doi 10.1139/E08-059, 2008.

Ridgwell, A. and Hargreaves, J. C.: Regulation of atmospheric CO2 by deep-sea sediments in an Earth system model, Global Biogeochem. Cycles, 21(2), doi:10.1029/2006GB002764, 2007.

Ridgwell, A., Hargreaves, J. C., Edwards, N. R., Annan, J. D., Lenton, T. M., Marsh, R., Yool, A. and Watson, A.: Marine geochemical data assimilation in an efficient Earth System Model of global biogeochemical cycling, Biogeosciences, 4(4), 87–104, doi:10.5194/bg-4-87-2007, 2007.

Roth, R., Ritz, S. P. and Joos, F.: Burial-nutrient feedbacks amplify the sensitivity of atmospheric carbon dioxide to changes in organic matter remineralisation, Earth Syst. Dyn., 5(2), 321–343, doi:10.5194/esd-5-321-2014, 2014.

Sarnthein, M., Schneider, B. and Grootes, P. M.: Peak glacial 14C ventilation ages suggest major draw-down of carbon into the abyssal ocean, Clim. Past, 9(6), 2595–2614, doi:10.5194/cp-9-2595-2013, 2013.

Schmitt, J., Schneider, R., Elsig, J., Leuenberger, D., Lourantou, A., Chappellaz, J., Kohler, P., Joos, F., Stocker, T. F., Leuenberger, M. and Fischer, H.: Carbon Isotope Constraints on the Deglacial CO2 Rise from Ice Cores, Science, 336(6082), 711–714, doi:10.1126/science.1217161, 2012.

Schmittner, A. and Somes, C. J.: Complementary constraints from carbon (13C) and nitrogen (15N) isotopes on the glacial ocean's soft-tissue biological pump, Paleoceanography, 31(6), 669–693, doi:10.1002/2015PA002905, 2016.

Schmittner, A., Urban, N. M., Shakun, J. D., Mahowald, N. M., Clark, P. U., Bartlein, P. J., Mix, A. C. and Rosell-Mele, A.: Climate Sensitivity Estimated from Temperature Reconstructions of the Last Glacial Maximum, Science (80-.)., 334(6061), 1385–1388, doi:10.1126/science.1203513, 2011.

Shin, S.-I., Liu, Z., Otto-Bliesner, B., Brady, E., Kutzbach, J. and Harrison, S.: A Simulation of the Last Glacial Maximum climate using the NCAR-CCSM, Clim. Dyn., 20(2), 127–151, doi:10.1007/s00382-002-0260-x, 2003.

Sigman, D. M. and Boyle, E. A.: Glacial/Interglacial Variations In Atmospheric Carbon Dioxide, Nature, 407(6806), 859–869, doi:10.1038/35038000, 2000.

Simmons, C. T., Mysak, L. A., and Matthews, H. D.: An investigation of carbon cycle dynamics since the Last Glacial Maximum: Complex interactions between the terrestrial biosphere, weathering, ocean alkalinity, and CO2 radiative warming in an Earth system model of intermediate complexity, Clim. Past Discuss., doi:10.5194/cp-2016-24, in review, 2016.

Singh, A. D., Jung, S. J. A., Darling, K., Ganeshram, R., Ivanochko, T. and Kroon, D.: Productivity collapses in the Arabian Sea during glacial cold phases, Paleoceanography, 26(3), doi:10.1029/2009PA001923, 2011.

Skinner, L. C., Fallon, S., Waelbroeck, C., Michel, E. and Barker, S.: Ventilation of the Deep Southern Ocean and Deglacial CO2 Rise, Science (80-.)., 328(5982), 1147–1151, doi:10.1126/science.1183627, 2010.

Skinner, L. C., Waelbroeck, C., Scrivner, A. E. and Fallon, S. J.: Radiocarbon evidence for alternating northern and southern sources of ventilation of the deep Atlantic carbon pool during the last deglaciation, Proc. Natl. Acad. Sci., 111(15), 5480–5484, doi:10.1073/pnas.1400668111, 2014.

Skinner, L., McCave, I. N., Carter, L., Fallon, S., Scrivner, A. E. and Primeau, F.: Reduced ventilation and enhanced magnitude of the deep Pacific carbon pool during the last glacial period, Earth Planet. Sci. Lett., 411, 45–52, doi:10.1016/j.epsl.2014.11.024, 2015.

Smith, H. J., Fischer, H., Wahlen, M., Mastroianni, D. and Deck, B.: Dual modes of the carbon cycle since the Last Glacial Maximum, Nature, 400(6741), 248–250, doi:10.1038/22291, 1999.

Stephens, B. B. and Keeling, R. F.: The influence of antarctic sea ice on glacial-interglacial CO2 variations, Nature, 404(6774), 171–174, doi:10.1038/35004556, 2000.

Sun, X. and Matsumoto, K.: Effects of sea ice on atmospheric p CO 2 : A revised view and implications for glacial and future climates, J. Geophys. Res., 115(G2), 1–8, doi:10.1029/2009JG001023, 2010.

~~Tagliabue, a., Bopp, L., Roche, D. M., Bouttes, N., Dutay, J. C., Alkama, R., Kageyama, M., Michel, E. and Paillard, D.: Quantifying the roles of ocean circulation and biogeochemistry in governing ocean carbon-13 and atmospheric carbon dioxide at the last glacial maximum, Clim. Past Discuss., 5(3), 1463–1491, doi:10.5194/cpd-5-1463-2009, 2009.~~

Tamburini, F. and Föllmi, K. B.: Phosphorus burial in the ocean over glacial-interglacial time scales, Biogeosciences, 6(4), 501–513, doi:10.5194/bg-6-501-2009, 2009.

Tiedemann, R. , Ronge, T. , Lamy, F. , Köhler, P. , Frische, M. , De Pol Holz, R. , Pahnke, K., Alloway, B. V. , Wacker, L. and Southon, J.: New Constraints on the Glacial Extent of the Pacific Carbon Pool and its Deglacial Outgassing , Nova Act Lc, 121 (408), 229-233, 2015.

Toggweiler, J. R., Russell, J. L. and Carson, S. R.: Midlatitude westerlies, atmospheric CO2, and climate change during the ice ages, Paleoceanography, 21(2), doi:10.1029/2005PA001154, 2006.

Tréguer, P. and Pondaven, P.:Global change: Silica control of carbon dioxide, Nature, 486, 358–359, 2000.

Vance, D., Teagle, D. A. H. and Foster, G. L.: Variable Quaternary chemical weathering fluxes and imbalances in marine geochemical budgets, Nature, 458(7237), 493–496, doi:10.1038/nature07828, 2009.

Völker, C. and Köhler, P.: Responses of ocean circulation and carbon cycle to changes in the position of the Southern Hemisphere westerlies at Last Glacial Maximum, Paleoceanography, 28(4), 726–739, doi:10.1002/2013PA002556, 2013.

Waelbroeck, C., Paul, A., Kucera, M., Rosell-Melé, A., Weinelt, M., Schneider, R., Mix, A. C., Abelmann, A., Armand, L., Bard, E., Barker, S., Barrows, T. T., Benway, H., Cacho, I., Chen, M. T., Cortijo, E., Crosta, X., De Vernal, A., Dokken, T., Duprat, J., Elderfield, H., Eynaud, F., Gersonde, R., Hayes, A., Henry, M., Hillaire-Marcel, C., Huang, C. C., Jansen, E., Juggins, S., Kallel, N., Kiefer, T., Kienast, M., Labeyrie, L., Leclaire, H., Londeix, L., Mangin, S., Matthiessen, J., Marret, F., Meland, M., Morey, A. E., Mulitza, S., Pflaumann, U., Pisias, N. G., Radi, T., Rochon, A., Rohling, E. J., Sbaffi, L., Schäfer-Neth, C., Solignac, S., Spero, H., Tachikawa, K. and Turon, J. L.: Constraints on the magnitude and patterns of ocean cooling at the Last Glacial Maximum, Nat. Geosci., 2(2), 127–132, doi:10.1038/ngeo411, 2009.

Wagner, M. and Hendy, I. L.: Trace metal evidence for a poorly ventilated glacial Southern Ocean, Clim. Past Discuss., https://doi.org/10.5194/cpd-11-637-2015, 2015.

Wallmann, K.: Is late Quaternary climate change governed by self-sustained oscillations in atmospheric CO2?, Geochim. Cosmochim. Acta, 132, 413–439, doi:10.1016/j.gca.2013.10.046, 2014.

Wallmann, A.: Effects of Eustatic Sea-Level Change on Atmospheric CO_2 and Glacial Climate. Nova Act Lc NF, 121, 241-245, 2015.

Watson, A. J. and Naveira Garabato, A. C.: The role of Southern Ocean mixing and upwelling in glacial-interglacial atmospheric CO2change, Tellus, Ser. B Chem. Phys. Meteorol., 58(1), 73–87, doi:10.1111/j.1600-0889.2005.00167.x, 2006.

Weber, S. L., Drijfhout, S. S., Abe-Ouchi, A., Crucifix, M., Eby, M., Ganopolski, A., Murakami, S., Otto-Bliesner, B., and Peltier, W. R.: The modern and glacial overturning circulation in the Atlantic ocean in PMIP coupled model simulations, Clim. Past, 3, 51-64, https://doi.org/10.5194/cp-3-51-2007, 2007.

Weitemeyer, K. A. and Buffett, B. A.: Accumulation and release of methane from clathrates below the Laurentide and Cordilleran ice sheets, Global Planet Change, 53(3), 176–187, 2006.

Williamson, M. S., Lenton, T. M., Shepherd, J. G. and Edwards, N. R.: An efficient numerical terrestrial scheme (ENTS) for Earth system modelling, Ecol. Modell., 198(3–4), 362–374, doi:10.1016/j.ecolmodel.2006.05.027, 2006.

Yu, J., Anderson, R. and Rohling, E.: Deep Ocean Carbonate Chemistry and Glacial-Interglacial Atmospheric CO2 Change, Oceanography, 27(1), 16–25, doi:10.5670/oceanog.2014.04, 2014.

Zech, R.: A permafrost glacial hypothesis – Permafrost carbon might help explaining the Pleistocene ice ages, Quat. Sci. J., 61(1), 84–92, doi:10.3285/eg.61.1.07, 2012.

Zech, R., Huang, Y., Zech, M., Tarozo, R., and Zech, W.: High carbon sequestration in Siberian permafrost loess-paleosols during glacials, Clim. Past, 7, 501-509, doi:10.5194/cp-7-501-2011, 2011.

Zeng, N.: Glacial-interglacial atmospheric CO2 changes – the Glacial Burial Hypothesis. – Advances in Atmospheric Sciences, 20: 677–693, 2003.

Zeng, N.: Quasi-100 ky glacial-interglacial cycles triggered by subglacial burial carbon release, Clim. Past, 3, 135–153, doi:10.5194/cpd-2-371-2006, 2007.

Zhang, X., Lohmann, G., Knorr, G., and Xu, X.: Different ocean states and transient characteristics in Last Glacial Maximum simulations and implications for deglaciation, Clim. Past, 9, 2319-2333, doi:10.5194/cp-9-2319-2013, 2013.

Ziegler, M., Diz, P., Hall, I. R. and Zahn, R.: Millennial-scale changes in atmospheric CO2 levels linked to the Southern Ocean carbon isotope gradient and dust flux, Nat. Geosci., 6, 457–461, 2013.

Zimov, S., Schuur, E. and III, F. C.: Permafrost and the global carbon budget, Science, 312(June), 1612–1613, doi:10.1126/science.1128908, 2006.

Zimov, N. S., Zimov, S. A., Zimova, A. E., Zimova, G. M., Chuprynin, V. I., and Chapin, F. S.: Carbon storage in permafrost and soils of the mammoth tundra-steppe biome: Role in the global carbon budget, Geophys. Res. Lett., 36, L02502, doi:10.1029/2008gl036332, 2009.